Arch. Rational Mech. Anal. 178 (2005) 149–226
Digital Object Identifier (DOI) 10.1007/s00205-005-0391-4

Discrete Crystal Elasticity and Discrete Dislocations in Crystals

M. P. ARIZA & M. ORTIZ

Communicated by the Editors

Abstract

This article is concerned with the development of a discrete theory of crystal elasticity and dislocations in crystals. The theory is founded upon suitable adaptations to crystal lattices of elements of algebraic topology and differential calculus such as chain complexes and homology groups, differential forms and operators, and a theory of integration of forms. In particular, we define the lattice complex of a number of commonly encountered lattices, including body-centered cubic and face-centered cubic lattices. We show that material frame indifference naturally leads to discrete notions of stress and strain in lattices. Lattice defects such as dislocations are introduced by means of locally lattice-invariant (but globally incompatible) eigendeformations. The geometrical framework affords discrete analogs of fundamental objects and relations of the theory of linear elastic dislocations, such as the dislocation density tensor, the equation of conservation of Burgers vector, Kröner's relation and Mura's formula for the stored energy. We additionally supply conditions for the existence of equilibrium displacement fields; we show that linear elasticity is recovered as the Γ-limit of harmonic lattice statics as the lattice parameter becomes vanishingly small; we compute the Γ-limit of dilute dislocation distributions of dislocations; and we show that the theory of continuously distributed linear elastic dislocations is recovered as the Γ-limit of the stored energy as the lattice parameter and Burgers vectors become vanishingly small.

Contents

1. Introduction

The work presented in this article is concerned with the development of a discrete theory of crystal elasticity and dislocations in crystals. The classical treatment of harmonic crystal lattices and their defects, e.g., within the context of lattice statics (cf., e.g., [4, 45]) and eigendeformations (cf., e.g., [36]), becomes unwieldy when applied to general boundary value problems and conceals the essential mathematical structure of the theory, often impairing insight and hindering analysis. Instead, here we endeavor to develop a theory founded upon suitable adaptations to crystal lattices of elements of algebraic topology and differential calculus such as chain complexes and homology groups, differential forms and operators, and a theory of integration of forms. These elements, and their connection to linear elasticity and topological defects, are often taken for granted in $\mathbb{R}^n$ but need to be carefully defined and formalized for general crystal lattices. The resulting discrete geometrical framework enables the formulation of a mechanics of lattices in a manner that parallels closely – and extends in important respects – the classical continuum theories.

While the theory of linear elastic dislocations in crystals is well known (e.g., [19, 3, 36]), it may stand a brief review, especially as a point of reference for the discrete theory. The classical geometrical theory of linear elastic dislocations (e. g., [47, 23, 30, 48, 36, 20–22]) starts by positing the existence of an elastic distortion field β^e with the defining property that

$$E(\beta^e) = \int_{\mathbb{R}^3} \frac{1}{2} c_{ijkl} \beta^e_{ij} \beta^e_{kl} dx \tag{1}$$

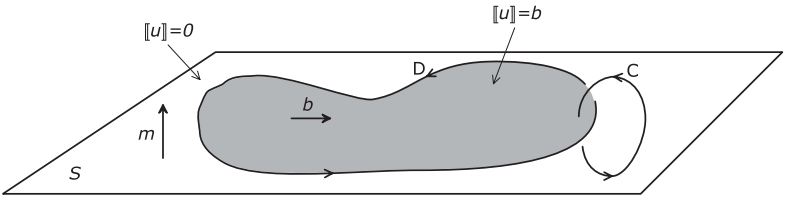

Fig. 1. Schematic representation of a perfect Volterra dislocation in a linear elastic solid. The plane S of unit normal m is the slip plane; D is the dislocation loop. The displacement field jumps discontinuously across the slip area (shown as the shaded region of the slip plane bounded by D) by one Burgers vector b. The presence of the dislocation may be detected by linking its elastic deformation field against a Burgers circuit C.

is the strain energy of the crystal. Here, $c_{ijkl} = c_{jikl} = c_{ijlk} = c_{klij}$ denote the elastic moduli of the crystal. A Volterra dislocation of Burgers vector b supported on a closed curve D is a field β^e such that

$$\int_C \beta^e_{ij} dx_j = -\mathrm{Link}(C, D) b_i \tag{2}$$

for all closed curves C (cf., Fig. 1). Here

$$\mathrm{Link}(C_1, C_2) = \frac{1}{8\pi} \int_{C_1} \int_{C_2} \frac{(dx_1 \times dx_2) \cdot (x_1 - x_2)}{|x_1 - x_2|^3} \tag{3}$$

is the Gauss linking number of two loops C_1 and C_2 in $\mathbb{R}^3$ (e.g., [21]). The test circuits C used in (2) to detect the presence of a dislocation are known as Burgers circuits. Consider now an element of oriented area A with boundary C. Then, the total Burgers vector of all dislocations crossing A is

$$b_i(A) = -\int_C \beta^e_{ij} dx_j. \tag{4}$$

By Stoke's theorem we have

$$b_i(A) = \int_A \alpha_{il} n_l dS, \tag{5}$$

where $n\,dS$ is the element of oriented area and

$$\alpha_{il} = -\beta^e_{ij,k} e_{kjl} \tag{6}$$

is NYE's dislocation density tensor [38]. The relation (6) between the elastic distortion field and the dislocation density field was presented by KRÖNER [26]. It follows immediately from this relation that

$$\alpha_{il,l} = 0, \tag{7}$$

i.e., the divergence of the dislocation density field is zero. This means, in particular, that the link between the dislocation lines and any closed surface, i.e., the number

of dislocation signed crossings through the surface, is zero. This property of dislocation lines is sometimes referred to as the conservation of Burgers vector property. Evidently, α measures the failure of the elastic distortion β^e to be a gradient and completely describes the distribution of dislocations in the crystal. In particular, if $\alpha = 0$ it follows that

$$\beta^e_{ij} = u_{i,j}, \tag{8}$$

i.e., β^e is the gradient of a displacement field u, and (1) reduces to the strain energy of a linear elastic solid.

At room temperature, dislocations in metals are predominantly the result of processes of crystallographic slip that build upon energetically and kinetically favorable lattice-preserving shears. By its crystallographic nature, slip results in dislocations that lie on well-characterized crystal planes and has Burgers vectors coincident with well-characterized crystal directions. Each possible slip plane and Burgers vector pair defines a slip system. The set of slip systems of a crystal is closely related to its crystal structure and often is known experimentally [19]. In a continuum setting, crystallographic slip may be described by identifying the elastic distortion β^e with the Lebesgue-regular part of the distributional gradient of the displacement field u (as in the Lebesgue decomposition theorem), and requiring the remaining singular part to be supported on a collection S of crystallographic slip planes. The extent of crystallographic slip on a plane in S is described by the displacement jump $[\![u]\!]$ across the plane. This displacement jump is required to be lattice preserving and, hence, an integer linear combination of Burgers vectors contained within the slip plane. Thus, the unknown fields of the theory are the elastic distortion β^e, which equals the displacement gradient ∇u in $\mathbb{R}^3 \backslash S$, and the displacement jump $[\![u]\!]$ on S. The elastic distortion β^e follows directly from the minimization of the strain energy (1) over $\mathbb{R}^3 \backslash S$ with respect to the displacement field u, subject to the prescribed $[\![u]\!]$ across S. This problem belongs to a classical class of problems in linear elasticity know as 'cut surfaces' [36]. By contrast, the evolution of the displacement jump $[\![u]\!]$ on S is governed by kinetics, including lattice friction, cross slip, and short-range dislocation-dislocation interactions resulting in jogs, junctions and other reaction products.

There are several essential shortcomings of the theory of linear-elastic dislocations just outlined which are a direct consequence of the continuum character of the theory. Firstly, linear-elastic Volterra dislocations as described above have infinite strain energy. The conventional 'fix' for this unphysical situation is to exclude in the computation of the strain energy a small tube of material, or core, around the dislocation line of radius a_0, the 'cut-off radius' (cf., e.g., [19, 3]). The resulting strain energies then diverge logarithmically in a_0. The introduction of a core is intended to account for the discreteness of the crystal lattice and its relaxation in the vicinity of the dislocation line. The cut-off radius is an ad-hoc parameter extraneous to linear elasticity which must be determined by fitting to experiment. In addition, the core cut-off radius is a poor representation of the structure of dislocation cores in general.

A superior regularization of the theory of linear-elastic dislocations may be accomplished by relaxing the requirement that the displacement jump $[\![u]\!]$ across

the singular set S be an integer linear combination of in-plane Burgers vectors, and instead introducing a PEIERLS potential ϕ [40] such that the total energy of the crystal is

$$E(u) = \int_{\mathbb{R}^3 \setminus S} \frac{1}{2} c_{ijkl} u_{i,j} u_{k,l} dx + \int_S \phi([\![u]\!]) dS. \tag{9}$$

The Peierls potential on a slip plane is periodic in shear and exhibits the translation invariance of the lattice (cf., e.g., [39]). The displacement field then follows by the minimization of $E(u)$ under the action of applied loads and subject to kinetic or topological constraints such as lattice friction, dislocation-dislocation and dislocation-obstacle interactions [24, 14, 25]. While the Peierls framework represents a vast improvement over the cut-off radius regularization, it falls short in a number of important aspects. Thus, since the crystal is regarded as a continuum, there is no natural notion of spacing between slip planes. Of course, the potential slip planes may be placed at the appropriate crystallographic interplanar distance, but then the assumption of interplanar linear elasticity becomes questionable.

A natural approach to the mechanics of crystal defects which is free of the pathologies just described is to acknowledge the discrete nature of crystal lattices from the outset. However, this requires foundational developments in two main areas: the formulation of a discrete differential calculus on crystal lattices; and the application of the said discrete differential calculus to the formulation of a discrete mechanics of lattices, including lattice defects. Thus, the geometrical theory of crystal defects outlined above relies heavily on the homotopy of closed Burgers circuits in $\mathbb{R}^3$ as a device for characterizing line defects. Homotopy also underlies fundamental rules governing dislocation reactions, such as Frank's rule (e.g., [19]) and topological transitions such as dislocation junctions [48]. In addition, the geometrical theory of crystal defects is tacitly founded on the homology of $\mathbb{R}^3$. It is well known that the singular homology of $\mathbb{R}^n$ is $H_p(\mathbb{R}^n) = \mathbb{Z}$ if $p = 0$, and $H_p(\mathbb{R}^n) = 0$ if $p \geqq 1$ (e.g., [34]). The identity $H_0(\mathbb{R}^n) = \mathbb{Z}$ follows directly from the path-connectedness of $\mathbb{R}^n$, i.e., the fact that every pair of points in $\mathbb{R}^n$ can be joined by a continuous path. The identities $H_p(\mathbb{R}^n) = 0$, $p \geqq 1$ imply in particular that every closed loop in $\mathbb{R}^n$ is the boundary of a surface and is contractible to a point, and that every closed surface is the boundary of a volume and is likewise contractible to a point. These properties of $\mathbb{R}^3$, and related topological invariants such as the Gauss linking number, underlie the definition (2) of a Volterra dislocation. Finally, the familiar differential operators of $\mathbb{R}^3$, such as div, grad and curl, and the integration of forms of various orders, including Stoke's theorem, arise frequently in relations such as (1), (2), (5), (6), (7) and (8).

In laying the groundwork for a discrete theory, these elements of algebraic topology and differential calculus need to be extended to crystal lattices. At the most fundamental level, the notions of point, curve, surface and volume and their boundary and coboundary connections need to be carefully redefined. These objects supply the natural domains of definition of mechanical fields and forms, as well as their natural domains of integration. Crystal lattices can be endowed with this requisite structure by regarding them as complexes (not necessarily simplicial). This

notion of crystal lattice is greatly expanded with respect to traditional representations of lattices [4, 44], and proves powerful as a foundation for a mechanics of lattices. The construction of lattice complexes is not entirely trivial, as the complex must be translation invariant, possess the symmetries of the crystal, and have the homology of the imbedding space, e.g., $\mathbb{R}^n$. In addition, the lattice complex must contain all the operative slip systems of the crystal. In Section 2 we define the lattice complex of a number of commonly encountered lattices, including body-centered cubic and face-centered cubic lattices.

In Section 3, we introduce the differential complex of a lattice, including fields and forms of all orders, the differential and codifferential operators, the wedge product, the Hodge-$*$ operator, integrals of forms of all orders, a discrete Stoke's theorem, a discrete Helmholtz-Hodge decomposition, and a discrete linking number. These tools enable the formulation of a discrete mechanics of crystal lattices and lattice defects that is formally indistinguishable from the continuum theory. In this approach, all specificity regarding the continuum or discrete nature of the system – and the structure of the crystal – is subsumed in the definition of the lattice complex and differential structures, and the physical governing equations are identical for all systems. In this sense, the present work may be regarded as part of an ongoing effort to develop mechanical and physical theories of discrete objects using discrete differential calculus (cf., e.g., [18, 28] and the extensive literature review therein).

In Section 4, we proceed to develop a mechanics of lattices and lattice defects. A key step in that regard is the realization that the essential structure of the theory is dictated by material-frame indifference, i.e., by the invariance of the energy of the crystal lattice under translations and rotations. Indeed, we show that material-frame indifference results in a natural discrete version of the Cauchy-Green deformation tensor field, and upon linearization, of the small-strain tensor field. The corresponding definitions of stress, traction and equilibrium, follow from duality and stationarity. For harmonic lattices, the theory precisely identifies the form of the stress-strain relations. It bears emphasis that these relations have a special structure due to material-frame indifference, and that the force-displacement relations of the crystal lattice inherit that structure. Conversely, arbitrary force constants violate material-frame indifference in general, with the unphysical consequence that lattice rotations may induce strain energy. The restrictions placed on the force constants of a crystal lattice by material-frame indifference do not appear to have been fully appreciated in the lattice statics literature (for notable exceptions, cf., [43, 45]).

In all these developments, the discrete differential calculus framework proves of great value. For instance, within that framework the various mechanical fields find a clear definition as functions over the lattice complex: the displacement field is a 0-form; the deformation field is a 1-form; the strain-tensor, metric-tensor and stress fields are scalar-valued functions over pairs of 1-cells; and so on. It is also interesting to note the notion of a tensor field which emerges from the theory. Thus, for instance, the strain and stress tensors, which provide examples of second-order tensors, are real-valued functions of pairs of cells. Also, the notion of metric that emerges naturally from the theory is noteworthy: the natural way to define the metric properties of the lattice is to provide the inner products of the differential of the

position vector for every pair of 1-cells. The availability of an efficient theory of integration of forms, including a Stoke's theorem, is also invaluable in deriving the equations of equilibrium of the crystal and establishing their structure.

In Section 5, we introduce the notion of discrete dislocation by means of the standard eigendeformation device (cf., [36, 39] for overviews of eigendeformations in the context of dislocation mechanics). Uniform eigendeformations represent lattice-invariant that cost no energy. Non-uniform eigendeformations are not gradients of a displacement field in general and, therefore, introduce dislocations into the lattice. The structure of the resulting dislocations is particularly revealing. Thus, it follows that the set of all discrete dislocation loops can be identified with the group B^2 of 2-coboundaries of the lattice; and the set of all Burgers circuits can be identified with the group Z_1 of 1-cycles of the lattice. The Burgers-circuit test (2) simply reflects the duality between these two groups. In particular, the coboundaries of all 1-cells of the lattice, which constitute a generator of B^2, may be regarded as elementary dislocation loops. All remaining dislocations loops are generated by the elementary loops in the sense of chains. Likewise, the boundaries of all 2-cells of the lattice constitute a generator of Z_1 and may be regarded as elementary – or the smallest possible – Burgers circuits. The theory also provides discrete versions of fundamental relations such as Kröner's formula (6), the conservation of Burgers vector relation (7), and others. The geometrical and physical insight into the structure of discrete dislocations afforded by the geometrical foundations of the theory can hardly be overemphasized.

While the primary focus of this paper is the formulation of a discrete mechanics of lattices, we nevertheless delve briefly into some questions of analysis. Thus, for instance, we give conditions for the existence of equilibrium displacement fields (Propositions 2 and 3) and discuss the equilibrium problem for slip and dislocation fields. We also show that linear elasticity is recovered as the Γ-limit of the harmonic lattice statics problem, as the lattice parameter becomes vanishingly small (Proposition 4). We also investigate two continuum limits of the stored energy of a dislocation ensemble. The first limit is attained by the application of a scaling transformation which expands – and rarefies – the dislocation ensemble, while leaving the lattice parameter unchanged (Proposition 5). The second limit of the stored energy is obtained by scaling down the lattice size and the Burgers vector sizes simultaneously, and leads to the classical theory of continuously distributed dislocations (Proposition 6). In conclusion we note that the investigation of the continuum limits just described fits within current efforts to understand continuum models as the limits of discrete systems (cf., [7] and the references therein).

2. Crystal lattices

The development of a general theory of the mechanics of lattices and lattice defects is greatly facilitated by a judicious use of elements of algebraic topology and differential calculus. These elements greatly streamline the notation and, perhaps more importantly, shed considerable insight into the general structure of the theory, especially in the presence of lattice defects. We begin by regarding crystal lattices

as chain complexes, a view that greatly expands previous mathematical models of lattices. In particular, the lattice complex encodes all information regarding points, curves, surfaces, volumes of the lattice and their adjacency relations. These algebraic elements provide the basis for the subsequent definition of a discrete lattice calculus. For instance, the boundary and coboundary operators induce differential and codifferential operators on forms and fields, and the cup product of cochains induces a wedge product of forms. Provided that it is appropriately defined, the lattice complex also encodes the geometry of the slip systems and discrete dislocations of the corresponding crystal class. We develop the complexes of commonly encountered lattices, such as the face-centered cubic lattice and the body-centered cubic lattice, and provide in tabular form all the fundamental operations required in applications.

2.1. Elementary properties of crystal lattices

2.1.1. Notation. We denote the group of integers by $\mathbb{Z}$, the real numbers by $\mathbb{R}$ and the complex numbers by $\mathbb{C}$. In indicial expressions involving vectors and tensors we adopt Einstein's summation convention unless explicitly stated.

The most elementary view of a crystal lattice is as a discrete subgroup [44]

$$L = \{x(l) = l^i a_i,\ l \in \mathbb{Z}^n\} \tag{10}$$

of $\mathbb{R}^n$, where $\{a_1, \ldots, a_n\}$ are linearly independent vectors defining a lattice basis. The dual basis $\{a^1, \ldots, a^n\}$ is characterized by the property

$$a^i \cdot a_j = \delta^i{}_j, \tag{11}$$

where the dot denotes scalar product in $\mathbb{R}^n$. Following common notation, we shall denote by Ω the volume of the unit cell of the lattice, or atomic volume. The dual and reciprocal lattices are the lattices spanned by the dual basis and by $\{2\pi a^1, \ldots, 2\pi a^n\}$, respectively. We recall that the first Brillouin zone B is the Voronoi cell of the reciprocal lattice at the origin. The volume of the dual unit cell is $1/\Omega$, whereas the volume $|B|$ of the first Brillouin zone, and of the reciprocal unit cell, is $(2\pi)^n/\Omega$.

A complex lattice may be defined as a collection of interpenetrating simple lattices having the same basis. Thus, the point set of a complex lattice is of the form:

$$L = \{x(l, \alpha) = l^i a_i + r_\alpha,\ l \in \mathbb{Z}^n,\ \alpha = 1, \ldots, N\}, \tag{12}$$

where α labels each constituent simple sublattice, and r_α is the relative translation vector of the α sublattice. Certain crystal lattices and certain sets of objects that arise naturally in the mechanics of crystals, such as the set of atomic bonds, possess the translational symmetry of a complex lattice. Even when a crystal lattice can be described as a simple lattice, it may be convenient to describe it as a complex lattice for indexing purposes. For instance, a body-centered cubic lattice can variously be described as a simple lattice or as a complex lattice consisting of two superposed simple-cubic lattices.

We recall that a symmetry of the lattice is an orthogonal transformation $Q \in O(n)$ that maps the lattice into itself (cf., e.g., [12]). The set $\mathcal{S}$ of all symmetry transformations is a subgroup of $O(n)$ known as the symmetry group of the lattice. In three dimensions there are 32 possible symmetry groups corresponding to each of the 32 crystallographic point groups [6]. If the inversion transformation belongs to $\mathcal{S}$, then the lattice is said to be centrosymmetric. A simple lattice is necessarily centrosymmetric. We also recall that two lattices L_1 and L_2 define the same Bravais lattice if there exists a linear isomorphism $\phi : \mathbb{R}^n \to \mathbb{R}^n$ such that $L_2 = \phi(L_1)$ and $\mathcal{S}(L_2) = \phi\mathcal{S}(L_1)\phi^{-1}$. For $n = 2$ there are exactly 5 Bravais lattices, whereas for $n = 3$ there are 14 Bravais lattices [44].

A crystallographic plane is conventionally defined by its Miller indices $m \in \mathbb{Z}^n$, defined such that the points $\{a_1/m_1, \ldots, a_n/m_n\}$ are the intercepts of the plane with the coordinate axes. A family of parallel crystallographic planes may be defined implicitly by the equation

$$x \cdot k \in \mathbb{Z} \tag{13}$$

for some dual vector k, where the symbol $\cdot$ signifies the duality pairing in $\mathbb{R}^n$. It is readily shown that the components of the vector k in the dual basis a^i coincide with the Miller indices. The distance between consecutive parallel planes is important in understanding processes of crystallographic slip. A trite calculation gives the distance between the two planes as

$$d^{-1} = |k|, \tag{14}$$

where $|\cdot|$ denotes the standard norm in $\mathbb{R}^n$.

The choice of lattice basis is clearly not unique. Any n-tuple $(a'_1, \ldots, a'_n)$ related linearly to the original basis as $a'_i = \mu_i{}^j a_j$ also defines a lattice basis of the same orientation provided that $\mu \in SP(\mathbb{Z}^n)$ [12], i.e., $\mu_i{}^j \in \mathbb{Z}$ and $\det(\mu) = \pm 1$. A far-reaching consequence of this fact is that any affine mapping F on $\mathbb{R}^n$ of the form

$$F = \mu_i{}^j a_j \otimes a^i \tag{15}$$

leaves the lattice invariant. A particularly important class of lattice-invariant deformations of relevance to processes of crystallographic slip is

$$F = I + (s^j a_j) \otimes (m_i a^i) \tag{16}$$

with $s, m \in \mathbb{Z}^n$ and $s^i m_i = 0$. These simple-shear deformations represent uniform crystallographic slip through a Burgers vector $b = s^j a_j$ on the plane of normal $m_i a^i$. Energetic considerations, such as the examination of core energies of linear-elastic dislocations, as well as kinetic considerations, such as those based on linear-elastic estimates of lattice friction, suggest that crystallographic slip occurs preferentially on closed-packed planes, i.e., planes for which the interplanar distance d, equation (14), is maximized. A tabulation of commonly observed slip planes may be found in the treatise of HIRTH & LOTHE [19].

2.2. The chain complex of a crystal lattice

2.2.1. Notation. Throughout this section we follow the notation and nomenclature of [34], which may be consulted for further details and background. We denote the interior of a subset A of a topological space by $\mathrm{Int}A$, its boundary by $\mathrm{Bd}A$, and its closure by $\bar{A}$. We also denote by B^n the unit n-ball, i.e., the set of all points x of $\mathbb{R}^n$ such that $|x| \leqq 1$, where $|\cdot|$ denotes the standard norm in $\mathbb{R}^n$. The unit sphere S^{n-1} is the set of points for which $|x| = 1$. If $f : G \to H$ is a group homomorphism, we denote by $\ker f$ the kernel of f, i.e., the subgroup $f^{-1}(\{0\})$ of G, and by $\mathrm{im}\, f$ the image of f, i.e., the subgroup $f(G)$ of H. Given two abelian groups G and H we denote by $\mathrm{Hom}(G, H)$ the abelian group of all homomorphisms of G into H.

In the preceding elementary view, a crystal lattice is regarded merely as a point set, each site being occupied by an atom. A more complete view of a crystal lattice includes objects such as atomic bonds, or pairs of atoms, elementary areas and elementary volumes. We shall refer to these higher-dimensionality objects as p-cells, where p is the dimension of the cell. p-cells supply the natural support for defining functions arising in the mechanics of lattices, such as displacement and deformation fields and dislocation densities. They also supply the natural framework for defining discrete differential operators and integrals. Naturally, we require the collection of all p-cells to be translation and symmetry invariant. There are a number of additional restrictions on p-cells that give mathematical expression to the intuitive notion of a perfect, or defect-free, crystal lattice. In this section, we proceed to develop this extended view of crystals.

Recall that a space e is called a cell of dimension p if it is homeomorphic with B^p, i.e., if there exists a continuous bijective function $f : B^p \to e$ such that its inverse is also continuous. It is called an open cell if it is homeomorphic to $\mathrm{Int}\, B^p$. We shall use the notation e_p and the term p-cell when we wish to make explicit the dimension of the cell. We recall that a regular CW complex is a space X and a collection of disjoint open cells whose union is X such that: (i) X is Hausdorff; (ii) for each open cell e there exists a homeomorphism $f : B^p \to X$ that maps $\mathrm{Int}B^p$ onto e and carries $\mathrm{Bd}B^p$ into a finite union of open cells, each of dimension less than p; (iii) a set A is closed in X if $A \cap \bar{e}$ is closed in $\bar{e}$ for each cell e. X is the underlying space of the complex. By a slight abuse of notation we shall use the symbol X to refer both to the complex and to the underlying space. In all subsequent developments the underlying space is always $\mathbb{R}^n$ and hence condition (i) is automatically satisfied. The cells contained in another cell e are the faces of e. The faces of e different from e itself are called the proper faces of e. The notation $e' \preceq e$ or $e \succeq e'$ signifies that e' is a face of e, whereas the notation $e' \prec e$ or $e \succ e'$ signifies that e' is a proper face of e. The subspace X_p of X that is the union of the open cells of X of dimension at most p is a subcomplex of X called the p-skeleton of X. In particular, X_0 is the set of 0-cells or vertex set. The dimension of a complex is the largest dimension of a cell of X.

We define an n-dimensional lattice complex to be a CW complex such that:

(A1) The underlying space is all of $\mathbb{R}^n$.
(A2) The vertex set defines an n-dimensional lattice.
(A3) The cell set is translation and symmetry invariant.

For $n \leqq 3$, we shall refer to the 1-cells of a lattice complex as elementary segments, to the 2-cells as elementary areas, and to the 3-cells as elementary volumes. The requirement that these elements form a CW complex gives mathematical expression to the intuitive notions that p-cells should be non-intersecting, and their boundaries the union of cells of lower dimension. Implied in axiom $A1$ is the requirement that the union of all cells in the complex be $\mathbb{R}^n$. Translation and symmetry invariance require that if a cell is in X, so must be all translates of the cell by translation vectors of the lattice, and all symmetry-related cells. The symmetry and CW complex requirements just stated place fundamental restrictions on the choice of elementary segment, elementary area and elementary volume sets.

There are additional restrictions on a lattice complex that are of a homological nature and that give mathematical expression to the intuitive notion of a perfect, defect-free lattice. As noted in the introduction, the geometrical theory of linear-elastic point and line defects is (tacitly or explicitly) built around the homology of $\mathbb{R}^3$, specifically on the fact that every closed loop in $\mathbb{R}^3$ is the boundary of a surface and is contractible to a point, and that every closed surface is the boundary of a volume and is likewise contractible to a point. Non-trivial homology groups are then associated with distributions of point and line defects in the continuum (e g., [47, 23, 30, 48, 36, 20–22]).

In order to carry these tools over to the discrete setting, we proceed to formulate a homology of crystal lattices. We begin by defining the chain complex of the lattice. By convention, vertices have one orientation only. Elementary segments, or 1-cells, are oriented by ordering their vertices. We shall use the symbol $[v, v']$ to denote the elementary segment defined by the vertices $\{v, v'\}$ together with the orientation determined by the ordering (v, v'). Two adjacent oriented elementary segments of the form $[v, v']$ and $[v', v'']$ are said to be oriented consistently. An elementary area, or 2-cell, is oriented by assigning consistent orientations to each of its elementary segments. An elementary volume, or 3-cell, has two possible orientations, *inward* and *outward*. Thus, a 2-cell is consistently oriented with an outwardly (or inwardly) oriented 3-cell if the boundary of the 2-cell is oriented clockwise (respectively, counter-clockwise) when seen from inside the 3-cell. We shall denote by $[v_0, \ldots, v_p]$ the p-simplex defined by the vertices $\{v_0, \ldots, v_p\}$ together with the orientation determined by the ordering $(v_0, \ldots, v_p)$ (cf., e.g., [34], § 39, for a general definition of the orientation of a cell).

We recall that a p-chain in a CW complex X is a function c from the set of oriented p-cells of X to the integers such that: (i) $c(e) = -c(e')$ if e and e' are opposite orientations of the same cell; and (ii) $c(e) = 0$ for all but finitely-many oriented p-cells e. Note that p-chains are added by adding their values. We shall use the notation c_p when we wish to make explicit the dimension of the chain. The resulting group of oriented p-chains is denoted C_p. In an n-dimensional complex, C_p is the trivial group if $p < 0$ or $p > n$. If e is an oriented cell, the elementary chain corresponding to e is defined by: (i) $c(e) = 1$; (ii) $c(e') = -c(e)$ if e' is the opposite orientation of e; and (iii) $c = 0$ otherwise. By an abuse of notation we shall use the same symbol to denote a cell and the corresponding elementary chain. It is straightforward to show (cf., e.g., [34], Lemma 5.1) that C_p is free-abelian, i.e., it is abelian and it has a basis. Indeed, once all cells are oriented, each p-chain c_p

can be written uniquely as a finite linear combination $c_p = \sum n_i e_i$ of elementary p-chains e_i with integer coefficients n_i. Thus, the chain c assigns the integer value n_i to e_i, $-n_i$ to $-e_i$ and 0 to all oriented p-cells not appearing in the sum.

Any function f from the oriented p-cells of X to an abelian group G extends uniquely to a homomorphism $C_p \to G$ provided that $f(-e_p) = -f(e_p)$ for all oriented p-cells e_p. The boundary operator is a homomorphism $\partial_p : C_p \to C_{p-1}$ that can be defined in this manner by setting

$$\partial_p e_p = \sum_{e_{p-1} \prec e_p} \pm e_{p-1}, \tag{17}$$

where the sign is chosen as $+$ (or $-$) if the orientation of e_{p-1} coincides with (respectively, is the opposite of) that induced by e_p. For instance, if $e = [v, v']$ is an oriented elementary segment, then $\partial_1 e = v' - v$. It is readily verified that $\partial_{p-1} \circ \partial_p = 0$. Indeed, $\partial_{p-1} \circ \partial_p e_p = \sum_{e_{p-1} \prec e_p} \sum_{e_{p-2} \prec e_{p-1}} \pm e_{p-2}$, and the terms in these two sums cancel in pairs. Then, $\ker \partial_p$ is called the group of p-cycles and denoted Z_p, while $\mathrm{im} \partial_{p+1}$ is called the group of p-boundaries and denoted B_p. Also $H_p = Z_p / B_p$ is the pth homology group of the lattice complex. Henceforth we shall omit the dimensional subscript from ∂_p whenever it can be deduced from the context.

We shall say that a lattice complex X is perfect, or defect-free, if its homology is identical to the homology of the underlying space. For instance, a lattice in $\mathbb{R}^n$ is perfect if $H_p = \mathbb{Z}$ for $p = 0$ for $H_p = 0$, if $p \geqq 1$, i.e., if the homology of the complex is identical to the singular homology of $\mathbb{R}^n$ (cf., e.g., [34], § 29, for a general discussion of singular homology). The identity $H_0 = \mathbb{Z}$ follows simply by ensuring that X is path connected (cf., e.g., [34], Theorem 7.2), i.e., that every pair of points in X is joined by a continuous path of elementary segments. This requires all lattice sites to be connected by elementary segments, without 'hanging' sites. The identities $H_p = 0$, $p \geqq 1$, imply in particular that every 1-cycle in X is the boundary of a 2-chain, and that every 2-cycle is the boundary of a 3-chain. In the applications of interest here, it is important that a lattice complex possess a reference configuration that is defect-free. In order to ensure this property we append the following axiom:

(A4) The lattice complex is perfect.

This requirement places fundamental restrictions on the choice of cell set. In applications, it also provides a useful screening test of the admissibility of a lattice complex, especially in three dimensions.

We note that, for a given lattice, the choice of lattice complex is not uniquely determined by axioms (A1)–(A4) in general. Consider for instance an n-dimensional simple lattice having the trivial symmetry group $\{E, I\}$, where E and I are the identity and inversion transformations, respectively. Then, for any lattice basis we can construct a complex in which the n-cells are the parallelepiped defined by the basis vectors and its translates, and the remaining cells are chosen so that the complex is homeomorphic to the simple-cubic complex described in Section 2.3.4. Clearly, each lattice basis determines a lattice complex, and the choice of complex is not unique. In applications, the lattice complex must be carefully constructed

so that it contains all the crystallographic elements of interest, including the full complement of slip planes, Burgers vectors, dislocation loops, Burgers circuits, interstitial sites, and others. These additional requirements tend to reduce the latitude–or eliminate it completely–in the choice of lattice complex.

We additionally define the group C^p of p-cochains as the group $\mathrm{Hom}(C_p, \mathbb{Z})$ of all homomorphisms of C_p into $\mathbb{Z}$. If c^p is a p-cochain and c_p is a p-chain, we denote by $\langle c^p, c_p \rangle$ the value of c^p on c_p. The coboundary operator $\delta^p : C^p \to C^{p+1}$ is then defined by the identity

$$\langle \delta^p c^p, c_{p+1} \rangle = \langle c^p, \partial_{p+1} c_{p+1} \rangle. \tag{18}$$

From the identity $\partial_{p-1} \circ \partial_p = 0$, it follows immediately that $\delta^{p+1} \circ \delta^p = 0$. Let e^* be the elementary cochain whose value is 1 on a cell e and 0 on all other cells. The mapping $(^*)$ extends to an isomorphism from C_p to the subgroup of C^p of cochains of finite support, whose inverse will also be denoted by $(^*)$. We shall also simply write $e^p = (e_p)^*$ and $e_p = (e^p)^*$ and leave the operator $*$ implied. With this notation, an arbitrary cochain can be expressed as the formal (possibly infinite) sum $c^p = \sum n_i e_i^*$, where $n_i \in \mathbb{Z}$, and we have the identity $\delta^p c^p = \sum n_i \delta^p e_i^*$. Thus, the coboundary operator can be defined by specifying $\delta^p e^p$ on each oriented p-cell e_p, namely,

$$\delta^p e^p = \sum_{e_{p+1} \succ e_p} \pm e^{p+1}, \tag{19}$$

where the sign is chosen as $+$ (or $-$) if the orientation of e_p coincides with (respectively, is the opposite of) that induced by e_{p+1}. Then, $\ker \delta^p$ is called the group of cocycles and denoted Z^p, while $\mathrm{im}\delta^{p-1}$ is called the group of coboundaries and denoted B^p. Also $H^p = Z^p / B^p$ is the pth cohomology group of the lattice complex. As before, we shall henceforth omit the dimensional subscript from δ^p whenever it can be deduced from the context.

As subsequent developments will demonstrate (cf. Sections 5.1 and 5.2), the cycle group Z_1 of a crystal lattice is the group of all Burgers circuits. The generators of Z_1 may be interpreted as elementary Burgers circuits. The coboundary group B^2 of a crystal lattice is the group of all dislocation loops. This makes precise the sense in which Burgers circuits and dislocation loops are dual to each other. The generators of B^2 may be interpreted as a set of elementary dislocation loops.

In addition, as we shall see in Section 3, the boundary and coboundary operators just defined induce a discrete lattice analog of the de Rham differential complex in $\mathbb{R}^n$. In particular, the cup product of cochains provides the basis for the introduction of a wedge product of discrete forms. Recall that in a simplicial complex X, the cup product of $c^p \in C^p$ and $c^q \in C^q$ is defined by the identity

$$\langle c^p \cup c^q, [v_0, \ldots, v_{p+q}] \rangle = \langle c^p, [v_0, \ldots, v_p] \rangle \langle c^q, [v_p, \ldots, v_{p+q}] \rangle \tag{20}$$

if $[v_0, \ldots, v_{p+q}]$ is a simplex such that $v_0 < \cdots < v_{p+q}$ in some partial ordering of the vertices of X which linearly orders the vertices of each of its simplices. The cup product is bilinear and associative, and satisfies the coboundary formula

$$\delta(c^p \cup c^q) = (\delta c^p) \cup c^q + (-1)^p c^p \cup (\delta c^q) \tag{21}$$

(cf., e.g., [34]). It is clear from its definition that the cup product depends on the choice of ordering of the vertices. For crystal lattices, the natural partial ordering of the vertices is obtained by introducing a translation-invariant orientation of the 1-cells such that $\{e_1(l,1),\ldots,e_1(l,N_1)\}$ have $e_0(l)$ as their first vertex, and then letting $v_1 \prec v_2$ if $v_1 \neq v_2$ and v_2 can be reached from v_1 by a path consisting of the 1-cells $\{e_1(l,1),\ldots,e_1(l,N_1)\}$. However, the cup product does induce an operation $\cup : H^p \times H^q \to H^{p+q}$ among cohomology classes which is independent of the ordering of the vertices, bilinear, associative and satisfies the coboundary formula. In addition, it is anticommutative in the sense

$$[z^p] \cup [z^q] = (-1)^{pq}[z^q] \cup [z^p], \tag{22}$$

where $z^p \in Z^p$ and $z^q \in Z^q$ are cocycles and $[z^p]$ and $[z^q]$ are the corresponding cosets. Recall in addition that a CW complex X is triangulable if there is a simplicial complex K such that each skeleton X_p of X is triangulated by a subcomplex of K of dimension at most p, which we denote K_p. The cup product then follows from the identity

$$\langle c^p \cup c^q, e_{p+q}\rangle = \sum_{\sigma_{p+q} \preceq e_{p+q}} \langle c^p \cup c^q, \sigma_{p+q}\rangle, \tag{23}$$

where the sum extends over the $(p+q)$-simplices in a triangulation of e_{p+q}, the cup product on the right had side is the simplicial cup product (20), and the cochains on the right-hand side are inclusions into K of the cochains on the left-hand side. It is immediate from this definition that bilinearity, associativity and the coboundary formula extend to triangulable CW complexes. A cap product can also be defined as a homomorphism $\cap : C^p \otimes C_{p+q} \to C_q$ such that $e^p \cap e_{p+q}$ is the unique cell e_q such that $e^p \cup e^q = e^{p+q}$. The boundary formula

$$\partial(c^p \cap c_{p+q}) = (-1)^q(\delta c^p \cap c_{p+q}) + c^p \cap \partial c_{p+q} \tag{24}$$

and the associativity property

$$c^p \cap (c^q \cap c_{p+q+r}) = (c^p \cup c^q) \cap c_{p+q+r} \tag{25}$$

follow readily from the definition (cf., e.g., [34], §66).

Matrix representations of the boundary and coboundary operators are often useful in applications. Let E_p be the set of all oriented p-cells of X. In general we shall have a linear relation of the form

$$(\partial_p c_p)(e_{p-1}) = \sum_{e_p \in E_p} L_p(e_{p-1}, e_p)c_p(e_p), \tag{26}$$

where the function $L_p : E_{p-1} \times E_p \to \mathbb{Z}$ is banded. In particular $L_p(e_{p-1}, e_p)$ is the value at e_{p-1} of the chain obtained by applying the boundary operator to the elementary chain e_p. By duality, the coboundary operator follows simply as

$$(\delta^{p-1}c^{p-1})(e_p) = \sum_{e_{p-1} \in E_{p-1}} L_p(e_{p-1}, e_p)c^{p-1}(e_{p-1}). \tag{27}$$

Hence, $L_p(e_{p-1}, e_p)$ is also the value at e_p of the cochain obtained by applying the coboundary operator to the elementary cochain e^{p-1}. As in the case of the boundary and coboundary operators, in the sequel we shall omit the dimensional label from the matrices L_p whenever it can be deduced from the context.

In the special case of lattice complexes, the functions L can be given more explicit indexed representations. Start by giving the cells of the lattice complex translation-invariant orientations. Introduce an equivalence relation T in C_p that identifies two chains when one can be obtained from the other by a translation. Denote by $[c_p]$ the equivalence class of c_p and by C_p/T the quotient set of equivalence classes. By translation invariance, the equivalence class $[e_p]$ of a p-cell can be indexed as a Bravais lattice, and the lattices of all p-cell classes jointly define a complex Bravais lattice. Thus, a p-cell in an n-dimensional lattice complex can be indexed as $e_p(l, \alpha)$, where $l \in \mathbb{Z}^n$, $\alpha \in \{1, \ldots, N_p\}$, and N_p is the number of simple p-cell sublattices. Using this indexing, lattice chains and cochains have the representation

$$c_p = \sum_{l\in\mathbb{Z}^n} \sum_{\alpha=1}^{N_p} c_p(l, \alpha) e_p(l, \alpha), \tag{28a}$$

$$c^p = \sum_{l\in\mathbb{Z}^n} \sum_{\alpha=1}^{N_p} c^p(l, \alpha) e^p(l, \alpha), \tag{28b}$$

where we write $c_p(l, \alpha) \equiv c_p\big(e_p(l, \alpha)\big)$ and $c^p(l, \alpha) \equiv \langle c^p, e_p(l, \alpha)\rangle$, respectively. An application of the boundary operator to (28a) yields

$$\partial c_p = \sum_{l\in\mathbb{Z}^n} \sum_{\alpha=1}^{N_p} c_p(l, \alpha) \partial e_p(l, \alpha). \tag{29}$$

In addition, by translation invariance,

$$\partial e_p(l, \alpha) = \sum_{l'\in\mathbb{Z}^n} \sum_{\beta=1}^{N_{p-1}} L_{\alpha\beta}(l - l') e_{p-1}(l', \beta), \tag{30}$$

where the function $L_{\alpha\beta}(\cdot)$ takes integer values and has finite support. Inserting (30) into (29) yields

$$(\partial c_p)(l', \beta) = \sum_{l\in\mathbb{Z}^n} \sum_{\alpha=1}^{N_p} L_{\alpha\beta}(l - l') c_p(l, \alpha). \tag{31}$$

By duality, the coboundary operator follows likewise as

$$(\delta c^{p-1})(l, \alpha) = \sum_{l'\in\mathbb{Z}^n} \sum_{\beta=1}^{N_{p-1}} L_{\alpha\beta}(l - l') c^{p-1}(l', \beta). \tag{32}$$

It therefore follows that the matrix representation of the boundary and coboundary operators is completely determined by the coefficients $L_{\alpha\beta}(l)$ in (30).

The discrete Fourier transform provides an additional means of exploiting the translation invariance of lattice complexes. Thus, the discrete Fourier transform of the p-chain c_p is (cf., Appendix A)

$$\hat{c}_p(\theta, \alpha) = \sum_{l \in \mathbb{Z}^n} c_p(l, \alpha) \mathrm{e}^{-i\theta \cdot l}, \tag{33}$$

and its inverse is

$$c_p(l, \alpha) = \frac{1}{(2\pi)^n} \int_{[-\pi,\pi]^n} \hat{c}_p(\theta, \alpha) \mathrm{e}^{i\theta \cdot l} d\theta. \tag{34}$$

Since chains take nonzero values over finitely many cells, the sum (33) also contains finitely many terms and $\hat{c}_p(\cdot, \alpha) \in C^\infty([-\pi, \pi]^n)$. As noted in Appendix A, $c_p(-l, \alpha)$ is the Fourier-series coefficient of $\hat{c}_p(\theta, \alpha)$, and hence the discrete Fourier transform defines an isomorphism ϕ_p between C_p and the group $\hat{C}_p$ of functions from $[-\pi, \pi]^n$ to $\mathbb{C}^{N_p}$ that have finitely-many nonzero integer Fourier-series coefficients. Let $\hat{C}^p = \mathrm{Hom}(\hat{C}_p, \mathbb{Z})$. We define the discrete Fourier transform of co-chains $\phi^p : C^p \to \hat{C}^p$ as the dual isomorphism of ϕ_p^{-1}, i.e., by the relation $\phi^p(c^p) = c^p \circ \phi_p^{-1}$, or, equivalently, by the identity

$$\langle c^p, c_p \rangle = \langle \hat{c}^p, \hat{c}_p \rangle, \tag{35}$$

Parseval's identity then yields the representation of ϕ^p:

$$\hat{c}^p(\theta, \alpha) = \sum_{l \in \mathbb{Z}^n} c^p(l, \alpha) \mathrm{e}^{-i\theta \cdot l}, \tag{36}$$

and the representation of its inverse:

$$c^p(l, \alpha) = \frac{1}{(2\pi)^n} \int_{[-\pi,\pi]^n} \hat{c}^p(\theta, \alpha) \mathrm{e}^{i\theta \cdot l} d\theta. \tag{37}$$

Thus, $c^p(-l, \alpha)$ is the Fourier-series coefficient of $\hat{c}^p(\theta, \alpha)$, and hence $\hat{C}^p$ can be identified with the group of functions from $[-\pi, \pi]^n$ to $\mathbb{C}^{N_p}$ that have (possibly infinitely-many nonzero) integer Fourier-series coefficients. We define the boundary operator $\hat{\partial}_p : \hat{C}_p \to \hat{C}_{p-1}$ so that ϕ_p defines a chain map between the chain complexes $\mathcal{C} = \{C_p, \partial_p\}$ and $\hat{\mathcal{C}} = \{\hat{C}_p, \hat{\partial}_p\}$, i.e., by enforcing the identity: $\hat{\partial}_p \circ \phi_p = \phi_{p-1} \circ \partial_p$ for all $p \geqq 1$ (cf., e.g., [34], § 13, for a general for the definition of a chain map). The group $\hat{H}_p = \ker \hat{\partial}_p / \mathrm{im} \hat{\partial}_{p+1}$ is the pth homology group of the chain complex $\hat{\mathcal{C}}$. Since ϕ^p is the dual of ϕ_p, it is a cochain map, and the coboundary operator follows equivalently as the dual of $\hat{\partial}_p$ or from the identity $\hat{\delta}^p \circ \phi^p = \phi^{p+1} \circ \delta^p$. The group $\hat{H}^p = \ker \hat{\delta}^p / \mathrm{im} \hat{\delta}^{p-1}$ is the pth cohomology group of the chain complex $\hat{\mathcal{C}}$.

Since ϕ is an isomorphism, it defines a chain equivalence and induces a homology isomorphism between $\mathcal{C}$ and $\hat{\mathcal{C}}$. It therefore follows that $\hat{\mathcal{C}}$ can be used interchangeably in place of $\mathcal{C}$ in order to compute the homology of X. This is significant in practice, since the operators $\hat{\partial}$ and $\hat{\delta}$ are pointwise algebraic operators. Thus,

applying the discrete Fourier transform to both sides of (31) and invoking the convolution theorem (cf., Appendix A) we obtain

$$\hat{\partial}\hat{c}_p(\theta, \beta) = \sum_{\alpha=1}^{N_p} P_{\beta\alpha}(\theta)\hat{c}_p(\theta, \alpha), \tag{38}$$

where we write

$$P_{\beta\alpha}(\theta) = \sum_{l\in\mathbb{Z}^n} L_{\alpha\beta}(l)\mathrm{e}^{i\theta\cdot l}. \tag{39}$$

By duality we immediately have

$$\hat{\delta}\hat{c}^{p-1}(\theta, \alpha) = \sum_{\beta=1}^{N_{p-1}} Q_{\alpha\beta}(\theta)\hat{c}^{p-1}(\theta, \beta), \tag{40}$$

where we write

$$Q_{\alpha\beta}(\theta) = P^*_{\beta\alpha}(\theta). \tag{41}$$

Thus, the matrices $P_p(\theta)$ represent the boundary operators $\hat{\partial}_p$, whereas their hermitian transpose $Q_p(\theta)$ represent the coboundary operators $\hat{\delta}^{p-1}$. In particular, the verification that the lattice complex is perfect reduces to the investigation of the kernels and images of the matrices P_p, namely, for fixed $\theta \neq 0$ and $p \geqq 1$, we must have $\ker P_p = \mathrm{im} P_{p+1}$. Then it follows that $B_p = Z_p$ and $H_p = 0$, as required.

2.3. Examples of lattice complexes

In this section we collect the chain complex representations of: the monatomic chain, the square lattice, the hexagonal lattice, the simple cubic (SC) lattice, the face-centered cubic (FCC) lattice and the body-centered cubic (BCC) lattice. The monatomic chain, the square lattice, the hexagonal lattice, and the SC lattice are discussed mainly for purposes of illustration. The square, SC and FCC lattices furnish examples of lattice complexes which are not simplicial. α-Polonium has the SC structure, which is otherwise rare. Metals which crystallize in the FCC class at room temperature include: Aluminum, copper, gold, lead, nickel, platinum, rhodium, silver and thorium; whereas metals which crystallize in the BCC class at room temperature include: Chromium, iron, lithium, molybdenum, niobium, potassium, rubidium, sodium, tantalum, tungsten and vanadium. We recall that the symmetry group of cubic crystals is the octahedral group $\mathcal{O}$, which is of order 24 and is generated by the transformations $\{E, C_2(6), C_3, C_3^2(8), C_4, C_4^3(6), C_4^2(3)\}$, where E is the identity and C_2, C_3 and C_4 are the abelian groups of rotations about 2, 3 and 4-fold axes [16].

The homology of these lattices is most readily analyzed with the aid of the matrix representations $P_p(\theta)$ and $Q_p(\theta)$ of the operators $\hat{\partial}_p$ and $\hat{\delta}^{p-1}$, respectively. In all of the examples collected below, the following properties are readily verified, e.g., with the aid of the singular-value decomposition of P_p:

(i) $P_p P_{p+1} = 0$, $1 \leqq p < n$, as required by the identity $\partial_p \circ \partial_{p+1} = 0$.
(ii) $Q_{p+1} Q_p = 0$, $1 \leqq p < n$, as required by the identity $\delta^p \circ \delta^{p-1} = 0$.
(iii) The complexes are connected, and hence $H_0 = \mathbb{Z}$.
(iv) $\hat{Z}_p = \ker P_p = \operatorname{im} P_{p+1} = \hat{B}_p$, $1 \leqq p < n$, and hence $\hat{H}_p = 0$.
(v) $\hat{Z}_n = \ker P_n = 0$, and hence $\hat{H}_n = 0$.
(vi) $\hat{Z}^0 = \ker Q_1 = 0$, and hence $\hat{H}^0 = 0$.
(vii) $\hat{Z}^p = \ker Q_{p+1} = \operatorname{im} Q_p = \hat{B}^p$, $1 \leqq p < n$, and hence $\hat{H}^p = 0$.

In particular, properties (iii)–(v) imply that the lattices are perfect, as required.

2.3.1. The monatomic chain. The most elementary example of a Bravais complex is the monatomic chain, whose simplicial complex representation is shown in Fig. 2. It is clear that the union of the cells in the complex is $\mathbb{R}$, as required. In addition, the symmetry group $\mathcal{S}$ reduces to $\{E, I\}$, where E is the identity and I the inversion, and the lattice complex is clearly translation and symmetry invariant. In this simple case, both the 0 and 1-cells can be indexed as Bravais lattices. The obvious indexing scheme is that which is shown in Fig. 2. The boundary and coboundary operators are determined by the identities

$$\partial e_1(l) = e_0(l+1) - e_0(l), \tag{42a}$$
$$\delta e^0(l) = e^1(l-1) - e^1(l), \tag{42b}$$

and their DFT representation (39) reduces to

$$Q = \mathrm{e}^{i\theta} - 1. \tag{43}$$

The monatomic lattice provides a simple illustration of the properties of the simplicial cup product (20). Thus, ordering the vertices from left to right, the resulting non-zero products are

$$e^0(l) \cup e^0(l) = e^0(l), \tag{44a}$$
$$e^0(l) \cup e^1(l) = e^1(l), \tag{44b}$$
$$e^1(l) \cup e^0(l+1) = e^1(l). \tag{44c}$$

Associativity and the coboundary formula are readily verified from this table. However, $e^1(l) \cup e^0(l) = 0$ and $e^0(l+1) \cup e^1(l) = 0$, which spoils anti-commutativity. If, by way of contrast, we order the vertices from right to left, then the resulting non-zero products are

$$e^0(l) \cup e^0(l) = e^0(l), \tag{45a}$$
$$e^0(l+1) \cup e^1(l) = e^1(l), \tag{45b}$$
$$e^1(l) \cup e^0(l) = e^1(l), \tag{45c}$$

which illustrates the dependence of the cup product on the ordering of the vertices.

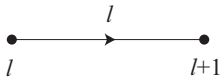

Fig. 2. Lattice complex representation of the monatomic chain and indexing scheme.

2.3.2. The square lattice. The square Bravais lattice is generated by the basis $\{(a, 0), (0, a)\}$ and its symmetry group is C_4, the abelian group of two-dimensional rotations by $\pi/2$. The lattice complex representation of the square lattice is shown in Fig. 3. The square lattice furnishes an example of a lattice complex that is not simplicial. The connectedness, and translation and symmetry invariance requirements are satisfied by choosing the elementary areas to be squares, as shown in Fig. 3. It is evident from this figure that the vertex and elementary area sets can be indexed as two-dimensional Bravais lattices. By contrast, there are two types of elementary segments, namely, horizontal segments and vertical segments. Hence, the segment set has the structure of a complex Bravais lattice comprising two simple sublattices. We choose the indexing scheme shown in Fig. 3, where $\varepsilon_1 = (1, 0)$ and $\varepsilon_2 = (0, 1)$. The boundary and coboundary operators are determined by the rules

$$\partial e_1(l, 1) = e_0(l + \varepsilon_1) - e_0(l), \tag{46a}$$

$$\partial e_2(l) = e_1(l, 1) + e_1(l + \varepsilon_1, 2) - e_1(l + \varepsilon_2, 1) - e_1(l, 2), \tag{46b}$$

$$\delta e^0(l) = -e^1(l, 1) - e^1(l, 2) + e^1(l - \varepsilon_1, 1) + e^1(l - \varepsilon_2, 2), \tag{46c}$$

$$\delta e^1(l, 1) = e^2(l) - e^2(l - \varepsilon_2), \tag{46d}$$

and all the symmetry-related identities. The corresponding DFT representation (39) is

$$Q_1 = \left(\mathrm{e}^{i\theta_1} - 1, \mathrm{e}^{i\theta_2} - 1\right), \tag{47a}$$

$$Q_2 = \begin{pmatrix} 1 - \mathrm{e}^{i\theta_2} \\ \mathrm{e}^{i\theta_1} - 1 \end{pmatrix}. \tag{47b}$$

A cup product can be defined by multiplying cells in the 1-skeleton, as in the monatomic chain, and appending the following non-zero products:

$$e^1(l, 1) \cup e^1(l + \varepsilon_1, 2) = e^2(l), \tag{48a}$$

$$e^1(l, 2) \cup e^1(l + \varepsilon_2, 1) = -e^2(l), \tag{48b}$$

$$e^0(l) \cup e^2(l) = e^2(l), \tag{48c}$$

$$e^2(l) \cup e^0(l + \varepsilon_1 + \varepsilon_2) = e^2(l). \tag{48d}$$

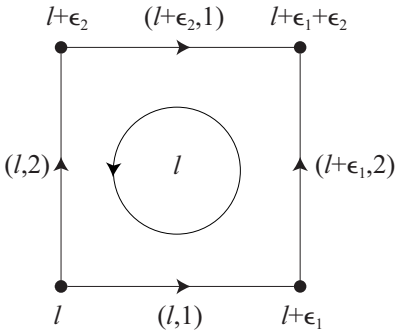

Fig. 3. Lattice complex representation of the square lattice and indexing scheme.

It is straightforward to verify that this product is associative and satisfies the coboundary formula (21). It is also interesting to note that every 2-cell is generated in two different ways by the multiplication of two pairs of 1-cells. In addition there are exactly two vertices which act on a 2-cell, one on the left and the other on the right.

2.3.3. The hexagonal lattice. The hexagonal lattice is generated by the basis $\{(a, 0), (a/2, \sqrt{3}a/2)\}$ and its symmetry group is C_6, the abelian group of two-dimensional rotations by $\pi/3$. The lattice complex representation of the hexagonal lattice is shown in Fig. 4. It is evident from this figure that there are three types of elementary segments and two types of elementary areas. Hence, the elementary segment and area sets have the structure of complex lattices comprising three and two simple sublattices, respectively. We choose the indexing scheme shown in Fig. 4, where $\varepsilon_1 = (1, 0)$, $\varepsilon_2 = (0, 1)$ and $\varepsilon_3 = \varepsilon_2 - \varepsilon_1 = (-1, 1)$. The boundary and coboundary operators are determined by the rules

$$\partial e_1(l, 1) = e_0(l + \varepsilon_1) - e_0(l), \tag{49a}$$

$$\partial e_2(l, 1) = e_1(l, 1) + e_1(l + \varepsilon_1, 3) - e_1(l, 2), \tag{49b}$$

$$\begin{aligned}\delta e^0(l) = {} & -e^1(l, 1) - e^1(l, 2) - e^1(l, 3) \\ & + e^1(l - \varepsilon_1, 1) + e^1(l - \varepsilon_2, 2) + e^1(l - \varepsilon_3, 3),\end{aligned} \tag{49c}$$

$$\delta e^1(l, 1) = e^2(l, 1) - e^2(l - \varepsilon_3, 2), \tag{49d}$$

and all symmetry-related identities. The corresponding DFT representation (39) is

$$Q_1 = (\mathrm{e}^{i\theta_1} - 1, \mathrm{e}^{i\theta_2} - 1, \mathrm{e}^{i\theta_3} - 1), \tag{50a}$$

$$Q_2 = \begin{pmatrix} 1 & -\mathrm{e}^{i\theta_3} \\ -1 & 1 \\ \mathrm{e}^{i\theta_1} & -1 \end{pmatrix}, \tag{50b}$$

where $\theta_3 = \theta_2 - \theta_1$. A cup product can be defined by adopting the partial ordering of the vertices implied by the orientation of the 1-cells. Cells in the 1-skeleton are

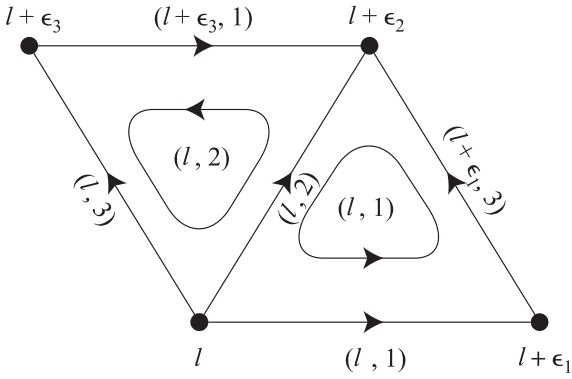

Fig. 4. Lattice complex representation of a hexagonal lattice and indexing scheme.

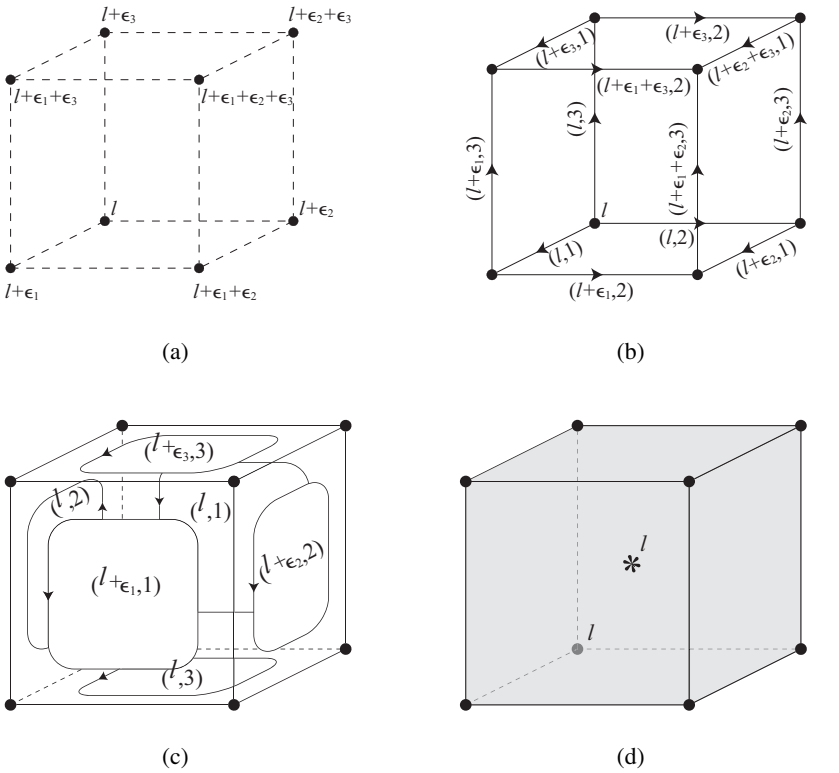

Fig. 5. Lattice complex representation of the simple-cubic lattice and indexing scheme. (a) Vertex set. (b) Elementary segment set. (c) Elementary area set. (d) Elementary volume set.

multiplied as in the monatomic chain. The remaining non-zero products are

$$e^0(l) \cup e^2(l,1) = e^2(l,1), \tag{51a}$$
$$e^2(l,1) \cup e^0(l+\varepsilon_2) = e^2(l,1), \tag{51b}$$
$$e^0(l) \cup e^2(l,2) = -e^2(l,2), \tag{51c}$$
$$e^2(l,2) \cup e^0(l+\varepsilon_2) = -e^2(l,2), \tag{51d}$$
$$e^1(l,1) \cup e^1(l+\varepsilon_1,3) = e^2(l,1), \tag{51e}$$
$$e^1(l,3) \cup e^1(l+\varepsilon_3,1) = -e^2(l,2). \tag{51f}$$

It is interesting to note that there is exactly one pair of 1-cells which generates each 1-cell by multiplication. Likewise, there is one vertex which operates on each 1-cell from the left, and another which operates from the right.

2.3.4. The simple cubic lattice. The simple-cubic (SC) Bravais lattice is generated by the basis $\{(a,0,0),(0,a,0),(0,0,a)\}$. The lattice complex representation

of the SC lattice is shown in Fig. 5. The cubic lattice furnishes an example of a three-dimensional lattice complex that is CW but not simplicial. The connectedness, and translation and symmetry invariance requirements are satisfied by choosing the elementary volumes to be cubes, as shown in Fig. 5c. It is evident from this figure that the vertex and elementary volume sets can be indexed as three-dimensional Bravais lattices. We also note that there are three types of elementary segments, along each of the cube directions, and three types of elementary areas. Hence, the segment and area sets have the structure of complex lattices comprising of three simple sublattices each. We choose the indexing scheme shown in Fig. 5, where $\varepsilon_1 = (1, 0, 0)$, $\varepsilon_2 = (0, 1, 0)$, and $\varepsilon_3 = (0, 0, 1)$. The boundary and coboundary operators are determined by the rules

$$\partial e_1(l, 1) = e_0(l + \varepsilon_1) - e_0(l), \tag{52a}$$

$$\partial e_2(l, 1) = e_1(l, 2) + e_1(l + \varepsilon_2, 3) - e_1(l + \varepsilon_3, 2) - e_1(l, 3), \tag{52b}$$

$$\begin{aligned}\partial e_3(l) = {} & e_2(l + \varepsilon_1, 1) - e_2(l, 1) + e_2(l + \varepsilon_2, 2) - e_2(l, 2) \\ & + e_2(l + \varepsilon_3, 3) - e_2(l, 3),\end{aligned} \tag{52c}$$

$$\begin{aligned}\delta e^0(l) = {} & -e^1(l, 1) - e^1(l, 2) - e^1(l, 3) + e^1(l - \varepsilon_1, 1) \\ & + e^1(l - \varepsilon_2, 2) + e^1(l - \varepsilon_3, 3),\end{aligned} \tag{52d}$$

$$\delta e^1(l, 1) = -e^2(l, 2) + e^2(l - \varepsilon_3, 2) + e^2(l, 3) - e^2(l - \varepsilon_2, 3), \tag{52e}$$

$$\delta e^2(l, 1) = -e^3(l) + e^3(l - \varepsilon_1), \tag{52f}$$

and all the symmetry-related identities. The corresponding DFT representation (39) is

$$Q_1 = \left(\mathrm{e}^{i\theta_1} - 1, \mathrm{e}^{i\theta_2} - 1, \mathrm{e}^{i\theta_3} - 1\right), \tag{53a}$$

$$Q_2 = \begin{pmatrix} 0, & \mathrm{e}^{i\theta_3} - 1, & 1 - \mathrm{e}^{i\theta_2} \\ 1 - \mathrm{e}^{i\theta_3}, & 0, & \mathrm{e}^{i\theta_1} - 1 \\ \mathrm{e}^{i\theta_2} - 1, & 1 - \mathrm{e}^{i\theta_1}, & 0 \end{pmatrix}, \tag{53b}$$

$$Q_3 = \begin{pmatrix} \mathrm{e}^{i\theta_1} - 1 \\ \mathrm{e}^{i\theta_2} - 1 \\ \mathrm{e}^{i\theta_3} - 1 \end{pmatrix}. \tag{53c}$$

A cup product can be defined by multiplying cells in the 2-skeleton, as in the square lattice, and appending the following non-zero products:

$$e^2(l, 1) \cup e^1(l + \varepsilon_2 + \varepsilon_3, 1) = e^3(l), \tag{54a}$$

$$e^1(l, 1) \cup e^2(l + \varepsilon_1, 1) = e^3(l), \tag{54b}$$

$$e^2(l, 2) \cup e^1(l + \varepsilon_1 + \varepsilon_3, 2) = e^3(l), \tag{54c}$$

$$e^1(l, 2) \cup e^2(l + \varepsilon_2, 2) = e^3(l), \tag{54d}$$

$$e^0(l) \cup e^3(l) = e^3(l), \tag{54e}$$

$$e^3(l) \cup e^0(l + \varepsilon_1 + \varepsilon_2 + \varepsilon_3) = e^3(l). \tag{54f}$$

It is straightforward to verify that this product is associative and satisfies the coboundary formula (21). As in the case of the square lattice, it is also interesting

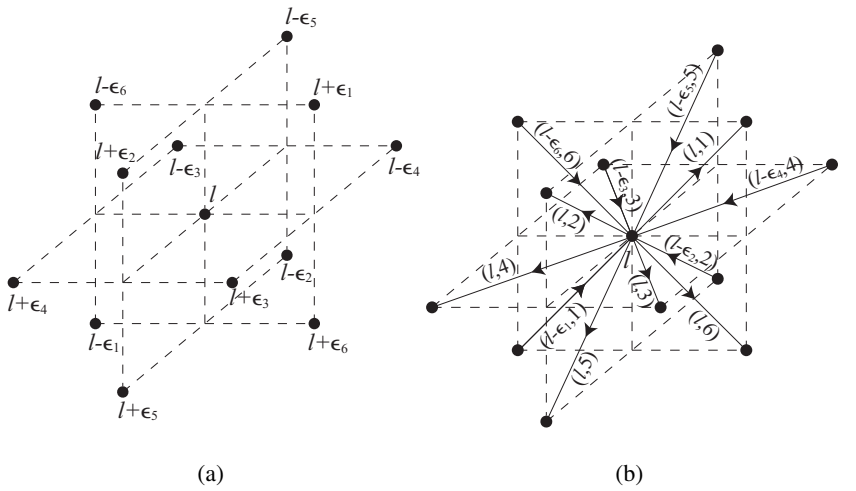

Fig. 6. Lattice complex representation of the face-centered cubic lattice and indexing scheme. (a) Vextex set. (b) Elementary segment set.

to note that every 3-cell is generated in four different ways by the multiplication of certain pairs of 1 and 2-cells. In addition there are exactly two vertices which act on a 3-cell, one on the left and the other on the right.

2.3.5. The face-centered cubic lattice. The face-centered cubic (FCC) Bravais lattice is generated by the basis $\{(0, a/2, a/2),\ (a/2, 0, a/2),\ (a/2, a/2, 0)\}$. A lattice complex representation of the FCC lattice is shown in Figs. 6, 7 and 8. The complex is chosen so as to contain the commonly observed $\frac{1}{2}\langle 110\rangle$ slip directions and $\{111\}$ slip planes. It is evident from the figures that the vertex set can be indexed as a simple lattice; the elementary segment set as a complex lattice comprising six simple sublattices; the elementary area set as a complex lattice comprising eight simple sublattices; and the elementary volume set as a complex lattice comprising of three sublattices. We choose the indexing scheme, shown in Figs. 6, 7 and 8, where $\varepsilon_1 = (1, 0, 0)$, $\varepsilon_2 = (0, 1, 0)$, $\varepsilon_3 = (0, 0, 1)$, $\varepsilon_4 = \varepsilon_2 - \varepsilon_1 = (-1, 1, 0)$, $\varepsilon_5 = \varepsilon_3 - \varepsilon_1 = (-1, 0, 1)$ and $\varepsilon_6 = \varepsilon_3 - \varepsilon_2 = (0, -1, 1)$. The boundary and coboundary operators are determined by the rules

$$\partial e_1(l, 1) = e_0(l + \varepsilon_1) - e_0(l), \tag{55a}$$

$$\partial e_2(l, 1) = e_1(l, 5) - e_1(l + \varepsilon_6, 4) - e_1(l, 6), \tag{55b}$$

$$\begin{aligned}\partial e_3(l, 1) = {} & e_2(l + \varepsilon_2, 1) + e_2(l + \varepsilon_2, 4) + e_2(l + \varepsilon_2, 6) + e_2(l + \varepsilon_2, 8) \\ & - e_2(l + \varepsilon_5, 5) - e_2(l + \varepsilon_5, 7) - e_2(l + \varepsilon_5, 2) - e_2(l + \varepsilon_5, 3),\end{aligned} \tag{55c}$$

$$\partial e_3(l, 2) = e_2(l + \varepsilon_6, 3) - e_2(l + \varepsilon_3, 6) + e_2(l + \varepsilon_5, 7) - e_2(l, 1), \tag{55d}$$

$$\begin{aligned}\delta e^0(l) = {} & -e^1(l, 1) - e^1(l, 2) - e^1(l, 3) - e^1(l, 4) \\ & - e^1(l, 5) - e^1(l, 6), + e^1(l - \varepsilon_1, 1) + e^1(l - \varepsilon_2, 2) \\ & + e^1(l - \varepsilon_3, 3) + e^1(l - \varepsilon_4, 4) + e^1(l - \varepsilon_5, 5) + e^1(l - \varepsilon_6, 6),\end{aligned} \tag{55e}$$

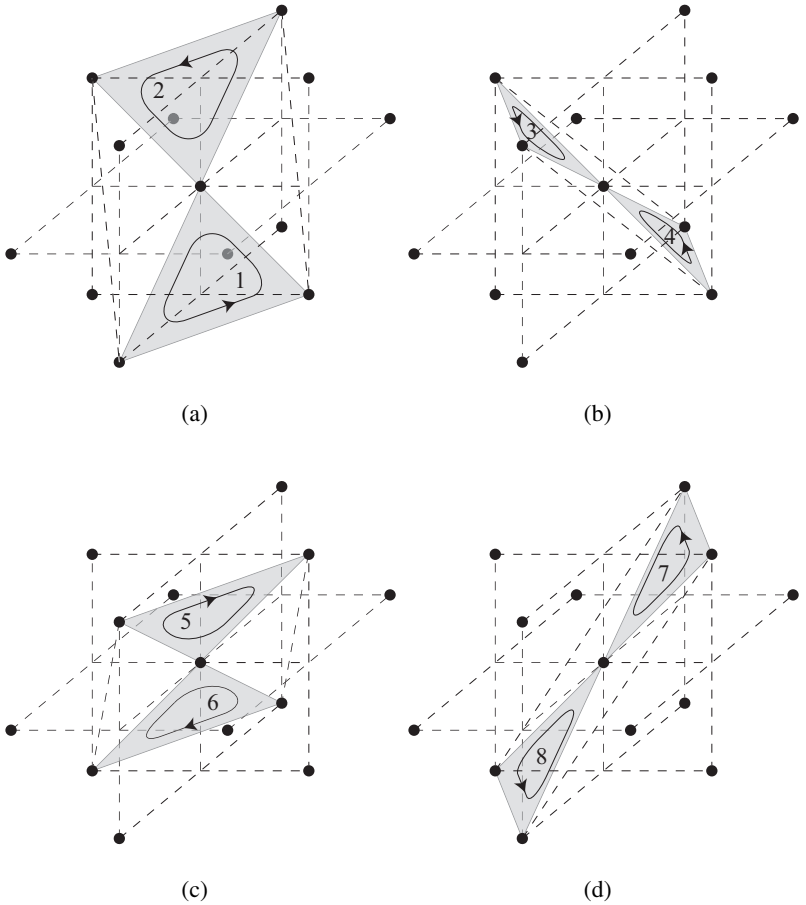

Fig. 7. Lattice complex representation of the face-centered cubic lattice and indexing scheme. Elementary area set.

$$\delta e^1(l,1) = e^2(l,7) - e^2(l+\varepsilon_1,8) - e^2(l,5) + e^2(l+\varepsilon_1,6), \tag{55f}$$
$$\delta e^2(l,1) = e^3(l-\varepsilon_2,1) - e^3(l,2), \tag{55g}$$

and all symmetry-related identities. The corresponding DFT representation (39) is

$$Q_1 = (\mathrm{e}^{i\theta_1}-1, \mathrm{e}^{i\theta_2}-1, \mathrm{e}^{i\theta_3}-1, \mathrm{e}^{i\theta_4}-1, \mathrm{e}^{i\theta_5}-1, \mathrm{e}^{i\theta_6}-1), \tag{56a}$$

$$Q_2 = \begin{pmatrix} 0 & 0 & 0 & 0 & -1 & \mathrm{e}^{-i\theta_1} & 1 & -\mathrm{e}^{-i\theta_1} \\ 0 & 0 & -1 & \mathrm{e}^{-i\theta_2} & 1 & -\mathrm{e}^{-i\theta_2} & 0 & 0 \\ 0 & 0 & \mathrm{e}^{-i\theta_6} & -\mathrm{e}^{-i\theta_2} & 0 & 0 & -\mathrm{e}^{-i\theta_5} & \mathrm{e}^{-i\theta_1} \\ -\mathrm{e}^{i\theta_6} & \mathrm{e}^{-i\theta_5} & 0 & 0 & -\mathrm{e}^{i\theta_1} & \mathrm{e}^{-i\theta_2} & 0 & 0 \\ 1 & -\mathrm{e}^{-i\theta_5} & 0 & 0 & 0 & 0 & \mathrm{e}^{-i\theta_5} & -1 \\ -1 & \mathrm{e}^{-i\theta_6} & -\mathrm{e}^{-i\theta_6} & 1 & 0 & 0 & 0 & 0 \end{pmatrix}, \tag{56b}$$

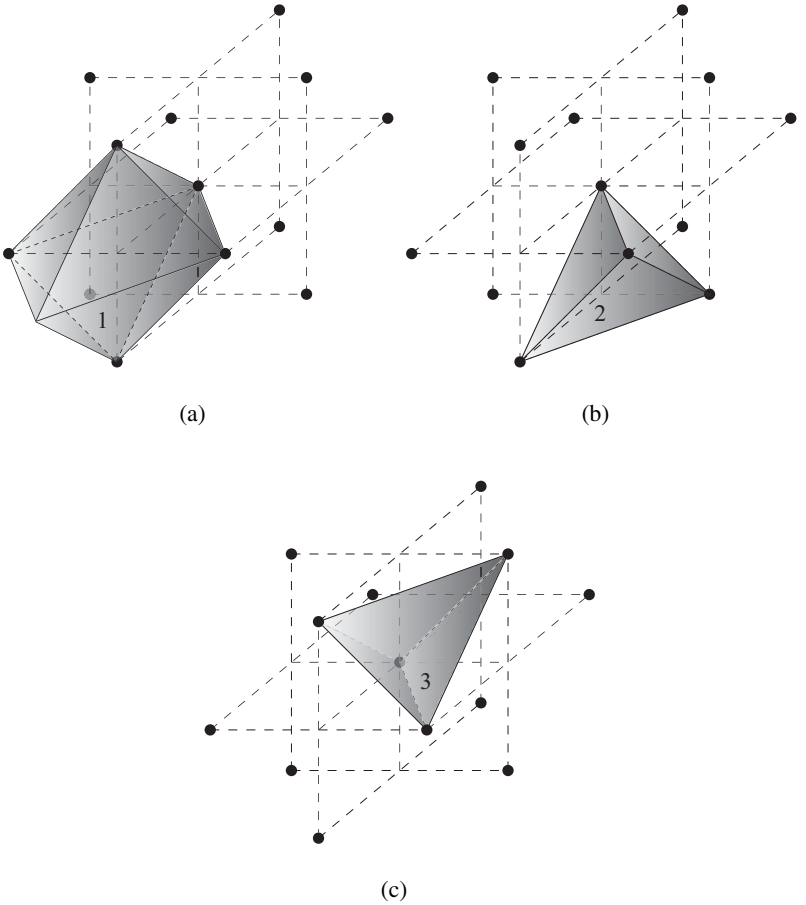

Fig. 8. Lattice complex representation of the face-centered cubic lattice and indexing scheme. Elementary volume set.

$$Q_3 = \begin{pmatrix} e^{i\theta_2} & -1 & 0 \\ -e^{i\theta_5} & 0 & e^{i\theta_3} \\ -e^{i\theta_5} & e^{i\theta_6} & 0 \\ e^{i\theta_2} & 0 & -e^{i\theta_2} \\ -e^{i\theta_5} & 0 & 1 \\ e^{i\theta_2} & -e^{i\theta_3} & 0 \\ -e^{i\theta_5} & e^{i\theta_5} & 0 \\ e^{i\theta_2} & 0 & -e^{i\theta_1} \end{pmatrix}. \tag{56c}$$

A cup product can be defined by multiplying cells in the 2-skeleton, as in the hexagonal lattice, and appending the following non-zero products:

$$e^2(l+\varepsilon_2,6)\cup e^1(l+\varepsilon_2,5)=e^3(l,1), \tag{57a}$$
$$e^2(l+\varepsilon_2,4)\cup e^1(l+\varepsilon_3,4)=e^3(l,1), \tag{57b}$$
$$e^2(l+\varepsilon_5,2)\cup e^1(l+\varepsilon_5,2)=e^3(l,1), \tag{57c}$$
$$e^2(l+\varepsilon_5,7)\cup e^1(l+\varepsilon_3,4)=e^3(l,1), \tag{57d}$$
$$e^2(l,1)\cup e^1(l+\varepsilon_5,1)=e^3(l,2), \tag{57e}$$
$$e^0(l)\cup e^3(l,1)=e^3(l,1), \tag{57f}$$
$$e^3(l,1)\cup e^0(l+\varepsilon_3+\varepsilon_4)=e^3(l,1), \tag{57g}$$
$$e^0(l)\cup e^3(l,2)=e^3(l,2), \tag{57h}$$
$$e^3(l,2)\cup e^0(l+\varepsilon_3)=e^3(l,2), \tag{57i}$$

and others related to these by symmetry. A straightforward calculation shows that this product is associative and satisfies the coboundary formula (21). The non-simplicial cell is obtained by the multiplication of four pairs of 1 and 2-cells, whereas the two simplicial cells are generated by one pair each. All 3-cells are acted upon by exactly two vertices, one acting on the left and another on the right.

2.3.6. The body-centered cubic lattice. The body-centered cubic (BCC) Bravais lattice is generated by the basis $\{(-a/2, a/2, a/2),\ (a/2, -a/2, a/2),\ (a/2, a/2, -a/2)\}$. A lattice complex representation of the BCC lattice is shown in Figs. 9, 10 and 11. The complex is chosen so as to contain the $\frac{1}{2}\langle 111\rangle$ slip directions and {110} slip planes. Complexes containing other commonly observed slip planes, such as {112}, may be constructed likewise. It is evident from the figures that the vertex set can be indexed as a simple lattice; the elementary segment set as a complex lattice comprising of seven simple sublattices; the elementary area set

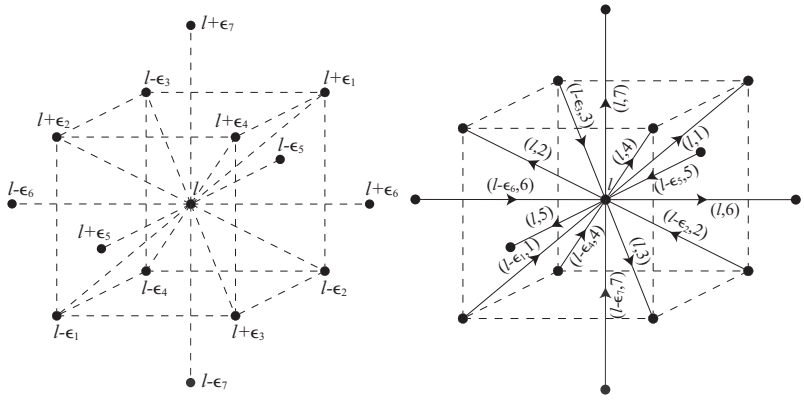

(a) (b)

Fig. 9. Lattice complex representation of the body-centered cubic lattice and complex lattice indexing scheme. (a) Vextex set. (b) Elementary segment set.

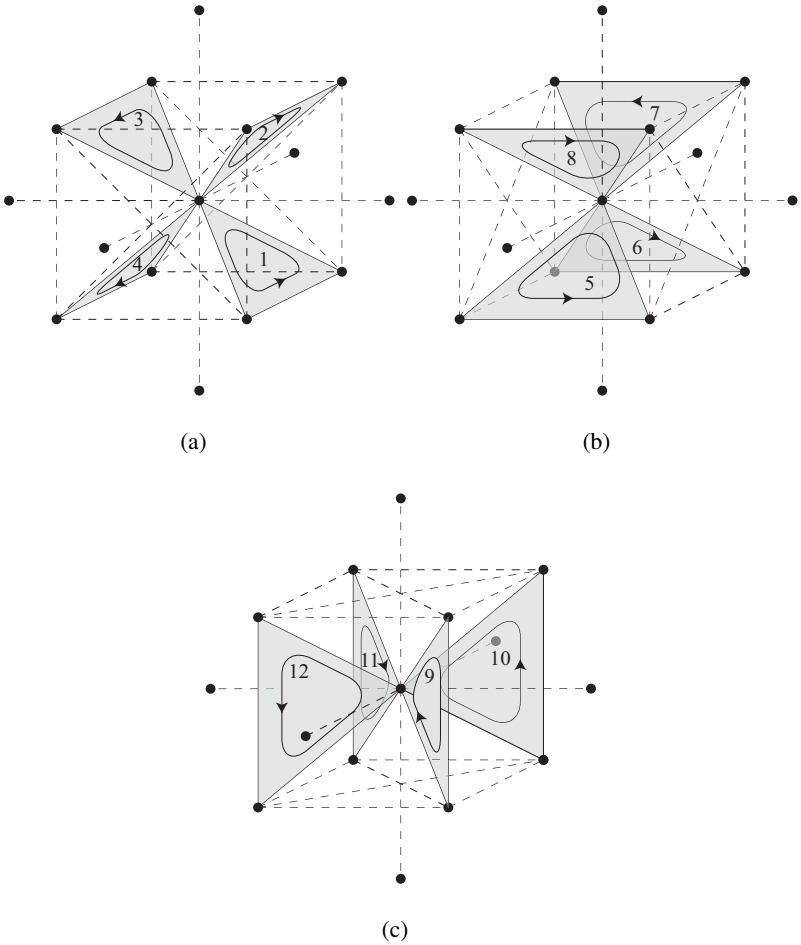

Fig. 10. Lattice complex representation of the body-centered cubic lattice and complex lattice indexing scheme. Elementary area set.

as a complex lattice comprising of twelve simple sublattices; and the elementary volume set as a complex lattice comprising of twelve sublattices. We choose the indexing scheme shown in Figs. 9, 10 and 11, where $\varepsilon_1 = (1, 0, 0)$, $\varepsilon_2 = (0, 1, 0)$, $\varepsilon_3 = (0, 0, 1)$, $\varepsilon_4 = (1, 1, 1)$, $\varepsilon_5 = (0, 1, 1)$, $\varepsilon_6 = (1, 0, 1)$ and $\varepsilon_7 = (1, 1, 0)$. The boundary and coboundary operators are determined by the rules

$$\partial e_1(l, 1) = e_0(l + \varepsilon_1) - e_0(l), \tag{58a}$$

$$\partial e_1(l, 5) = e_0(l + \varepsilon_5) - e_0(l), \tag{58b}$$

$$\partial e_2(l, 1) = -e_1(l - \varepsilon_2, 5) + e_1(l - \varepsilon_2, 2) + e_1(l, 3), \tag{58c}$$

$$\partial e_3(l, 1) = -e_2(l + \varepsilon_2, 1) + e_2(l + \varepsilon_5, 7) + e_2(l, 8) - e_2(l + \varepsilon_4, 4), \tag{58d}$$

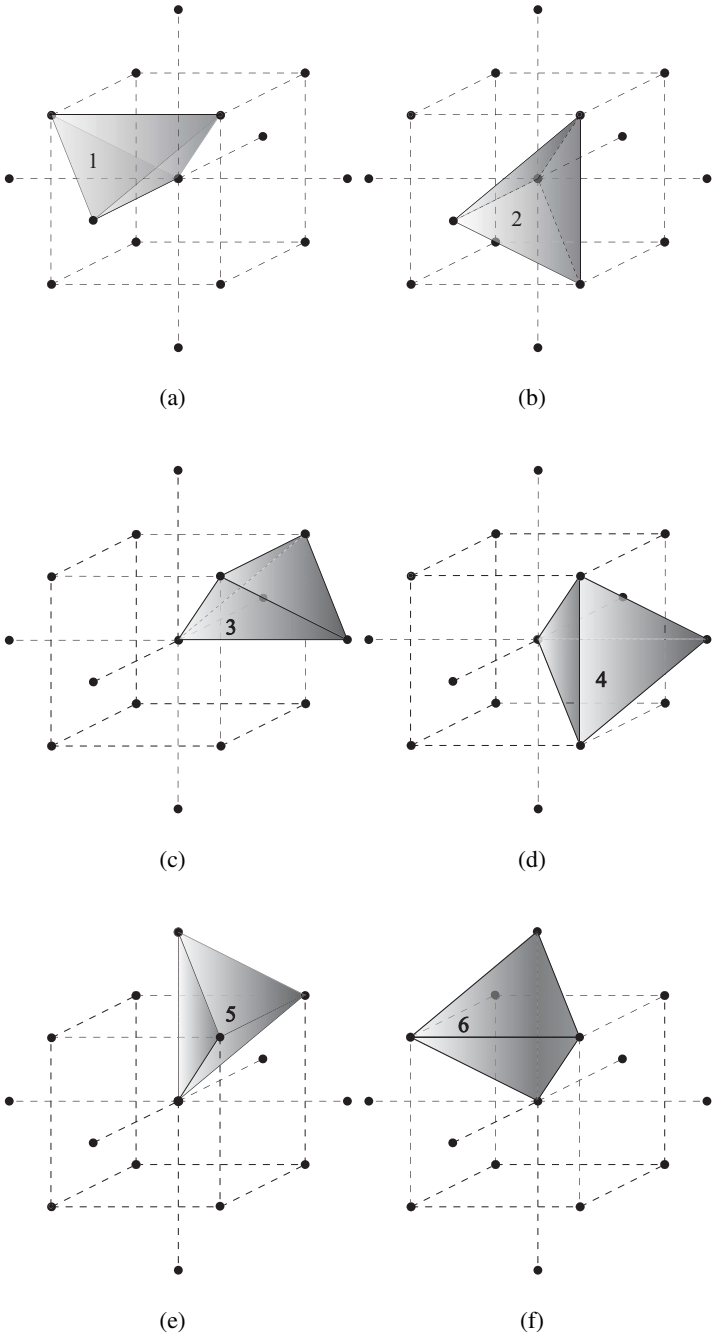

Fig. 11. Lattice complex representation of the body-centered cubic lattice and complex lattice indexing scheme. Elementary volume set.

$$\begin{aligned}
\delta e^0(l) = &-e^1(l,1) - e^1(l,2) - e^1(l,3) - e^1(l,4) \\
&-e^1(l,5) - e^1(l,6) - e^1(l,7) + e^1(l-\varepsilon_1,1) \\
&+e^1(l-\varepsilon_2,2) + e^1(l-\varepsilon_3,3) + e^1(l-\varepsilon_4,4) \\
&+e^1(l-\varepsilon_5,5) + e^1(l-\varepsilon_6,6) + e^1(l-\varepsilon_7,7), \qquad (58e)\\
\delta e^1(l,1) = &-e^2(l,2) + e^2(l+\varepsilon_1,4) - e^2(l+\varepsilon_1,5) \\
&+e^2(l,7) - e^2(l,10) + e^2(l+\varepsilon_1,12), \qquad (58f)\\
\delta e^1(l,5) = &-e^2(l+\varepsilon_2,1) - e^2(l-\varepsilon_1,2) + e^2(l+\varepsilon_3,3) \\
&+e^2(l+\varepsilon_4,4), \qquad (58g)\\
\delta e^2(l,1) = &-e^3(l-\varepsilon_2,1) + e^3(l-\varepsilon_7,5), \qquad (58h)
\end{aligned}$$

and all symmetry-related identities. The corresponding DFT representation (39) is

$$Q_1 = (\mathrm{e}^{i\theta_1} - 1, \mathrm{e}^{i\theta_2} - 1, \mathrm{e}^{i\theta_3} - 1, \mathrm{e}^{i\theta_4} - 1, \mathrm{e}^{i\theta_5} - 1, \mathrm{e}^{i\theta_6} - 1, \mathrm{e}^{i\theta_7} - 1), \qquad (59a)$$

$$Q_2 = \begin{pmatrix}
0 & -1 & 0 & \mathrm{e}^{-i\theta_1} & -\mathrm{e}^{-i\theta_1} & 0 & 1 & 0 & 0 & -1 & 0 & \mathrm{e}^{-i\theta_1} \\
\mathrm{e}^{-i\theta_2} & 0 & -1 & 0 & 0 & -\mathrm{e}^{-i\theta_2} & 0 & 1 & 0 & -\mathrm{e}^{-i\theta_2} & 0 & 1 \\
1 & 0 & -\mathrm{e}^{-i\theta_3} & 0 & -1 & 0 & \mathrm{e}^{-i\theta_3} & 0 & -1 & 0 & \mathrm{e}^{-i\theta_3} & 0 \\
0 & 1 & 0 & -\mathrm{e}^{-i\theta_4} & 0 & \mathrm{e}^{-i\theta_4} & 0 & -1 & 1 & 0 & -\mathrm{e}^{-i\theta_4} & 0 \\
-\mathrm{e}^{-i\theta_2} & -\mathrm{e}^{i\theta_1} & \mathrm{e}^{-i\theta_3} & \mathrm{e}^{-i\theta_4} & 0 & 0 & 0 & 0 & 0 & 0 & 0 & 0 \\
0 & 0 & 0 & 0 & \mathrm{e}^{-i\theta_1} & -\mathrm{e}^{-i\theta_4} & -\mathrm{e}^{-i\theta_3} & \mathrm{e}^{i\theta_2} & 0 & 0 & 0 & 0 \\
0 & 0 & 0 & 0 & 0 & 0 & 0 & 0 & -\mathrm{e}^{i\theta_3} & \mathrm{e}^{-i\theta_2} & \mathrm{e}^{-i\theta_4} & -\mathrm{e}^{-i\theta_1}
\end{pmatrix}, \qquad (59b)$$

$$Q_3 = \begin{pmatrix}
-\mathrm{e}^{i\theta_2} & 0 & 0 & 0 & \mathrm{e}^{i\theta_7} & 0 \\
0 & 0 & 1 & 0 & -1 & 0 \\
0 & -\mathrm{e}^{i\theta_3} & \mathrm{e}^{i\theta_6} & 0 & 0 & 0 \\
-\mathrm{e}^{i\theta_4} & \mathrm{e}^{i\theta_4} & 0 & 0 & 0 & 0 \\
0 & 0 & -\mathrm{e}^{i\theta_1} & 0 & 0 & \mathrm{e}^{i\theta_7} \\
0 & 0 & -\mathrm{e}^{i\theta_4} & \mathrm{e}^{i\theta_4} & 0 & 0 \\
\mathrm{e}^{i\theta_5} & 0 & 0 & -\mathrm{e}^{i\theta_3} & 0 & 0 \\
1 & 0 & 0 & 0 & 0 & -1 \\
0 & 1 & 0 & -1 & 0 & 0 \\
0 & \mathrm{e}^{i\theta_5} & 0 & 0 & 0 & -\mathrm{e}^{i\theta_2} \\
0 & 0 & 0 & 0 & -\mathrm{e}^{i\theta_4} & \mathrm{e}^{i\theta_4} \\
0 & 0 & 0 & \mathrm{e}^{i\theta_6} & -\mathrm{e}^{i\theta_1} & 0
\end{pmatrix}. \qquad (59c)$$

A cup product is induced by adopting the partial ordering of the vertices implied by the orientation of 1-cells. Cells in the 2-skeleton are multiplied as in the hexagonal complex. The remaining non-zero products are

$$\begin{aligned}
e^0(l) \cup e^3(l,1) &= e^3(l,1), \qquad (60a)\\
e^3(l,1) \cup e^0(l+\varepsilon_4) &= e^3(l,1), \qquad (60b)\\
e^2(l+\varepsilon_2,1) \cup e^1(l+\varepsilon_5,1) &= -e^3(l,1), \qquad (60c)\\
e^1(l,2) \cup e^2(l+\varepsilon_5,7) &= e^3(l,1), \qquad (60d)
\end{aligned}$$

and those obtained from these by symmetry. Again it is interesting to note the uniqueness of the representations of the 3-cells as products of their faces.

3. Calculus on lattices

The objective of this section is to develop a lattice analog of the de Rham complex in $\mathbb{R}^n$ (cf., e.g., [5]). In particular, we wish to extend to lattices the notions of forms and differential operators, as well as the theory of integration of forms and currents. This extension results in natural definitions of boundaries and generalizations of Stoke's theorem, the Hodge decomposition theorem, the Gauss linking number and other classical results and objects. As we shall see, the resulting framework is ideally suited for the development of a mechanics of lattices, with and without defects. In particular, the discrete version of the Gauss linking number which we develop in Section 3.3 provides a natural measure of the degree of entanglement of a dislocation ensemble. This entanglement contributes to the work-hardening of crystals. In addition, the discrete analog of discrete dislocations loops and Burgers circuits will be introduced in Section 5.1. As in the continuum setting, the discrete linking number also provides a natural device for relating those classes and types of objects.

3.1. The differential complex of a lattice

Consider a lattice complex X and its chain complex $\{C_p, \partial\}$. Let E_p be the set of p-cells of the lattice. A real-valued exterior differential form of order p, or a p-form, is a cochain with real coefficients. Thus, p-forms have the representation

$$\omega = \sum_{e_p \in E_p} f(e_p) e^p, \tag{61}$$

where $f : E_p \to \mathbb{R}$. Also p-forms with coefficients in an arbitrary abelian group G may be defined likewise. The case $G = \mathbb{R}^n$ will arise frequently in subsequent applications. In this context, we shall refer to the elementary p-cochains e^p as elementary p-forms, and we shall denote by Ω^p the set of p-forms over the lattice. The value of the p-form (61) on a general p-chain c_p is

$$\langle \omega, c_p \rangle = \sum_{e_p \in E_p} f(e_p) \langle e^p, c_p \rangle. \tag{62}$$

The exterior derivative of a p-form is the $(p+1)$-form

$$d\omega = \sum_{e_p \in E_p} f(e_p) \delta e^p. \tag{63}$$

Since $\delta^2 = 0$, we have immediately $d^2 = 0$. It also follows immediately from the properties of the coboundary operator that

$$\langle d\omega, c_{p+1} \rangle = \langle \omega, \partial c_{p+1} \rangle \tag{64}$$

for all p-forms $\omega \in \Omega^p$. Let now Y be a subcomplex of X. Let $\alpha, \beta \in \Omega^p$ and suppose that $\alpha_{|Y} = \beta_{|Y}$. Then,

$$\langle \alpha, \partial e_{p+1} \rangle = \langle \beta, \partial e_{p+1} \rangle \tag{65}$$

and

$$\langle d\alpha, e_{p+1}\rangle = \langle d\beta, e_{p+1}\rangle \tag{66}$$

for all $(p+1)$-cells e_{p+1} of Y. Hence, $d\alpha_{|Y} = d\beta_{|Y}$, which shows that d is a local operator. All the above definitions and operations rely solely on the abelian-group structure of $\mathbb{R}$ under addition and, therefore, extend immediately to forms with coefficients in an arbitrary abelian group G. When such an extension is necessary, we shall denote by $\Omega^p(X, G)$ the set of p-forms over X with coefficients in G.

The wedge-product of a real-valued p-form $\alpha = \sum f e^p$ and a real-valued q-form $\beta = \sum g e^q$ may be defined as the real-valued $(p+q)$-form

$$\alpha \wedge \beta = \sum_{e_p \in E_p} \sum_{e_q \in E_q} f(e_p) g(e_q) e^p \cup e^q. \tag{67}$$

The wedge product confers $\Omega^* = \oplus_{p=0}^n \Omega^p$ a graded algebra structure, and it inherits the essential properties of the cup product, namely, bilinearity, associativity, and the coboundary formula

$$d(\alpha \wedge \beta) = (d\alpha) \wedge \beta + (-1)^p \alpha \wedge (d\beta) \tag{68}$$

for all $\alpha \in \Omega^p$ and $\beta \in \Omega^q$.

The graded algebra Ω^* together with the operator d may be regarded as a discrete de Rham complex on the lattice X. A form $\alpha \in \Omega^p$ is closed if $d\alpha = 0$, and exact if there is a form $\beta \in \Omega^{p-1}$ such that $\alpha = d\beta$. The kernel of d are the closed forms and the image of d are the exact forms. The pth de Rham cohomology of X is the vector space $H^p = (\ker d \cap \Omega^p)/(\mathrm{im} d \cap \Omega^p)$. The cohomology of X is the direct sum $H^* = \oplus_{p\in\mathbb{Z}} H^p$. In $\mathbb{R}^n$, Poincaré's lemma states that $H^* = \mathbb{R}$ if $n = 0$ and $H^* = 0$ otherwise. We will require the cohomology of a perfect n-dimensional lattice to be identical to that of $\mathbb{R}^n$.

Considerations of duality lead naturally to the definition of p-vector fields and the codifferential operator. A real-valued vector field of order p, or a p-vector field, is a chain with real coefficients and arbitrary (not necessarily finite) support. Thus, p-vector fields have the representation

$$u = \sum_{e_p \in E_p} f(e_p) e_p, \tag{69}$$

where $f : E_p \to \mathbb{R}$. We shall denote by Ω_p the space of all p-vector fields over X. If $u = \sum f e_p$ is a p-vector field and $\alpha = \sum g e^p$ is a p-form we write

$$\langle \alpha, u\rangle = \sum_{e_p \in E_p} f(e_p) g(e_p). \tag{70}$$

We define the codifferential operator $\delta : \Omega_p \to \Omega_{p-1}$ by the identity

$$\langle \alpha, \delta u\rangle = \langle d\alpha, u\rangle \tag{71}$$

for all $\alpha \in \Omega^{p-1}$. It follows from (18) that the codifferential operator of a p-vector field $u = \sum f e_p$ admits the representation

$$\delta u = \sum_{e_p \in E_p} f(e_p) \partial e_p. \tag{72}$$

The preceding definitions and operations retain there meaning for p-forms and p-vector fields with coefficients in an inner-product space H. In applications the case $H = \mathbb{R}^n$, endowed with the standard inner product, will arise frequently. However, in this simple case we may equivalently perform all differential operations and duality operations component by component.

The exterior derivative of a p-form α inherits the matrix representation

$$d\alpha(e_{p+1}) = \sum_{e_p \in E_p} L(e_p, e_{p+1}) \alpha(e_p) \tag{73}$$

directly from (63) and the matrix representation (27) of the coboundary operator. In addition, the complex Bravais lattice representation (32) and the discrete Fourier representation (40) of the coboundary operator carry over *mutatis mutandis* to the exterior derivative. Likewise, the codifferential operator of a p-vector field u inherits the matrix representation

$$\delta u(e_{p-1}) = \sum_{e_p \in E_p} L(e_{p-1}, e_p) u(e_p) \tag{74}$$

directly from (72) and the matrix representation (26). Here again, the complex Bravais lattice representation (31) and the discrete Fourier representation (38) of the boundary operator carry over *mutatis mutandis* to the codifferential.

Given forms $\alpha = \sum f e^p$, $\beta = \sum g e^p$ and fields $u = \sum a e_p$, $v = \sum b e_p$ taking values in a Hilbert space H, the corresponding L^2-products are

$$\langle \alpha, \beta \rangle = \sum_{e_p \in E_p} \langle f(e_p), g(e_p) \rangle, \tag{75a}$$

$$\langle u, v \rangle = \sum_{e_p \in E_p} \langle a(e_p), b(e_p) \rangle. \tag{75b}$$

These products enable the introduction of the flat and sharp operators, $\flat : \Omega_p \to \Omega^p$ and $\sharp : \Omega^p \to \Omega_p$, respectively, through the usual identities (cf., [2])

$$\langle \alpha, u^\flat \rangle = \langle \alpha, u \rangle, \tag{76a}$$

$$\langle \alpha^\sharp, u \rangle = \langle \alpha, u \rangle. \tag{76b}$$

Clearly, $\alpha^\sharp = \sum f e_p$ and $u^\flat = \sum a e^p$, and thus the flat and sharp operators simply extend to forms and fields with the mappings $* : C^p \to C_p$ and $* : C_p \to C^p$ defined in Section 2.2. Using the sharp and flat operators it is possible to extend the differential and codifferential operators to fields and forms, respectively, by setting:

$\delta\alpha = (\delta(\alpha^\sharp))^\flat$ and $du = (d(u^\flat))^\sharp$. It is also possible to define a discrete Hodge $*$-operator, i.e., and isomorphism $* : \Omega^p \to \Omega^{n-p}$, through the identity

$$\langle \alpha, \beta \rangle = \langle \alpha \wedge *\beta, \mu \rangle = \langle \beta \wedge *\alpha, \mu \rangle, \tag{77}$$

where $\mu = \sum e_n$ is the unit n-chain, or volume form, taking the value 1 on all n-cells. By linearity, in suffices to specify the $*$-operator for all elementary p-cochains e^p. It can be readily verified that $*e^p$ is the unique elementary $(n-p)$-cochain e^{n-p} such that $e^p \cup e^{n-p} = e^n$ for some elementary n-cochain e^n. Indeed,

$$\langle \alpha \wedge *e^p, \mu \rangle = \alpha(e_p) = \langle \alpha, e^p \rangle \tag{78}$$

and (77) is satisfied identically. Thus, the Hodge $*$-operator is related to the cap product (cf. Section 2.2) through the identity

$$*\alpha = \sum_{e_p \in E_p} f(e_p)(e^p \cap \mu)^*, \tag{79}$$

where $\alpha = \sum f e^p$.

As in the conventional Hodge-de Rham theory we can define the discrete Laplace-de Rham operator $\Delta : \Omega^p \to \Omega^p$ by the formula $\Delta = d\delta + \delta d$. A form α such that $\Delta\alpha = 0$ is said to be harmonic. We shall denote by K^p the vector space of harmonic p-forms. Then we have the following discrete analog of the classical Hodge decomposition theorem.

Proposition 1. *The following equation holds:*

$$\Omega^p = d\Omega^{p-1} \oplus \delta\Omega^{p+1} \oplus K^p, \tag{80}$$

where the decomposition is L^2-orthogonal.

Proof. (cf., [2], Theorem 7.5.3). Let $\alpha \in \Omega^p$. Then $\Delta\alpha = 0$ if and only if $d\alpha = 0$ and $\delta\alpha = 0$. Indeed, if $d\alpha = 0$ and $\delta\alpha = 0$ then $\Delta\alpha = d\delta\alpha + \delta d\alpha = 0$. Conversely, let $\Delta\alpha = 0$. Then $\langle \Delta\alpha, \alpha \rangle = \langle d\delta\alpha + \delta d\alpha, \alpha \rangle = \langle d\delta\alpha, \alpha \rangle + \langle \delta d\alpha, \alpha \rangle = \langle d\alpha, d\alpha \rangle + \langle \delta\alpha, \delta\alpha \rangle = 0$, whence it follows that $d\alpha = 0$ and $\delta\alpha = 0$. Suppose now that $\omega = d\alpha + \delta\beta + \gamma$, with $\omega \in \Omega^p$, $\alpha \in \Omega^{p-1}$, $\beta \in \Omega^{p+1}$ and $\gamma \in K^p$. Then $\langle d\alpha, \delta\beta \rangle = \langle d^2\alpha, \beta \rangle = \langle \alpha, \delta^2\beta \rangle = 0$. In addition, $\langle d\alpha, \gamma \rangle = \langle \alpha, \delta\gamma \rangle = 0$, and $\langle \delta\beta, \gamma \rangle = \langle \beta, d\gamma \rangle = 0$. Thus, the spaces $d\Omega^{p-1}$, $\delta\Omega^{p+1}$ and K^p are orthogonal. Let now $\mathcal{C}^p$ be the orthogonal complement of $d\Omega^{p-1} \oplus \delta\Omega^{p+1}$. Clearly, $K^p \subset \mathcal{C}^p$. Conversely, let $\gamma \in \mathcal{C}^p$. Then $\langle d\alpha, \gamma \rangle = \langle \alpha, \delta\gamma \rangle = 0$ for all $\alpha \in \Omega^{p-1}$, and $\delta\gamma = 0$. In addition, $\langle \delta\beta, \gamma \rangle = \langle \beta, d\gamma \rangle = 0$ for all $\beta \in \Omega^{p+1}$, and $d\gamma = 0$. Hence, $\Delta\gamma = 0$, and $\mathcal{C}^p \subset K^p$. □

The Hodge decomposition theorem supplies the following direct link between harmonic functions and cohomology.

Corollary 1. *K^p and H^p are isomorphic.*

Proof. (cf., [2], Corollary 7.5.4). Let $\gamma \in K^p$. Then $\Delta\gamma = 0$, $d\gamma = 0$ and $\gamma \in \ker d^p$. Hence, K^p can be mapped to $\ker d^p$ by inclusion, and then to H^p by projection, i.e., by assigning to γ its equivalence class $[\gamma]$. We wish to show that the mapping $K^p \to H^p$ thus defined is an isomorphism. Suppose $[\gamma] = 0$. This requires that there is a $\beta \in \Omega^{p-1}$ such that $\gamma = d\beta$, i.e., that γ be exact. But, since γ is harmonic we additionally have $\delta\gamma = 0$. Therefore, $\langle \gamma, \gamma \rangle = \langle \gamma, d\beta \rangle = \langle \delta\gamma, \beta \rangle = 0$. Hence $\gamma = 0$ and the map $\gamma \to [\gamma]$ is one-to-one. Suppose now that $[\omega] \in H^p$. By the Hodge theorem we can write $\omega = d\alpha + \delta\beta + \gamma$, where $\gamma \in K^p$. But $0 = d\omega = d\delta\beta$. Hence $\langle \delta\beta, \delta\beta \rangle = \langle \beta, d\delta\beta \rangle = 0$ and $\delta\beta = 0$. This leaves $\omega = d\alpha + \gamma$ and $[\omega] = [\gamma]$, and thus the map $\gamma \to [\gamma]$ is onto. □

For perfect lattices, the Hodge decomposition theorem reduces to the following form.

Corollary 2. *Let X be a perfect lattice complex. Let ω be a p-form over X. Then,*

$$\omega = d\alpha + \delta\beta, \tag{81}$$

where

$$\alpha = \Delta^{-1}\delta\omega, \tag{82a}$$

$$\beta = \Delta^{-1}d\omega. \tag{82b}$$

Proof. For a perfect lattice, $K^p = H^p = 0$ and the Hodge decomposition reduces to (81). In addition, we have the identities: $d\Delta^{-1}\delta\omega = \Delta^{-1}d\delta\omega$ and $\delta\Delta^{-1}d\omega = \Delta^{-1}\delta d\omega$. The first of these identities is verified as follows: $\Delta d\Delta^{-1}\delta\omega = (d\delta + \delta d)d\Delta^{-1}\delta\omega = d\delta d\Delta^{-1}\delta\omega = d(\delta d + d\delta)\Delta^{-1}\delta\omega = d\Delta\Delta^{-1}\delta\omega = d\delta\omega$. The second identity is verified as follows: $\Delta\delta\Delta^{-1}d\omega = (\delta d + d\delta)\delta\Delta^{-1}d\omega = \delta d\delta\Delta^{-1}d\omega = \delta(d\delta + \delta d)\Delta^{-1}d\omega = \delta\Delta\Delta^{-1}d\omega = \delta d\omega$. By virtue of the preceding identities we have $d\alpha + \delta\beta = d\Delta^{-1}\delta\omega + \delta\Delta^{-1}d\omega = \Delta^{-1}d\delta\omega + \Delta^{-1}\delta d\omega = \Delta^{-1}(d\delta + \delta d)\omega = \Delta^{-1}\Delta\omega = \omega$. □

3.2. Integration on lattices

The characteristic chain of a subset A of E_p is

$$\chi_A = \sum_{e_p \in A} e_p. \tag{83}$$

The integral of a p-form α over A is defined as

$$\int_A \alpha \equiv \langle \alpha, \chi_A \rangle. \tag{84}$$

We may equivalently regard $\langle \alpha, \chi_A \rangle$ as the action of A on the form α, and A as a current, i.e., a linear functional on forms (cf., e.g., [31]). If $\alpha = \sum f(e_p)e^p$ then

$$\int_A \alpha = \sum_{e_p \in A} f(e_p). \tag{85}$$

Suppose now that $A \subset E_{p+1}$ and $\omega \in \Omega^p$. Then

$$\int_A d\omega = \langle d\omega, \chi_A \rangle = \langle \omega, \partial \chi_A \rangle. \tag{86}$$

We define the integral of ω over the boundary of A as

$$\int_{\partial A} \omega = \langle \omega, \partial \chi_A \rangle. \tag{87}$$

Then we have

$$\int_A d\omega = \int_{\partial A} \omega, \tag{88}$$

which may be regarded as a discrete version of Stoke's theorem. As an example of an application, the integration-by-parts formula

$$\int_{\partial A} \alpha \wedge \beta = \int_A (d\alpha) \wedge \beta + \int_A (-1)^p \alpha \wedge (d\beta), \tag{89}$$

where $\alpha \in \Omega^p$, $\beta \in \Omega^q$, and $A \subset E_{p+q+1}$, follows directly by integrating the coboundary formula (68) over A and applying Stoke's theorem to the left-hand side of the resulting equation.

3.3. The Gauss linking number

Throughout this section we restrict our attention to three-dimensional lattices, i.e., $n = 3$. The linking number of two 1-forms $\omega, \omega' \in \Omega^1$ is defined to be

$$\mathrm{Link}(\omega, \omega') = \int_{E_3} \omega \wedge d\omega'. \tag{90}$$

From the integration by parts formula (89) it follows that

$$\mathrm{Link}(\omega, \omega') = \int_{E_3} d\omega \wedge \omega'. \tag{91}$$

Clearly, $\mathrm{Link}(\omega, \omega') = 0$ if either ω or ω' is exact. In particular, let $A \in E_0$ and let χ_A be its characteristic chain, regarded as a 0-form. Then $d\chi_A$ is a 1-form which represents the closed oriented boundary ∂A of A. It then follows that $\mathrm{Link}(d\chi_A, \omega') = 0$, i.e., the linking number of a closed oriented surface with any other 1-form is necessarily zero. Suppose instead that $\omega = \chi_B \wedge d\chi_A$ for some $B \in E_0$ intersecting A. Then, ω represents a subset C of ∂A determined by its intersection with B. In addition, it follows from an application of the coboundary formula (68) that $d\omega = d\chi_B \wedge d\chi_A = d\chi_A \wedge d\chi_B$, which represents the loop D obtained by intersecting the boundaries ∂A and ∂B. Likewise, let $\omega' = \chi_{B'} \wedge d\chi_{A'}$ for some distinct but intersecting sets $A', B' \in E_0$, and let the oriented area C'

and oriented loop D' be defined as before. Now suppose that D and C' intersect transversally, i.e., $d\omega \wedge \omega'$ is supported on isolated 3-cells. Then,

$$\text{Link}(D, D') = \sum_{D \cap C'} \pm 1, \tag{92}$$

where the sum extends over the support of $d\omega \wedge \omega'$ and the sign is positive at intersections where the orientations of D and C' are consistent, and negative otherwise. It is readily shown (e.g., [5], §17) that $\text{Link}(D, D')$ is independent of the choices made in the preceding definition (cf., [5] also for the connection between the linking number and the Hopf invariant).

If the lattice is perfect, then ω may be written in the form (81). Inserting this representation into (90) we obtain

$$\text{Link}(\omega, \omega') = \int_{E_3} d\alpha \wedge d\omega' + \int_{E_3} \delta\beta \wedge d\omega'. \tag{93}$$

But the first term on the right-hand side vanishes by virtue of (89) and we have

$$\text{Link}(\omega, \omega') = \int_{E_3} \delta\beta \wedge d\omega'. \tag{94}$$

Furthermore, inserting (82b) into this expression we obtain

$$\text{Link}(\omega, \omega') = \int_{E_3} \delta\Delta^{-1} d\omega \wedge d\omega'. \tag{95}$$

This identity generalizes the well-known integral formula (3) for the Gauss linking number of two loops C_1 and C_2 in $\mathbb{R}^3$ (e.g., [21]).

3.4. Examples of linking relations

By way of illustration, we may examine the linking number for the cases of the simple cubic, BCC and FCC lattices described in Sections 2.3.4, 2.3.6 and 2.3.5. By the bilinearity of the linking number, it suffices to provide rules for the linking of pairs of elementary 1-cells.

3.4.1. The simple cubic lattice. In the simple cubic lattice the links that can be formed with a 1-cell, such as $e^1(l, 2)$, are:

$$\text{Link}\big(e^1(l + \varepsilon_2 + \varepsilon_3, 1), e^1(l, 2)\big) = 1, \tag{96a}$$

$$\text{Link}\big(e^1(l + \varepsilon_1 + \varepsilon_2, 3), e^1(l, 2)\big) = 1, \tag{96b}$$

$$\text{Link}\big(e^1(l + \varepsilon_2, 3), e^1(l, 2)\big) = 1, \tag{96c}$$

$$\text{Link}\big(e^1(l + \varepsilon_2, 1), e^1(l, 2)\big) = 1. \tag{96d}$$

All other linking relations may be deduced by symmetry.

3.4.2. The body-centered cubic lattice. In the BCC lattice the 1-cells in the cube direction, such as $e^1(l, 5)$, $e^1(l, 6)$ and $e^1(l, 7)$, do not form any links. The links that can be formed with a diagonal 1-cell, such as $e^1(l, 1)$, are:

$$\mathrm{Link}\big(e^1(l + \varepsilon_6, 2), e^1(l, 1)\big) = 1, \tag{97a}$$

$$\mathrm{Link}\big(e^1(l + \varepsilon_7, 3), e^1(l, 1)\big) = 1, \tag{97b}$$

$$\mathrm{Link}\big(e^1(l + \varepsilon_1, 2), e^1(l, 1)\big) = 1, \tag{97c}$$

$$\mathrm{Link}\big(e^1(l + \varepsilon_1, 3), e^1(l, 1)\big) = 1, \tag{97d}$$

with all other linking relations following by symmetry.

3.4.3. The face-centered cubic lattice. In the FCC lattice all 1-cells are symmetry related. It therefore suffices to enumerate the links that can be formed with one 1-cell, with all other linking relations following by symmetry. Taking $e^1(l, 1)$ as the representative 1-cell we obtain

$$\mathrm{Link}\big(e^1(l - \varepsilon_4, 4), e^1(l, 1)\big) = 1, \tag{98a}$$

$$\mathrm{Link}\big(e^1(l + \varepsilon_2, 6), e^1(l, 1)\big) = 1, \tag{98b}$$

$$\mathrm{Link}\big(e^1(l + \varepsilon_1, 4), e^1(l, 1)\big) = 1, \tag{98c}$$

$$\mathrm{Link}\big(e^1(l - \varepsilon_5, 6), e^1(l, 1)\big) = 1, \tag{98d}$$

with all other linking relations following by symmetry.

4. Harmonic lattices

In this section we apply the machinery developed in the preceding sections to the formulation of a mechanics of lattices. An important observation is that the essential structure of that mechanics follows from material-frame indifference, possibly combined with additional assumptions of locality. In particular, invariance of the energy with respect to rigid-body rotations and translations determines the form of the deformation and stress fields, both for finite and linearized kinematics. The equilibrium equations then follow from stationarity, and can be given a compact expression using discrete differential operators. In addition, we briefly delve into basic questions of analysis pertaining to the equilibrium problem, and investigate the continuum limit of the energy function of harmonic lattices in the sense of Γ-convergence.

4.1. The mechanics of lattices

Consider a crystal lattice described by its corresponding lattice complex X. A deformation of a crystal is a mapping $y : E_0 \to \mathbb{R}^n$. Thus, $y(e_0)$ is the position of vertex $e_0 \in E_0$ in the deformed configuration of the crystal. We shall assume that the energy of a deformed crystal can be written as a function of the form $E(y)$, i.e., as a function $E : \Omega^0(X, \mathbb{R}^n) \to \mathbb{R}$. For instance $E(y)$ may be approximated

by means of a suitable empirical potential. Examples of commonly used empirical or semi-empirical potentials include: pairwise potentials such as Lennard-Jones [1]; the embedded-atom method (EAM) for FCC metals [11]; the modified embedded-atom method (MEAM) for BCC metals [50]; the FINNIS-SINCLAIR potential for transition metals [13]; MGPT pseudo-potentials [32]; STILLINGER-WEBER for covalent crystals [46]; bond-order potentials [41]; and others.

Energy functions can often be simplified by recourse to suitable assumptions regarding the nature of the atomic interactions. Atoms in a crystal can be grouped by shells, according to their distance to a reference atom. Then, nearest-neighbor interactions refer to interactions extending to the first shell of atoms; next-to-nearest neighbor interactions consist of interactions extending to the second shell of atoms; and so on. Some empirical potentials restrict the range of interactions between atoms to a few atom shells. For instance, the simplest implementations of the EAM account for nearest-neighbor interactions only. Another common set of restrictions underlying empirical potentials concerns the extent of multi-body interactions. Thus, the energy function $E(y)$ is said to consist of two-body interactions if it can be written as a sum over energy functions depending on the positions of pairs of atoms; it is said to consist of three-body interactions if $E(y)$ can be written as a sum over functions depending of the positions of three atoms; and so on. For instance, the Lennard-Jones potential accounts for pairwise interactions only.

The energy function $E(y)$ must be material-frame indifferent, i.e., invariant under superposed rigid-body motions. Thus we must have

$$E(Ry + c) = E(y) \tag{99}$$

for all $R \in SO(n)$ and $c \in \mathbb{R}^n$. Let $y_1 \sim y_2$ if and only if $y_2 = y_1 + c$ for some $c \in \mathbb{R}^n$. Then $\sim$ is an equivalence relation, and translation invariance requires that E be expressible as a function of the quotient space $\Omega^0(X, \mathbb{R}^n)/\sim$. But $\Omega^0(X, \mathbb{R}^n)/\sim$ may be identified with the range of $\Omega^0(X, \mathbb{R}^n)$ by d. Thus, if $y_1 \sim y_2$ then clearly $dy_1 = dy_2$. Conversely, if $dy_1 = dy_2$, then y_1 and y_2 differ by a constant. Hence it follows that the energy function is expressible as a function of the deformation $dy : E_1 \to \mathbb{R}^n$. We shall denote $E(dy)$ the resulting energy function. Rotation invariance further requires that

$$E(Rdy) = E(dy) \tag{100}$$

for all $R \in SO(n)$, i.e., the function $E(dy)$ is isotropic. From Cauchy's representation formula for isotropic functions of an arbitrary number of vectors (cf., e.g., [49]) it follows that the energy must be expressible as a function $E(C)$ of the discrete right Cauchy-Green deformation field $C : E_1 \times E_1 \to \mathbb{R}$ defined as

$$C(e_1, e_1') = dy(e_1) \cdot dy(e_1') \tag{101}$$

for every pair of 1-cells e_1 and e_1'. Note that no assumption of locality is implied in the representation $E(C)$, which in principle may depend on the value of C for all pairs of 1-cells.

The stable configurations of interest are the minimizers of $E(y)$, possibly over a finite domain subject to appropriate boundary conditions and under the action of

applied loads. However, the energy landscape defined by $E(y)$ is typically of great complexity, with numerous energy wells, e.g., corresponding to lattice-invariant deformations. In order to make progress we shall resort to two main approximations, namely, the harmonic approximation and the eigendeformation formalism.

A harmonic crystal is a crystal whose energy is quadratic in the displacement field $u(e_0) = y(e_0) - x(e_0)$. We may obtain the harmonic approximation of the energy by expanding the function $E(x + u)$ in the Taylor series of u. The result is a quadratic function of the form

$$E(u) = \int_{E_1}\int_{E_1}\int_{E_1}\int_{E_1} \frac{1}{2}C(e_1, e_1', e_1'', e_1''')\varepsilon(e_1, e_1')\varepsilon(e_1'', e_1''') \equiv \frac{1}{2}\langle C\varepsilon, \varepsilon\rangle, \quad (102)$$

where $\varepsilon : E_1 \times E_1 \to \mathbb{R}$, defined as

$$\varepsilon(e_1, e_1') = \frac{1}{2}\left[du(e_1) \cdot dx(e_1') + dx(e_1) \cdot du(e_1')\right] = \varepsilon(e_1', e_1), \quad (103)$$

is the discrete strain field. We shall also denote by $\varepsilon(u)$ the operator that maps a displacement to its corresponding strain field. Then, the energy (102) can be rewritten as

$$E(u) = \frac{1}{2}\langle C\varepsilon(u), \varepsilon(u)\rangle. \quad (104)$$

The coefficients $C : E_1^4 \to \mathbb{R}$ are harmonic moduli which measure the strength of the interactions between 1-cells of the lattice. Owing to the symmetry of the strain field, in (102) we may suppose

$$C(e_1, e_1', e_1'', e_1''') = C(e_1', e_1, e_1'', e_1''') = C(e_1, e_1', e_1''', e_1'') \quad (105)$$

without loss of generality. We verify that the discrete strain field is indeed invariant under superposed rigid-body displacements, i.e., under transformations of the form $u \to u + c + \omega x$, $c \in \mathbb{R}^n$, $\omega \in so(3)$, and therefore the energy (102) is infinitesimally material-frame indifferent. Inserting (103) into (102) we obtain the representation

$$E(u) = \int_{E_1}\int_{E_1} \frac{1}{2}du(e_1) \cdot B(e_1, e_1')du(e_1') \equiv \frac{1}{2}\langle Bdu, du\rangle, \quad (106)$$

where

$$B(e_1, e_1') = \int_{E_1}\int_{E_1} C(e_1, e_1'', e_1', e_1''')dx(e_1'') \otimes dx(e_1'''). \quad (107)$$

In addition, using the representation (73) of the differential we obtain

$$E(u) = \int_{E_0}\int_{E_0} \frac{1}{2}u(e_0) \cdot A(e_0, e_0')u(e_0') \equiv \frac{1}{2}\langle Au, u\rangle, \quad (108)$$

where

$$A(e_0, e_0') = \int_{E_1}\int_{E_1} L(e_0, e_1)L(e_0', e_1')B(e_1, e_1'). \quad (109)$$

The function $A : E_0^2 \to \mathrm{sym}\mathbb{R}^{n\times n}$ collects the harmonic force constants of the crystal. All moduli arising in the preceding representations of the energy must be translation and symmetry invariant. In addition, we have the symmetry relations

$$C(e_1, e_1', e_1'', e_1''') = C(e_1'', e_1''', e_1, e_1'), \tag{110a}$$

$$B(e_1, e_1') = B^T(e_1', e_1), \tag{110b}$$

$$A(e_0, e_0') = A^T(e_0', e_0). \tag{110c}$$

Finally, by translation invariance we have the representations

$$Bdu = \Psi * du, \tag{111a}$$

$$Au = \Phi * u, \tag{111b}$$

where Ψ and Φ are the force-constant fields of the lattice. Since (111a) and (111b) are in convolution form, an application of Parseval's identity and the convolution theorem yields the additional representations:

$$E(u) = \frac{1}{(2\pi)^n} \int_{[-\pi,\pi]^n} \frac{1}{2} \langle \hat{\Phi}(\theta)\hat{u}(\theta), \hat{u}^*(\theta)\rangle \, d\theta, \tag{112a}$$

$$E(u) = \frac{1}{(2\pi)^n} \int_{[-\pi,\pi]^n} \frac{1}{2} \langle \hat{\Psi}(\theta) P^*(\theta)\hat{u}(\theta), P(\theta)\hat{u}^*(\theta)\rangle \, d\theta, \tag{112b}$$

which will be extensively used in subsequent analyses.

Taking variations of (102) we obtain

$$\dot{E} = \int_{E_1} \int_{E_1} \sigma(e_1, e_1')\dot{\varepsilon}(e_1, e_1') \equiv \langle \sigma, \dot{\varepsilon}\rangle, \tag{113}$$

where

$$\sigma(e_1, e_1') = \int_{E_1} \int_{E_1} C(e_1, e_1', e_1'', e_1''')\varepsilon(e_1'', e_1''') \tag{114}$$

or, in invariant notation,

$$\sigma = C\varepsilon \tag{115}$$

is the discrete stress field. This relation may be regarded as a discrete version of Hooke's law. We note that the stress field is symmetric, i.e.,

$$\sigma(e_1, e_1') = \sigma(e_1', e_1). \tag{116}$$

Inserting (103) in (113) we further obtain

$$\dot{E} = \int_{E_1} \tau(e_1) \cdot d\dot{u}(e_1) \equiv \langle \tau, d\dot{u}\rangle, \tag{117}$$

where

$$\tau(e_1) = \int_{E_1} \sigma(e_1, e_1')dx(e_1') \tag{118}$$

or, in invariant notation,

$$\tau = \sigma dx \tag{119}$$

is an internal force field. The equilibrium equation is, therefore,

$$\delta\tau = 0. \tag{120}$$

The equilibrium conditions across the boundary of a domain can be ascertained likewise. Let $A \subset E_1$. Then (117) can be split as

$$\begin{aligned}\dot{E} &= \int_A \tau(e_1)\cdot d\dot{u}(e_1) + \int_{E_1-A} \tau(e_1)\cdot d\dot{u}(e_1)\\ &= \int_{E_1} \chi_A\tau(e_1)\cdot d\dot{u}(e_1) + \int_{E_1} \chi_{E_1-A}\tau(e_1)\cdot d\dot{u}(e_1),\end{aligned} \tag{121}$$

and stationarity requires that

$$\delta(\chi_A\tau)(e_0) + \delta(\chi_{E_1-A}\tau)(e_0) = 0 \tag{122}$$

which, for vertices e_0 on the boundary ∂A, may be regarded as a discrete traction-equilibrium equation. An equation of equilibrium in terms of the displacement field can be obtained as follows. From (120) we have that, for any test field $v \in \Omega^0(X, \mathbb{R}^n)$,

$$0 = \langle\delta\tau, v\rangle = \langle\tau, dv\rangle = \langle\sigma dx, dv\rangle = \langle C\varepsilon(u), \varepsilon(v)\rangle = \langle Au, v\rangle \tag{123}$$

and, hence, the equations of equilibrium take the form

$$\delta\tau = Au = 0, \tag{124}$$

which can also be derived by taking variations of (104) directly.

Further restrictions on the force constants, which facilitate their identification, are obtained from macroscopic properties of the lattice such as the elastic moduli. In order to make this connection, consider a stress field $\sigma : E_1 \times E_1 \to \mathbb{R}$ over the lattice and let $\tau : E_1 \to \mathbb{R}^n$ be the corresponding internal force field. Suppose in addition that an incremental deformation $\dot{u} : E_0 \to \mathbb{R}^n$ is applied to the stressed lattice. Let Y be a subcomplex of X consisting of n-cells and their faces, henceforth referred to as a sub-body, and let $|Y|$ be its volume. The tractions on the boundary of Y are given by $\delta(\chi_{E_1(Y)}\tau)$, equation (122), and their deformation power is

$$\begin{aligned}\dot{E}(Y) &= \int_{E_0} \delta(\chi_{E_1(Y)}\tau)(e_0)\cdot\dot{u}(e_0)\\ &= \int_{E_1} (\chi_{E_1(Y)}\tau)(e_1)\cdot d\dot{u}(e_1)\\ &= \int_{E_1(Y)} \tau(e_1)\cdot d\dot{u}(e_1)\\ &= \int_{E_1(Y)}\int_{E_1} \sigma(e_1, e_1')dx(e_1')\cdot d\dot{u}(e_1)\\ &= \int_{E_1(Y)}\int_{E_1} \sigma(e_1, e_1')\dot{\varepsilon}(e_1, e_1').\end{aligned} \tag{125}$$

Suppose that the incremental deformation is of the form $d\dot{u} = \dot{\bar{\varepsilon}} dx$, where $\dot{\bar{\varepsilon}} \in \mathrm{sym}\mathbb{R}^{n\times n}$ represents a uniform macroscopic strain rate. For this particular case we have

$$\dot{E}(Y) = \left\{ \int_{E_1(Y)} \int_{E_1} \sigma(e_1, e_1') dx(e_1) \otimes dx(e_1') \right\} \cdot \dot{\bar{\varepsilon}} \tag{126}$$

and, hence, the average macroscopic stress over Y is

$$\begin{aligned} \bar{\sigma}(Y) &= \frac{1}{|Y|} \int_{E_1(Y)} \int_{E_1} \sigma(e_1, e_1') dx(e_1) \otimes dx(e_1') \\ &= \frac{1}{|Y|} \int_{E_1(Y)} \tau(e_1) \otimes dx(e_1), \end{aligned} \tag{127}$$

so that $\dot{E}(Y) = |Y| \bar{\sigma}(Y) \cdot \dot{\bar{\varepsilon}}$. Assume now that the state of stress is itself the result of a uniform macroscopic strain $\bar{\varepsilon} \in \mathrm{sym}\mathbb{R}^{n\times n}$, i.e.,

$$\sigma(e_1, e_1') = \left\{ \int_{E_1} \int_{E_1} C(e_1, e_1', e_1'', e_1''') dx(e_1'') \otimes dx(e_1''') \right\} \bar{\varepsilon}, \tag{128}$$

which follows from (114) by setting $du = \bar{\varepsilon} dx$. Since, in this case, the state of stress and deformation of the lattice is uniform, it follows that, for sufficiently large Y, $\bar{\sigma}(Y)$ converges to

$$\bar{\sigma}_{ij} = c_{ijkl} \bar{\varepsilon}_{kl}, \tag{129}$$

where

$$\begin{aligned} c_{ijkl} &\sim \frac{1}{|Y|} \int_{E_1(Y)} \int_{E_1} \int_{E_1} \int_{E_1} C(e_1, e_1', e_1'', e_1''') \\ &\qquad dx_i(e_1) dx_j(e_1') dx_k(e_1'') dx_l(e_1''') \\ &\sim \frac{1}{|Y|} \int_{E_1(Y)} \int_{E_1} B_{ik}(e_1, e_1'') dx_j(e_1) dx_l(e_1'') \end{aligned} \tag{130}$$

are the elastic moduli of the lattice. We note that the requisite major and minor symmetries $c_{ijkl} = c_{klij} = c_{jikl} = c_{ijlk}$ of the elastic moduli follow directly from (105).

An alternative expression for the elastic moduli in terms of force constants may be obtained as follows: insert representation (73) of dx into (130) to obtain

$$c_{ijkl} \sim \frac{1}{|Y|} \int_{E_0} \int_{E_0} \int_{E_1(Y)} \int_{E_1} L(e_0, e_1) L(e_0', e_1') B_{ik}(e_1, e_1') x_j(e_0) x_l(e_0'). \tag{131}$$

Using (109) we have, asymptotically for large Y,

$$c_{ijkl} \sim \frac{1}{|Y|} \int_{E_0(y)} \int_{E_0} A_{ik}(e_0, e_0') x_j(e_0) x_1(e_0') \tag{132}$$

or, equivalently,

$$c_{ijkl} \sim -\frac{1}{2|Y|} \int_{E_0(Y)} \int_{E_0} A_{ik}(e_0, e_0') (x_j(e_0) - x_j(e_0'))(x_l(e_0) - x_l(e_0')) \tag{133}$$

For a simple lattice, by translation invariance and representation (111b) we have, explicitly,

$$c_{ijkl} = \frac{-1}{2\Omega} \sum_{l \in \mathbb{Z}^n} \Phi_{ik}(l) x_j(l) x_l(l), \tag{134}$$

where the elastic moduli are now expressed simply in terms of the force constants of the lattice.

It is interesting to note that the minor symmetries of c_{ijkl} are not evident in (134). Indeed, those minor symmetries do not hold for arbitrary choices of the force-constant field Φ, but only for force-constant fields of the form (109) dictated by material-frame indifference. The restrictions imposed by material-frame indifference on the force constants have been addressed in [43, 45], but have not always been recognized in the literature, where the force constants are often mistakenly regarded as fundamental and subject to no restrictions other than material symmetry.

4.2. Equilibrium problem

Suppose now that a crystal lattice is acted upon by a distribution of forces $f \in \Omega_0$. We wish to determine the equilibrium configurations of the crystal, i. e., the solutions of the equilibrium equation

$$Au = f \tag{135}$$

under appropriate boundary and forcing conditions. Problems arising in applications frequently fall into the following categories: (i) f has bounded support and u decays to 0 at infinity; (ii) f and u are periodic; (iii) f and u are periodic in certain directions, and f has bounded support and u decays to 0 at infinity in the remaining directions. Examples of problems of the first type include the deformation of a crystal under the action of an applied point load or in the presence of a dilatation point. Taylor dislocation lattices fall in the second class of problems, straight dislocations in the third.

The equilibrium equation (135) may be analyzed – and its solutions characterized – by means of the fundamental solution formalism (cf., e.g., [42]). Recall that, by translation invariance, the equilibrium equation can be expressed in convolution form as

$$\Phi * u = f, \tag{136}$$

where Φ is the force-constant field of the lattice. The following proposition covers a broad class of problems often encountered in applications.

Proposition 2. *Suppose that*

(i) Φ *has finite support;*
(ii) $\hat{\Phi}^{-1} \in L^1([-\pi, \pi]^n)$*;*
(iii) f *has finite support.*

Let

$$G(l) = \frac{1}{(2\pi)^n} \int_{[-\pi,\pi]^n} \hat{\Phi}^{-1}(\theta) \mathrm{e}^{i\theta\cdot l}\, d\theta. \tag{137}$$

Then,

$$u = G * f \tag{138}$$

is a solution of the equilibrium equation (136).

Note that assumptions (i) and (iii) state that Φ and f are zero everywhere except on a finite set of vertices, whereas assumption (ii) implies that $\hat{\Phi}$ is invertible almost everywhere in $[-\pi, \pi]^n$ and its inverse is integrable. The function G is the fundamental solution, or Green's function, of the lattice. Condition (ii) of the proposition is easily verified directly for specific force-constant models. Clearly, solutions need not be unique in general, e.g., they may be determined up to translations and infinitesimal rotations.

Proof. We verify that, since $\hat{\Phi}^{-1}(\theta)\mathrm{e}^{i\theta\cdot l} \in L^1([-\pi,\pi]^n)$, $G(l)$ in (137) is defined for all $l \in \mathbb{Z}^n$. In addition,

$$\begin{aligned}(\Phi * G)(l) &= \sum_{l'\in\mathbb{Z}^n} \Phi(l-l')G(l') \\ &= \sum_{l'\in\mathbb{Z}^n} \Phi(l-l') \left\{ \frac{1}{(2\pi)^n} \int_{[-\pi,\pi]^n} \hat{\Phi}^{-1}(\theta)\mathrm{e}^{i\theta\cdot l}\, d\theta \right\}. \end{aligned} \tag{139}$$

Since the sum over l extends over a finite number of terms, we have

$$\begin{aligned}(\Phi * G)(l) &= \frac{1}{(2\pi)^n} \int_{[-\pi,\pi]^n} \hat{\Phi}^{-1}(\theta) \left\{ \sum_{l'\in\mathbb{Z}^n} \Phi(l-l')\mathrm{e}^{i\theta\cdot l} \right\} d\theta \\ &= \frac{1}{(2\pi)^n} \int_{[-\pi,\pi]^n} I\mathrm{e}^{i\theta\cdot l}\, d\theta \\ &= I\delta(l), \end{aligned} \tag{140}$$

where

$$\delta(l) = \begin{cases} 1 & \text{if } l = 0, \\ 0 & \text{otherwise,} \end{cases} \tag{141}$$

and I is the identity in $\mathbb{R}^{n\times n}$. Also, we note that (138) is well defined since by assumption f has finite support. Then

$$(\Phi * u)(l) = \sum_{l'\in\mathbb{Z}^n} \Phi(l-l') \left\{ \sum_{l''\in\mathbb{Z}^n} G(l'-l'')f(l'') \right\}. \tag{142}$$

Since both sums are finite, we have

$$\begin{aligned}(\Phi * u)(l) &= \sum_{l''\in\mathbb{Z}^n}\left\{\sum_{l'\in\mathbb{Z}^n}\Phi(l-l')G(l'-l'')\right\}f(l'')\\ &= \sum_{l''\in\mathbb{Z}^n}\delta(l-l'')f(l'')\\ &= f(l),\end{aligned}\tag{143}$$

which shows that u is indeed a solution of (136). □

The solution of the periodic problem is elementary. Suppose that the periodic unit cell of the problem is in the form of a set $Y \subset \mathbb{Z}^n$, and that the translates $\{Y + L^i A_i,\ L \in \mathbb{Z}^n\}$ define a partition of $\mathbb{Z}^3$ for some translation vectors $A_i \in \mathbb{Z}^n$, $i = 1, \ldots, n$. Let A^i be the corresponding dual basis, and $B^i = 2\pi A^i$ the reciprocal basis. Using the convolution theorem for periodic lattice functions, equation (A.293), the equilibrium equations (136) reduce to the finite problem

$$\hat{\Phi}(\theta)\hat{u}(\theta) = \hat{f}(\theta), \quad \theta \in Z,\tag{144}$$

where Z is the intersection of the lattice spanned by B^i and $[-\pi, \pi]^n$, and $\hat{f}(\theta)$ is given by (A.289). Supposing that $\hat{\Phi}(\theta)$ is invertible for all $\theta \neq 0$, the sole remaining difficulty in solving (144) is that $\hat{\Phi}(\theta)$ necessarily vanishes at the origin. Thus, the solvability of problem (144) necessitates $\hat{f}_0 = 0$. In view of (A.294), this condition simply amounts to the requirement that the average force $\langle f \rangle$ be zero, i.e., the applied forces $f(l)$ must be in static equilibrium. The solution $\hat{u}(\theta)$ is then indeterminate at $\theta = 0$, i.e., the lattice displacement field $u(l)$ is determined up to a rigid translation. This situation can also be understood from the standpoint of the Fredholm alternative. Thus, consider the operator $(T\hat{u})(\theta) = \hat{\Phi}(\theta)\hat{u}(\theta)$. The kernel $\mathcal{N}(T)$ is the space of rigid translations. For problem (144) to have solutions, $\hat{f}$ must be orthogonal to $\mathcal{N}(T)$, i.e., $\hat{f}_0$ must be zero or, equivalently, $f(l)$ must have zero average. If this condition is satisfied, the solution is determined modulo $\mathcal{N}(T)$, i.e., up to a rigid translation. If $\hat{u}(\theta)$ is a solution of (144), the corresponding lattice displacement field $u(l)$ follows by an application of the inverse discrete Fourier transform formula (A.290).

Conditions for existence and uniqueness of the solutions of the equilibrium problem follow from standard theory (e.g., [10]). To this end, recall that the space $X = H^1(\mathbb{R}^n)/\mathbb{R}^n$, defined as the space of equivalence classes with respect to the relation: $u \sim v \Leftrightarrow u - v$ is a constant, is a Banach space under the norm $||\dot{u}||_X = ||\nabla u||_{L^2}$, where $u \in \dot{u}, \dot{u} \in X$ (cf., e.g., [8], proposition 3.40). For present purposes, it is advantageous to express the equilibrium problem in variational form. To this end, let $f \in X^*$ and let

$$F(u) = \begin{cases} E(u) - \langle f, u\rangle & \text{if } \operatorname{supp}(\hat{u}) \in [-\pi, \pi]^n,\\ +\infty & \text{otherwise,}\end{cases}\tag{145}$$

be the potential energy of the crystal, where the energy $E(u)$ is defined as in (112a). Then, we wish to find the minimum

$$m_X(F) = \inf_{u\in X} F(u)\tag{146}$$

and the set of minimizers

$$M_X(F) = \{u \in X \text{ s. t. } F(u) = m_X(F)\}. \tag{147}$$

The following proposition collects standard conditions guaranteeing the existence and uniqueness of solutions of problem (146).

Proposition 3. *Suppose that $\hat{\Phi}$ is measurable and that there exists a constant $C > 0$ such that*

$$\langle \hat{\Phi}(\theta)\zeta, \zeta^* \rangle \geqq C|\theta|^2|\zeta|^2, \quad \forall \theta \in [-\pi, \pi]^n, \ \zeta \in \mathbb{C}^n. \tag{148}$$

Then F has a unique minimum in X.

Proof. Under the assumptions, F is sequentially coercive in X. In fact, the sets $\{F \leqq t\}$ are bounded in the reflexive space X and therefore relatively compact in its weak topology. In addition, F is continuous in the strong topology of X and convex, and therefore sequentially lower semicontinuous in the weak topology of X. Hence, F has a minimum in X. The uniqueness of the minimizer follows directly from the strict convexity of F. Thus, let $u, v \in M_X(F)$ so that $F(u) = F(v) = m_X(F)$. If $u \neq v$ we have

$$F\left(\frac{u}{2} + \frac{v}{2}\right) < \frac{1}{2}F(u) + \frac{1}{2}F(v) = m_X(F), \tag{149}$$

which is impossible. Hence $u = v$. □

The results cited in this proof are standard (e.g., [10], Examples 1.14, 1.22 and 1.23, Propositions 1.18 and 1.20, Theorem 1.15).

4.3. Continuum limit

In this section we study the *continuum limit* of the equilibrium problem (135), i.e., the behavior of the lattice as the lattice parameter is allowed to become vanishingly small, or, equivalently, in the long wavelength limit. It is widely appreciated that harmonic lattices behave like elastic continua in that limit. A common way of understanding this limiting behavior is to refer to the asymptotic form of the dynamical matrix, or, equivalently, of the phonon dispersion relation as the wave number $k \to 0$. Here, instead, we seek to understand the continuum limit in the sense of the Γ-convergence of the energy functional (104). As it is well known, Γ-convergence of the energy functional also guarantees convergence of the energy minimizers under rather general conditions (cf., e.g., [10], Corollary 7.24). For simplicity, throughout this section we restrict our attention to simple lattices.

We begin by adopting the wave number representation of the Fourier transform (cf. Section A.2), which is more natural in the continuum setting. In this representation the energy (112a) takes the form

$$E(u) = \frac{1}{(2\pi)^n} \int_B \frac{1}{2} \langle D(k)\hat{u}(k), \hat{u}^*(k) \rangle \, dk, \tag{150}$$

where

$$D(k) = \frac{1}{\Omega^2}\hat{\Phi}(k) = \frac{1}{\Omega}\sum_{l\in\mathbb{Z}^n}\Phi(l)\mathrm{e}^{-ik\cdot x(l)} \tag{151}$$

is the dynamical matrix of the lattice. For a simple lattice and assuming sufficient differentiability, the properties

$$D^T(k) = D^*(k), \tag{152a}$$
$$D(-k) = D^T(k), \tag{152b}$$
$$D(0) = 0, \tag{152c}$$
$$\partial_k D(0) = 0 \tag{152d}$$

follow simply from reciprocity, translation invariance and the centrosymmetry of the lattice. In particular, property (152a) implies that $D(k)$ is hermitian. The behavior of $D(k)$ for small k is of particular importance in the continuum limit. From (151), (152c), (152d) and (134) we obtain

$$\lim_{\varepsilon\to 0}\varepsilon^{-2}D_{ik}(\varepsilon k) = \lim_{\varepsilon\to 0}\varepsilon^{-2}\frac{1}{\Omega}\sum_{l\in\mathbb{Z}^n}\Phi(l)\mathrm{e}^{-i\varepsilon k\cdot x(l)} = c_{ijkl}k_jk_l \equiv (D_0)_{ik}(k), \tag{153}$$

where D_0 is the dynamical matrix of the linear elastic solid of moduli c_{ijkl}.

Consider now the sequence of functions $E_\varepsilon : H^1(\mathbb{R}^n) \to \bar{\mathbb{R}}$ defined as:

$$E_\varepsilon(u) = \begin{cases} \frac{1}{(2\pi)^n}\int_{B/\varepsilon}\frac{1}{2}\langle\varepsilon^{-2}D(\varepsilon k)\hat{u}(k), \hat{u}^*(k)\rangle\,dk & \text{if } \mathrm{supp}(\hat{u}) \in B/\varepsilon, \\ +\infty & \text{otherwise,} \end{cases} \tag{154}$$

obtained by scaling down the lattice size by a factor of ε. We wish to ascertain the limiting behavior of the sequence E_ε as $\varepsilon \to 0$. We surmise that the likely limit is the linear elastic energy

$$E_0(u) = \int_{\mathbb{R}^n}\frac{1}{2}c_{ijkl}u_{i,j}u_{k,l}dx = \frac{1}{(2\pi)^n}\int_{\mathbb{R}^n}\frac{1}{2}c_{ijkl}k_jk_l\hat{u}_i\hat{u}_k^*dk, \tag{155}$$

where c_{ijkl} are the elastic moduli of the material and a comma denotes partial differentiation. Simple conditions under which this limit is indeed realized are provided by the following proposition.

Proposition 4. *Suppose that:*

(i) *for every $\zeta \in \mathbb{C}^n$ the function $\langle D(\cdot)\zeta, \zeta^*\rangle$ is measurable on B;*
(ii) *there is a constant C such that*

$$0 \leqq \langle D(k)\zeta, \zeta^*\rangle \leqq C|k|^2|\zeta|^2 \tag{156}$$

for a. e. $k \in B$ and for every $\zeta \in \mathbb{C}^n$;

(iii) *for every* $\zeta \in \mathbb{C}^n$, *the functions* $\varepsilon^{-2}\langle D(\varepsilon k)\zeta, \zeta^*\rangle$ *converge for a. e.* k *to*

$$\langle D_0(k)\zeta, \zeta^*\rangle = c_{ijkl}k_j k_l \zeta_i \zeta_k^* \tag{157}$$

Then,

$$\Gamma - \lim_{\varepsilon\to 0} E_\varepsilon(u) = E_0(u) \tag{158}$$

in the weak topology of $H^1(\mathbb{R}^n)$.

Proof. Let $u \in H^1(\mathbb{R}^n)$, and let u_ε the sequence of $H^1(\mathbb{R}^n)$-functions converging to u obtained by restricting $\hat{u}$ to B/ε (cf. Section A.4.1). Then,

$$E_\varepsilon(u_\varepsilon) = \frac{1}{(2\pi)^n}\int_{B/\varepsilon} \frac{1}{2}\langle \varepsilon^{-2} D(\varepsilon k)\hat{u}(k), \hat{u}^*(k)\rangle\, dk. \tag{159}$$

By assumptions (ii)–(iii) and dominated convergence, it follows that

$$\lim_{\varepsilon\to 0}\int_{B/\varepsilon} \langle \varepsilon^{-2} D(\varepsilon k)\hat{u}(k), \hat{u}^*(k)\rangle dk = \int \langle D_0(k)\hat{u}(k), \hat{u}^*(k)\rangle dk \tag{160}$$

and, hence,

$$\lim_{\varepsilon\to 0} E_\varepsilon(u_\varepsilon) = E_0(u). \tag{161}$$

Let now $u_\varepsilon \rightharpoonup u$ in $H^1(\mathbb{R}^n)$. We need to show that

$$E_0(u) \leqq \liminf_{\varepsilon\to 0} E_\varepsilon(u_\varepsilon). \tag{162}$$

Suppose that $\liminf_{\varepsilon\to 0} E_\varepsilon(u_\varepsilon) < +\infty$, otherwise there is nothing to prove. We pass to a subsequence, to be renamed u_ε, which gives the lim inf as a limit. In view of (160) it suffices to prove that

$$\lim_{\varepsilon\to 0}\int_{B/\varepsilon} \big(\langle \varepsilon^{-2} D(\varepsilon k)\hat{u}_\varepsilon(k), \hat{u}_\varepsilon^*(k)\rangle - \langle \varepsilon^{-2} D(\varepsilon k)\hat{u}(k), \hat{u}^*(k)\rangle\big) dk \geqq 0. \tag{163}$$

Consider the identity

$$\begin{aligned}
&\langle \varepsilon^{-2} D(\varepsilon k)\hat{u}_\varepsilon(k), \hat{u}_\varepsilon^*(k)\rangle - \langle \varepsilon^{-2} D(\varepsilon k)\hat{u}(k), \hat{u}^*(k)\rangle \\
&\quad = \langle \varepsilon^{-2} D(\varepsilon k)\big(\hat{u}_\varepsilon(k) - \hat{u}(k)\big), \hat{u}_\varepsilon^*(k) - \hat{u}^*(k)\rangle \\
&\qquad + 2\langle \varepsilon^{-2}|k|^{-1} D(\varepsilon k)\hat{u}(k), \big(\hat{u}_\varepsilon^*(k) - \hat{u}^*(k)\big)|k|\rangle.
\end{aligned} \tag{164}$$

In the last term, $\big(\hat{u}_\varepsilon(k) - \hat{u}(k)\big)|k| \rightharpoonup 0$ in L^2, whereas, by dominated convergence, $\varepsilon^{-2}|k|^{-1} D(\varepsilon k)\hat{u}(k) \to |k|^{-1} D_0(k)\hat{u}(k)$ also in L^2. Hence,

$$\int_{B/\varepsilon} \langle \varepsilon^{-2}|k|^{-1} D(\varepsilon k)\hat{u}(k), \big(\hat{u}_\varepsilon^*(k) - \hat{u}^*(k)\big)|k|\rangle\, dk \to 0, \tag{165}$$

and

$$\begin{aligned}
&\lim_{\varepsilon\to 0}\int_{B/\varepsilon} \big(\langle \varepsilon^{-2} D(\varepsilon k)\hat{u}_\varepsilon(k), \hat{u}_\varepsilon^*(k)\rangle - \langle \varepsilon^{-2} D(\varepsilon k)\hat{u}(k), \hat{u}^*(k)\rangle\big)\, dk \\
&\quad = \lim_{\varepsilon\to 0}\int_{B/\varepsilon} \langle \varepsilon^{-2} D(\varepsilon k)\big(\hat{u}_\varepsilon(k) - \hat{u}(k)\big), \hat{u}_\varepsilon^*(k) - \hat{u}^*(k)\rangle\, dk \geqq 0
\end{aligned} \tag{166}$$

as required. □

If $D(k)$ is sufficiently smooth at the origin then, by (152c) and (152d),

$$\lim_{\varepsilon \to 0} \varepsilon^{-2} D_{ik}(\varepsilon k) = \frac{1}{2} \frac{\partial^2 D_{ik}}{\partial k_j \partial k_l}(0) k_j k_l. \tag{167}$$

Comparing this expression with (153) we find the identity

$$c_{ijkl} + c_{ilkj} = \frac{\partial^2 D_{ik}}{\partial k_j \partial k_l}(0), \tag{168}$$

which provides an alternative means, equivalent to (134), of computing the elastic moduli of the lattice. Identity (168) shows that, as expected, the elastic moduli fully describe the behavior of the lattice in the continuum limit.

If the first of inequalities (156) can be strengthened to

$$C|k|^2|\zeta|^2 \leqq \langle D(k)\zeta, \zeta^* \rangle \tag{169}$$

for some constant $C > 0$, for all $\varepsilon > 0$, a. e. $k \in B$ and for every $\zeta \in \mathbb{C}^n$, then the sequence of functions $E_\varepsilon(u)$ is equicoercive in the space $X = H^1(\mathbb{R}^n)/\mathbb{R}^n$ defined in Section 4.2. If, in addition, the conditions of Theorem 3 are satisfied, then the unique minimizer of $E_\varepsilon(u)$ converges weakly in X to the unique minimizer of $E_0(u)$ (cf., e.g., [10] for the connection between equicoercivity and convergence of minimizers).

4.4. Simple illustrative examples

The consideration of complex interatomic potentials describing specific materials is beyond the scope of this paper. Therefore, we shall confine our attention to two simple examples, namely, the square and simple cubic lattices with nearest neighbor interactions, mainly for purposes of illustration and for developing insight and intuition.

4.4.1. The square lattice. As a first simple example we consider the case of a square lattice undergoing anti-plane shear. The lattice complex is as described in Section 2.3.2. In the nearest-neighbor approximation, the single non-zero harmonic force constant is $C(e_1, e_1) = \mu/a$, where μ is the shear modulus of the crystal. The remaining nonzero force constants (111a) and (111b) are

$$\Psi\begin{pmatrix} 0 \\ 1, 1 \end{pmatrix} = \Psi\begin{pmatrix} 0 \\ 2, 2 \end{pmatrix} = \mu a, \tag{170}$$

and

$$\Phi(1, 0) = \Phi(0, 1) = \Phi(-1, 0) = \Phi(0, -1) = -\mu a, \tag{171a}$$

$$\Phi(0, 0) = -\Phi(1, 0) - \Phi(0, 1) - \Phi(-1, 0) - \Phi(0, -1) = 4\mu a. \tag{171b}$$

Here $\Psi\binom{l}{\alpha,\beta}$ designates the force constant that couples $du(0,\alpha)$ to $du(l,\beta)$, and $\Phi(l)$ designates the force constant that couples $u(0)$ and $u(l)$. A straightforward computation yields

$$\hat{\Phi}(\theta) = 4\mu a\left(\sin^2\frac{\theta_1}{2} + \sin^2\frac{\theta_2}{2}\right), \tag{172}$$

whence the dynamical matrix follows as

$$D(k) = \frac{4\mu}{a^2}\left(\sin^2\frac{k_1 a}{2} + \sin^2\frac{k_2 a}{2}\right), \tag{173}$$

which in this simple example reduces to a scalar. We verify that $(1/2)\partial_{k_1}\partial_{k_1}D(0) = \mu$ and $(1/2)\partial_{k_2}\partial_{k_2}D(0) = \mu$, as required.

4.4.2. The simple cubic lattice. Consider now the simple cubic lattice complex described in Section 2.3.4. In the nearest-neighbor approximation, the non-zero harmonic force constants are: $C(e_1, e_1, e_1, e_1) \equiv F$; $C(e_1, e_1, e_1', e_1') \equiv G$; and $C(e_1, e_1', e_1, e_1') \equiv H$. Here e_1 and e_1' denote 1-cells having a common vertex. Thus, F is the strength of the pairwise component of the energy, G measures the strength of the coupling between the elongations of adjacent 1-cells, or Poisson effect, and H measures the strength of the bond-angle interactions. The corresponding force-constant fields are

$$\Psi\binom{0}{1,1} = a^2\begin{pmatrix} F & 0 & 0 \\ 0 & 4H & 0 \\ 0 & 0 & 4H \end{pmatrix}, \tag{174a}$$

$$\Psi\binom{0}{1,2} = a^2\begin{pmatrix} 0 & G & 0 \\ H & 0 & 0 \\ 0 & 0 & 0 \end{pmatrix}, \tag{174b}$$

and

$$\Phi(1,0,0) = a^2\begin{pmatrix} -F & 0 & 0 \\ 0 & -4H & 0 \\ 0 & 0 & -4H \end{pmatrix}, \tag{175a}$$

$$\Phi(1,1,0) = a^2\begin{pmatrix} 0 & -G-H & 0 \\ -H-G & 0 & 0 \\ 0 & 0 & 0 \end{pmatrix}, \tag{175b}$$

$$\Phi(0,0,0) = a^2\begin{pmatrix} 2F+16H & 0 & 0 \\ 0 & 2F+16H & 0 \\ 0 & 0 & 2F+16H \end{pmatrix}, \tag{175c}$$

whence all the remaining force constants follow by symmetry. Lengthy but straightforward calculations yield

$$\hat{\Phi}_{11}(\theta) = a^2\left[4F\sin^2\frac{\theta_1}{2} + 16H\left(\sin^2\frac{\theta_2}{2} + \sin^2\frac{\theta_3}{2}\right)\right], \tag{176a}$$

$$\hat{\Phi}_{12}(\theta) = 4a^2(G+H)\sin\theta_1\sin\theta_2, \tag{176b}$$

whence the dynamical matrix follows as

$$D_{11}(k) = \frac{1}{a}\left[4F\sin^2\frac{k_1 a}{2} + 16H\left(\sin^2\frac{k_2 a}{2} + \sin^2\frac{k_3 a}{2}\right)\right], \tag{177a}$$

$$D_{12}(k) = \frac{4}{a}(G+H)\sin(k_1 a)\sin(k_2 a) \tag{177b}$$

with all remaining components following by symmetry. Finally, the elastic moduli follow from (168) as

$$c_{11} = aF, \tag{178a}$$

$$c_{12} = 4aG, \tag{178b}$$

$$c_{44} = 4aH. \tag{178c}$$

Thus, for this simple model all the forces constants can be identified directly from the elastic moduli and the lattice parameter.

5. Eigendeformation theory of crystallographic slip

The total energy of a crystal is invariant under lattice-invariant deformations (cf. Section 2.1) and, therefore, it is a nonconvex function of the atomic displacements. This lack of convexity in turn permits the emergence of lattice defects such as dislocations. A seeming deficiency of the harmonic approximation described earlier – which would appear to disqualify it as a suitable framework for the study of dislocations – is that the energy (108) is a convex function of the displacements and, in particular, not invariant under lattice-invariant deformations. However, this limitation can be overcome by recourse to the theory of eigendeformations (cf., e.g., [36]), which we proceed to formulate in this section.

5.1. The energy of a plastically deformed crystal

Consider a uniform lattice-invariant deformation of the form (16), corresponding to a homogeneous crystallographic slip on planes of normal $m_i a^i$ through a translation vector $s^j a_j$. This uniform deformation has the matrix representation

$$F = I + \frac{\xi}{d} b \otimes m, \tag{179}$$

where m is the unit normal to the slip plane, b is the Burgers vector, d is the distance between consecutive slip planes, and $\xi \in \mathbb{Z}$ is the slip amplitude in quanta of Burgers vector. The corresponding linearized eigendeformation 1-form $\beta \in \Omega^1$ is

$$\beta(e_1) \approx (F - I)dx(e_1) = (dx(e_1)\cdot m)\,\xi b. \tag{180}$$

We note that, by a suitable choice of lattice complex, 1-cells either lie on a slip plane, in which case $dx(e_1)\cdot m = 0$, or join two consecutive slip planes, in which

case $dx(e_1) \cdot m = d$. Let $E_1(m)$ be the set of 1-cells of the second type, i.e., $E_1(m) = \{e_1 \in E_1, \text{ s. t. } dx(e_1) \cdot m = d\}$. Then we have the representation

$$\beta = \sum_{e_1 \in E_1(m)} \xi b\, e^1. \tag{181}$$

The general eigendeformation 1-form resulting from the activation of the slip system defined by b and m is obtained by *localizing* (181) 1-cell by 1-cell, with the result

$$\beta = \sum_{e_1 \in E_1(m)} \xi(e_1) b\, e^1, \tag{182}$$

where now ξ is an integer-valued function on $E_1(m)$. Suppose now that crystallographic slip can take place on N crystallographic systems defined by Burgers vectors and normals (b^s, m^s), $s = 1, \ldots, N$, respectively. The resulting eigendeformation 1-form is

$$\beta = \sum_{s=1}^{N} \sum_{e_1 \in E_1(m^s)} \xi^s(e_1) b^s\, e^1, \tag{183}$$

where $\xi^s : E_1(m^s) \to \mathbb{Z}$ is the slip field corresponding to slip system s. We shall assume that exact, or compatible, eigendeformations of this general type cost no energy. A simple device for building this feature into the theory is to assume an elastic energy of the form

$$E(u, \xi) = \frac{1}{2} \langle B(du - \beta),\, du - \beta \rangle, \tag{184}$$

which replaces representation (106) in the presence of eigendeformations. Clearly, if $\beta = dv$, i.e., if the eigendeformations are exact, or compatible, then the energy-minimizing displacements are $u = v$ and $E = 0$. However, because slip is crystallographically constrained, β must necessarily be of the form (183) and, therefore, is not compatible in general. By virtue of this lack of compatibility, a general distribution of slip induces residual stresses in the lattice and a nonvanishing elastic energy, or stored energy.

A compelling geometrical interpretation of eigendeformations can be given with the aid of a discrete version of the Nye dislocation density tensor [38], namely,

$$\alpha = d\beta. \tag{185}$$

This simple relation may be regarded as the discrete version of KRÖNER's formula (6) (see [26]). From (185) it follows immediately that

$$d\alpha = 0, \tag{186}$$

which generalizes the conservation of the Burgers vector identity (7). Note that α is a 2-form, i.e., $\alpha \in \Omega^2$. Clearly, if the eigendeformations are compatible, i.e., if $\beta = dv$, then $\alpha = d^2 v = 0$. Thus, the dislocation density 2-form α measures the

degree of incompatibility of the eigendeformations. Furthermore, it follows from the definition (90) of the linking number that

$$\int_{E_3} \omega \wedge \alpha = \mathrm{Link}(\omega, \beta). \tag{187}$$

Thus, suppose that α is supported on a collection of closed loops, and ω is a subset of $d\chi_A$, where χ_A is the characteristic chain of a subset $A \in E_0$. Then by the intersection interpretation of the linking number it follows that (187) counts the number of signed intersections of the dislocation loops with ω. In particular, if $\omega = d\chi_A$, then $\mathrm{Link}(\omega, \beta) = 0$, which shows that the number of dislocation loops entering a closed surface must necessarily equal the number of dislocation loops exiting the surface.

Further insight into the geometry of dislocations may be derived by inserting representation (183) into (185), which yields

$$\alpha = \sum_{s=1}^{N} \sum_{e_1 \in E_1(m^s)} \xi^s(e_1) b^s \, \delta e^1 \equiv \sum_{s=1}^{N} \alpha^s. \tag{188}$$

Thus, each slip system s contributes a certain dislocation density α^s to α. Furthermore, the dislocation density α^s has a constant direction b^s and consists of the superposition of *elementary dislocation loops* $\delta e^1 \in B^2$ with multiplicities $\xi^s(e_1)$. Each elementary loop δe^1 is an elementary 2-coboundary. Equivalently, since the lattice complex is assumed to be perfect, the elementary dislocation loops may be regarded as 2-cocycles surrounding the 1-cells of the lattice, hence their designation as loops.

5.2. Examples of dislocation systems

A compilation of experimentally observed slip systems metallic crystals may be found in [19]. Thus, for instance, FCC crystals are commonly found to deform plastically through the activation of 12 slip systems consisting of {111} slip planes and [110] slip directions. Likewise, BCC crystals exhibit activity on 24 main slip systems consisting of {110} and {112} slip planes and [111] slip directions. Table 1 collects the slip directions and plane normals for the square, hexagonal, simple cubic, FCC and BCC crystals for ease of reference.

In perfect lattices, the sets $\{\partial e_2(l, \alpha),\ l \in \mathbb{Z}^n, \alpha = 1, \ldots, N_2\}$ and $\{\delta e^1(l, \alpha),\ l \in \mathbb{Z}^n, \alpha = 1, \ldots, N_1\}$ generate Z_1 and B^2, respectively. These 1-cycles and 2-coboundaries may be regarded as sets of elementary Burgers circuits and dislocation loops, respectively. All Burgers circuits and dislocation distributions can be obtained by taking integer combinations of the elementary circuits and loops, respectively. In two-dimensional lattices, the elementary loops take the form of dipoles. The geometry of the elementary circuits and dipoles of the square and hexagonal lattices is shown in Fig. 12 by way of illustration. In three-dimensional lattices, the elementary dislocation loops consist of rings of oriented 2-cells incident on 1-cells. In particular, it is somewhat misleading – and best avoided – to represent elementary dislocation loops as closed curves in space. The geometry of

Table 1. Slip-system sets in Schmid and Boas' nomenclature. The vector m is the unit normal to the slip plane, and s is the unit vector in the direction of the Burgers vector of the system. All vectors are expressed in cartesian coordinates.

Square	Slip System	A3	B3				
	s	$[001]$	$[001]$				
	m	(100)	(010)				
Hexagonal	Slip System	A3	B3	C3			
	s	$[001]$	$[001]$	$[001]$			
	$2m$	$(0\bar{2}0)$	$(\sqrt{3}\bar{1}0)$	$(\sqrt{3}\bar{1}0)$			
SC	Slip System	A2	A3	B1	B3	C1	C2
	s	$[0\bar{1}0]$	$[001]$	$[\bar{1}00]$	$[00\bar{1}]$	$[\bar{1}00]$	$[0\bar{1}0]$
	m	(100)	(100)	(010)	(010)	(001)	(001)
FCC	Slip System	A2	A3	A6	B2	B4	B5
	$\sqrt{2}s$	$[01\bar{1}]$	$[101]$	$[\bar{1}\bar{1}0]$	$[0\bar{1}1]$	$[\bar{1}0\bar{1}]$	$[\bar{1}10]$
	$\sqrt{3}m$	$(\bar{1}11)$	$(\bar{1}11)$	$(\bar{1}11)$	(111)	(111)	(111)
	Slip System	C1	C3	C5	D1	D4	D6
	$\sqrt{2}s$	$[011]$	$[\bar{1}0\bar{1}]$	$[1\bar{1}0]$	$[0\bar{1}\bar{1}]$	$[\bar{1}01]$	$[110]$
	$\sqrt{3}m$	$(\bar{1}\bar{1}1)$	$(\bar{1}\bar{1}1)$	$(\bar{1}\bar{1}1)$	$(1\bar{1}1)$	$(1\bar{1}1)$	$(1\bar{1}1)$
BCC	Slip System	A2	A3	A6	B2	B4	B5
	$\sqrt{3}\,s$	$[\bar{1}11]$	$[\bar{1}11]$	$[\bar{1}11]$	$[111]$	$[111]$	$[111]$
	$\sqrt{2}\,m$	$(0\bar{1}1)$	(101)	(110)	$(0\bar{1}1)$	$(\bar{1}01)$	$(\bar{1}10)$
	Slip System	C1	C3	C5	D1	D4	D6
	$\sqrt{3}\,s$	$[11\bar{1}]$	$[11\bar{1}]$	$[11\bar{1}]$	$[1\bar{1}1]$	$[1\bar{1}1]$	$[1\bar{1}1]$
	$\sqrt{2}\,m$	(011)	(101)	$(\bar{1}10)$	(011)	$(\bar{1}01)$	(110)

the elementary Burgers circuits and dislocation loops of the cubic, FCC and BCC lattices is shown in Fig. 13.

5.3. The stored energy of a fixed distribution of dislocations

If the distribution of eigendeformations is known, and in the absence of additional constraints, the energy of the lattice can be readily minimized with respect to the displacement field. Suppose that the crystal is acted upon by a distribution of forces $f \in \Omega_0(X, \mathbb{R}^n)$. The total potential energy of the lattice is then

$$F(u, \xi) = E(u, \xi) - \langle f, u \rangle. \tag{189}$$

Minimization of $F(u, \xi)$ with respect to u yields the equilibrium equation

$$Au = f + \delta B\beta, \tag{190}$$

where $\delta B\beta$ may be regarded as a distribution of eigenforces corresponding to the eigendeformations β. The equilibrium displacements, are, therefore,

$$u = A^{-1}(f + \delta B\beta) \equiv u_0 + A^{-1}\delta B\beta, \tag{191}$$

where $u_0 = A^{-1}f$ is the displacement field induced by the applied forces in the absence of eigendeformations and we write, formally,

$$A^{-1}f \equiv G * f \tag{192}$$

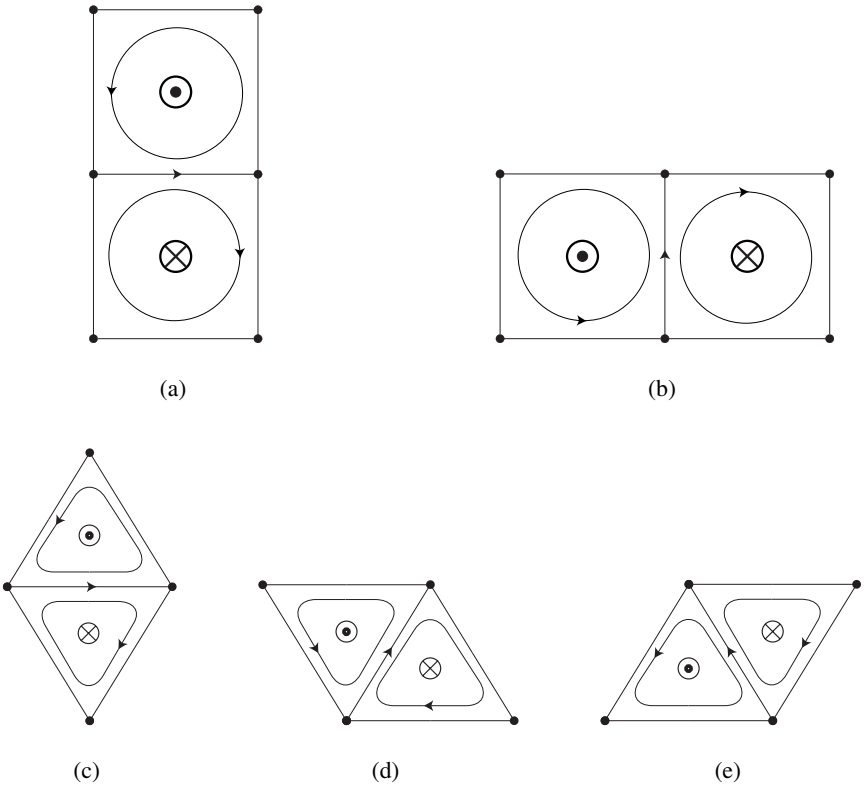

Fig. 12. Elementary dislocation dipoles (generators of the group B^2) for the square (a and b) and hexagonal lattices (c, d and e). The dipoles consist of a dislocation segment pointing into the plane (shown as $\otimes$), and a dislocation segment pointing away from the plane (shown as $\odot$). The corresponding Burgers circuits (generators of the group Z_1) are shown as oriented circles. The 1-cell to which the dipoles are attached is shown as an oriented 1-cell.

(cf. equation (138)). Conditions under which the minimum problem just described is well-posed and delivers a unique energy-minimizing displacement field have been given in Section 4.2. The corresponding minimum potential energy is

$$\begin{aligned} F(\beta) &= \frac{1}{2}\langle B\beta, \beta\rangle - \frac{1}{2}\langle A^{-1}(f + \delta B\beta),\ f + \delta B\beta\rangle \\ &= \frac{1}{2}\langle B\beta, \beta\rangle - \frac{1}{2}\langle A^{-1}\delta B\beta,\ \delta B\beta\rangle - \langle A^{-1}\delta B\beta,\ f\rangle - \frac{1}{2}\langle A^{-1}f,\ f\rangle \\ &= \frac{1}{2}\langle B\beta, \beta\rangle - \frac{1}{2}\langle A^{-1}\delta B\beta,\ \delta B\beta\rangle - \langle B\beta,\ du_0\rangle - \frac{1}{2}\langle Au_0,\ u_0\rangle. \quad (193) \end{aligned}$$

The first two terms

$$E(\beta) = \frac{1}{2}\langle B\beta, \beta\rangle - \frac{1}{2}\langle A^{-1}\delta B\beta,\ \delta B\beta\rangle \quad (194)$$

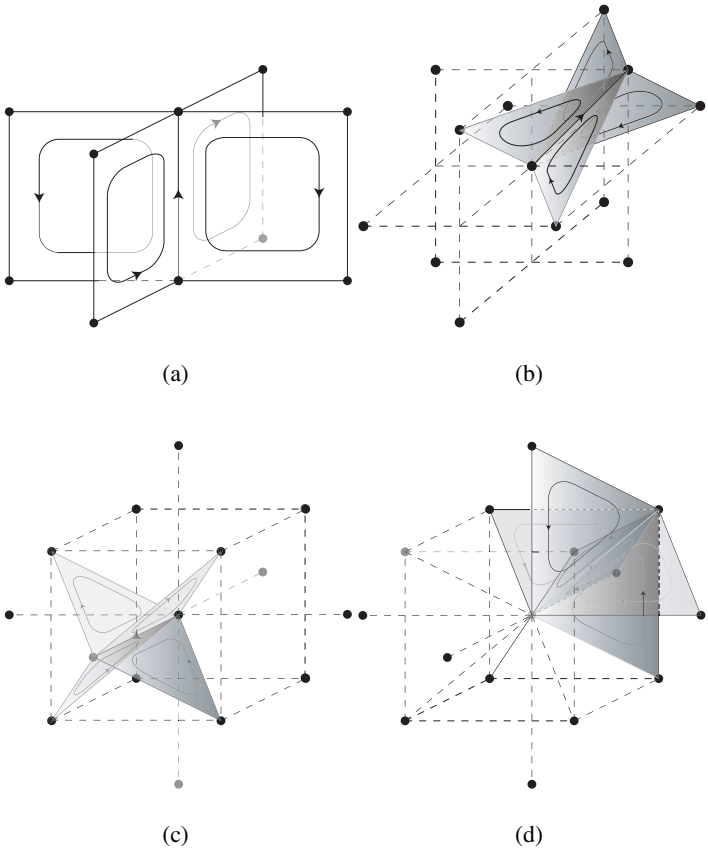

Fig. 13. Elementary dislocation loops (generators of the group B^2) for: (a) the simple cubic lattice; (b) the face-centered cubic lattice; and (c) and (d) the body-centered cubic lattice. The remaining elementary circuits and loops may be obtained by symmetry from those shown in the figure. The elementary loops consist of rings of oriented 2-cells incident on a 1-cell. The oriented 2-cells are the elementary Burgers circuits (generators of the group Z_1). The 1-cell to which the elementary dislocation loops are attached is shown as an oriented 1-cell.

in (193) give the self-energy of the distribution of lattice defects represented by the eigendeformation field β, or stored energy; the third term in (193) is the interaction energy between the lattice defects and the applied forces; and the fourth term in (193) is the elastic energy of the applied forces.

In the theory of continuously distributed elastic dislocations, a result of MURA [35] shows that the energy $E(\beta)$ can in fact be expressed directly as a function $E(\alpha)$ of the dislocation density field α, and is independent of the choice of slip distribution β used to induce α. In particular, two distributions of slip which differ by an exact form and, hence, represent the same dislocation density, have the same stored energy. In linear elasticity, this situation also arises in the theory of cut surfaces,

where an application of Stoke's theorem shows that the energy is independent of the choice of cut [3]. The corresponding discrete analog may be derived as follows. By virtue of the Hodge-Helmholtz decomposition (81) for perfect lattices we have the respresentation

$$\beta = dv + \delta\Delta^{-1}\alpha, \tag{195}$$

where $v = \Delta^{-1}\delta\beta$, (cf., equation (82a)). Inserting this representation in (194) and redefining $u - v$ as u, an altogether identical derivation to that leading to (193) now gives

$$E(\alpha) = \frac{1}{2}\langle B\delta\Delta^{-1}\alpha, \delta\Delta^{-1}\alpha\rangle - \frac{1}{2}\langle A^{-1}\delta B\delta\Delta^{-1}\alpha,\ \delta B\delta\Delta^{-1}\alpha\rangle \tag{196}$$

for the stored energy of the crystal, and

$$F(\alpha) = E(\alpha) - \langle B\delta\Delta^{-1}\alpha,\ du_0\rangle - \frac{1}{2}\langle Au_0,\ u_0\rangle \tag{197}$$

for the potential energy. We thus verify that, as in the case of linear elastic dislocations, the stored energy corresponding to a distribution of slip β can be expressed directly in terms of the dislocation density $\alpha = d\beta$.

Suppose that the crystal under consideration possesses N slip systems and its eigendeformations admit the representation (183) in terms of an integer-valued slip field $\xi \equiv \{\xi^s, s = 1, \ldots, N\}$. Because of the integer-valuedness condition, each component ξ^s corresponding to a particular slip system s defines a 1-cochain and, consequently, ξ belongs to the group C_1^N. Additionally we recall that values of ξ^s on 1-cells e_1 such that $dx(e_1)$ is contained in the corresponding slip plane, i.e., such that $dx(e_1) \cdot m^s = 0$, contribute nothing to the eigendeformation field β and, therefore, may be set to zero for definiteness. This normalization will be left implied – but is tacitly in force – throughout all subsequent developments. Then, the stored energy (194) can be written in the form

$$E(\xi) = \frac{1}{2}\langle H\xi, \xi\rangle, \tag{198}$$

where the operator H is defined by the identity

$$\langle H\xi, \xi\rangle = \frac{1}{2}\langle B\beta, \beta\rangle - \frac{1}{2}\langle A^{-1}\delta B\beta,\ \delta B\beta\rangle, \tag{199}$$

in which β and ξ are related through (183). By translation invariance we must have

$$H\xi = \Upsilon * \xi \tag{200}$$

for some discrete hardening-moduli field Υ. If $\xi \in l^2$, then (198) admits the Fourier representation

$$E(\xi) = \frac{1}{(2\pi)^n}\int_{[-\pi,\pi]^n} \frac{1}{2}\langle \hat{\Upsilon}(\theta)\hat{\xi}(\theta), \hat{\xi}^*(\theta)\rangle\, d\theta. \tag{201}$$

If, in addition, the crystal is acted upon by a force field f, the resulting potential energy is (cf. equation (193))

$$F(\xi) = E(\xi) - \langle \tau, \xi \rangle - \frac{1}{2}\langle A^{-1} f,\ f \rangle, \tag{202}$$

where the forcing field τ follows from the identity

$$\langle \tau, \xi \rangle = \langle f, A^{-1} \delta B \beta \rangle, \tag{203}$$

in which β and ξ are again related through (183). We note that $\tau(e_1)$ is the energetic force conjugate to $\xi(e_1)$ and, therefore, may be regarded as a collection of N discrete Peach-Koehler forces, or resolved shear stresses, acting on the 1-cell e_1. According to this interpretation, $H\xi$ represents the resolved shear-stress field resulting from a slip distribution ξ, and therefore H can be regarded as an atomic-level hardening matrix (cf., e.g., [9] for an account of the classical notion of a hardening matrix in crystal plasticity).

The preceding framework may be taken as a basis for formulating abstract versions of a number of classical problems in dislocation mechanics. For instance, a central problem in physical metallurgy and crystal plasticity is the characterization of the dislocation structures that arise as a result of the plastic working of ductile crystals (cf., e.g., [17, 27]). Insight into those structures can sometimes be derived from knowledge of energy-minimizing dislocation structures. The corresponding variational problem concerns the minimization of (197) subject to the constraint (186) of conservation of Burgers vector and the additional constraint

$$||\alpha||_1 \equiv \sum_{s=1}^{N} \sum_{e_2 \in E_2} |d\xi^s(e_2)| = M \tag{204}$$

that fixes the total mass of dislocation in the crystal. The resulting problem lacks lower-semicontinuity and its minimizers may be expected to exhibit fine oscillations. Numerical studies of energy-minimizing dislocation structures do indeed exhibit such patterns [37, 29].

Another longstanding problem in physical metallurgy concerns the determination of the patterns of slip activity which occur in plastically worked metals and attendant macroscopic properties such as yield stresses and hardening rates (cf., e.g., [33]). On a first approach to the problem, it might seem tempting to attempt the minimization of the potential energy (202) as a means of characterizing the slip fields likely to occur under the action of applied loads. However, this approach fails due to the lack of coerciveness of the function $F(\xi)$. We demonstrate this lack of coerciveness by means of a counterexample. Consider the case of a square lattice undergoing anti-plane shear, cf. Section 5.4.1. Suppose that the lattice deforms under the action of a point load $f > 0$ applied to the origin. For $h \in \mathbb{Z}$, $h \geqq 1$, consider a sequence of displacements such that $u_h(l) = hb$ at $l = 0$, and $u_h(l) = 0$ elsewhere. In addition, let $(\xi_h)_{A3}(l, 1) = -h$, $(\xi_h)_{B3}(l, 2) = -h$, $(\xi_h)_{A3}(l - \varepsilon_1, 1) = h$, $(\xi_h)_{B3}(l - \varepsilon_2, 2) = hb$, and $\xi_h = 0$ otherwise. Then, it can be readily verified that $du_h = \beta_h$ and $\alpha_h = 0$, and thus the strain-energy of the crystal is zero. Therefore, $F(\xi_h) = -hfb$ which tends to $-\infty$ as $h \to +\infty$. Thus,

$F(\xi)$ lacks coerciveness and the corresponding minimum problem fails to deliver solutions in general.

This degeneracy can be remedied, and the mathematical problem rendered well posed, by a careful accounting of physical sources of resistance, or obstacles, to the motion of dislocations (cf., e.g., [19]). For instance, when two dislocation lines cross each other, reactions take place that result in jogs, junctions and other reaction products. This source of work hardening is referred to as *forest hardening*. A simple limiting case is obtained by assuming that an infinite energy is required for dislocations to cross each other. This effectively rules outs crossings, a constraint that can be expressed in terms of the linking number (90) in the form

$$\mathrm{Link}\big(\xi^r(e_1), \xi^s(e_1')\big) = 0, \quad \forall e_1, e_1' \in E_1,\ r, s = 1, \ldots, N,\ r \neq s, \quad (205)$$

This constraint introduces a topological obstruction that restricts the configurations accessible to the dislocation ensemble. A rigorous analysis of the interaction between dislocations and obstacles has recently been performed by GARRONI and MÜLLER [14, 15].

5.4. Simple illustrative examples of stored energies

In this section we present two simple examples of stored energy corresponding to the simple cubic and square lattices. While these examples are of limited relevance to actual materials, they nevertheless serve the purpose of illustrating the structure of stored energies.

5.4.1. The square lattice. A particularly simple example concerns a square lattice undergoing anti-plane shear. The nearest-neighbor force constants and dynamical matrix for this case have been collected in (170), (171a), (171b) and (173). The relation between the eigendeformations and the slip field is

$$\beta\big(e_1(l,1)\big) = b\xi_{A3}\big(e_1(l,1)\big), \quad (206a)$$
$$\beta\big(e_1(l,2)\big) = b\xi_{B3}\big(e_1(l,2)\big), \quad (206b)$$

where the nomenclature for the slip systems can be referred to in Table 1. In addition, we conventionally set $\xi_{A3}\big(e_1(l,2)\big) = 0$ and $\xi_{B3}\big(e_1(l,1)\big) = 0$. From (184) the energy of the crystal per unit length in the anti-plane shear direction follows as

$$E(u,\xi) = \frac{1}{(2\pi)^2}\int_{-\pi}^{\pi}\int_{-\pi}^{\pi}\frac{\mu}{2}\big\{|(\mathrm{e}^{i\theta_1}-1)\hat{u}(\theta) - b\hat{\xi}_{A3}(\theta)|^2 + |(\mathrm{e}^{i\theta_2}-1)\hat{u}(\theta) - b\hat{\xi}_{B3}(\theta)|^2\big\}\,d\theta_1 d\theta_2. \quad (207)$$

Minimization with respect to u gives

$$\hat{u}(\theta) = i\frac{b}{2}\frac{\sin\frac{\theta_1}{2}\hat{\eta}_{A3}(\theta) + \sin\frac{\theta_2}{2}\hat{\eta}_{B3}(\theta)}{\sin^2\frac{\theta_1}{2} + \sin^2\frac{\theta_2}{2}}, \quad (208)$$

and the corresponding stored energy per unit length is computed to be

$$E(\xi) = \frac{1}{(2\pi)^2}\int_{-\pi}^{\pi}\int_{-\pi}^{\pi}\frac{\mu b^2}{2}\frac{|\sin\frac{\theta_2}{2}\hat{\eta}_{A3}(\theta) - \sin\frac{\theta_1}{2}\hat{\eta}_{B3}(\theta)|^2}{\sin^2\frac{\theta_1}{2}+\sin^2\frac{\theta_2}{2}}\,d\theta_1 d\theta_2, \tag{209}$$

where we write $b^2 \equiv |b|^2$ and

$$\hat{\eta}_{A3}(\theta) = \hat{\xi}_{A3}(\theta)\mathrm{e}^{i\theta_1/2}, \tag{210a}$$
$$\hat{\eta}_{B3}(\theta) = \hat{\xi}_{B3}(\theta)\mathrm{e}^{i\theta_2/2} \tag{210b}$$

may be regarded as translates of the fields ξ_{A3} and ξ_{B3} to the center of the corresponding 1-cells. Alternatively, using (47b) and (185), the energy (209) may be recast in the form

$$E(\alpha) = \frac{1}{(2\pi)^2}\int_{-\pi}^{\pi}\int_{-\pi}^{\pi}\frac{\mu b^2}{2}\frac{|\hat{\alpha}(\theta)|^2}{\sin^2\frac{\theta_1}{2}+\sin^2\frac{\theta_2}{2}}\,d\theta_1 d\theta_2, \tag{211}$$

which is a special case of (196) and exemplifies the general result that the stored energy of a crystal can be written in terms of the dislocation density α. In the special case in which slip is confined to a single plane, e.g., the plane $\{e_1(l,2)\text{ s. t. } l^2 = 0\}$, the energies (209) and (211) reduce to

$$E(\xi) = \frac{1}{2\pi}\int_{-\pi}^{\pi}\frac{\mu b^2}{2}\frac{\left|\sin\frac{\theta_1}{2}\right|}{\sqrt{1+\sin^2\frac{\theta_1}{2}}}|\hat{\xi}_{B3}(\theta_1)|^2 d\theta_1 \tag{212}$$

and

$$E(\alpha) = \frac{1}{2\pi}\int_{-\pi}^{\pi}\frac{\mu b^2}{2}\frac{|\hat{\alpha}(\theta_1)|^2}{\sqrt{\sin^2\frac{\theta_1}{2}+\sin^4\frac{\theta_1}{2}}}\,d\theta_1, \tag{213}$$

respectively.

5.4.2. The simple cubic lattice. The relation between eigendeformations and the slip field in a simple-cubic lattice is

$$\beta\big(e_1(l,1)\big) = b_{A2}\xi_{A2}\big(e_1(l,1)\big) + b_{A3}\xi_{A3}\big(e_1(l,1)\big), \tag{214a}$$
$$\beta\big(e_1(l,2)\big) = b_{B1}\xi_{B1}\big(e_1(l,2)\big) + b_{B3}\xi_{B3}\big(e_1(l,2)\big), \tag{214b}$$
$$\beta\big(e_1(l,3)\big) = b_{C1}\xi_{C1}\big(e_1(l,3)\big) + b_{C2}\xi_{C2}\big(e_1(l,3)\big), \tag{214c}$$

where the designation of the slip systems is as in Table 1. In addition, the components of ξ not appearing in the preceding relations are conventionally set to zero. Suppose, for simplicity, that activity takes place in the single system C1 and that $c_{12} = 0$ and $c_{11} = 2c_{44}$. The elastic moduli thus obtained are isotropic, and Poisson's ratio is zero. Assume, in addition, that $\hat{\xi}_{C1}$ is independent of θ_1, corresponding to a distribution of straight screw dislocations. Then, using moduli (174a) and (174b) the energy per unit length of dislocation is computed to be

$$E(\xi) = \frac{1}{(2\pi)^2}\int_{-\pi}^{\pi}\int_{-\pi}^{\pi}2ab^2H\frac{\sin^2\frac{\theta_2}{2}}{\sin^2\frac{\theta_2}{2}+\sin^2\frac{\theta_3}{2}}|\hat{\xi}_{C1}|^2 d\theta_2 d\theta_3. \tag{215}$$

Finally, if slip is confined to the single plane $\{e_1(l, 3) \text{ s. t. } l^3 = 0\}$, the energy per unit length reduces to

$$E(\xi) = \frac{1}{(2\pi)} \int_{-\pi}^{\pi} 2ab^2 H \frac{\left|\sin \frac{\theta_1}{2}\right|}{\sqrt{1 + \sin^2 \frac{\theta_1}{2}}} |\hat{\xi}_{C1}|^2 d\theta_2. \tag{216}$$

We verify that (212) is recovered from this expression by making the identification $4aH = c_{44} = \mu$.

5.5. Continuum limit of the stored energy

We conclude this article by returning to the connection between the discrete and continuum theories investigated in Section 4.3. Here again, the aim of the analysis is to identify limiting situations in which the mechanics of the crystal can effectively be described by means of linear elasticity, thus achieving considerable simplification with respect to the full discrete theory. However, the continuum limit of the stored energy is somewhat subtle due to the logarithmic divergence of the energy of linear elastic dislocations. This difficulty notwithstanding, a well-defined continuum limit is attained by letting the dislocations become *well-separated*, i.e., in the *dilute limit*. Another useful limit of the discrete theory is attained by letting both the lattice size and the Burgers vector become vanishingly small. As shown subsequently, this limit coincides with the classical theory of *continuously-distributed dislocations* (cf., e.g., [36]).

5.5.1. Well-separated or dilute dislocations. Recall that the stored energy has the representation (201) in terms of the hardening moduli $\hat{\Upsilon}(\theta)$ and the complex Bravais lattice representation $\hat{\xi}(\theta, \alpha)$ of the discrete slip field. Recall that the support of the slip field ξ^s is $E_1^s = \{e_1 \in E_1, \text{ s. t. } dx(e_1) \cdot m^s = d^s\}$. With a view to facilitating the passage to the continuum, we rewrite the stored energy (201) in wavenumber form and require the Fourier transforms $\hat{\xi}^s$ of the slip functions to be supported on the Brillouin zone B of the lattice. The resulting form of the stored energy is

$$E(\xi) = \frac{1}{(2\pi)^n} \int_B \frac{1}{2} \langle G(k)\hat{\xi}(k), \hat{\xi}^*(k) \rangle \, dk, \tag{217}$$

where

$$G^{rs}(k) = \frac{1}{\Omega} \sum_{\alpha \in I^r} \sum_{\beta \in I^s} \hat{\Upsilon}^{rs}_{\alpha\beta}(k) \mathrm{e}^{ik\cdot(r_\alpha - r_\beta)} \tag{218}$$

and Ω is the volume of the unit cell of the lattice. In this expression, the labels r and s refer to a pair of slip systems, whereas the labels α and β range over the sublattices of E_1^r and E_1^s, respectively, and r_α is the shift of sublattice α.

In order to attain the limit of interest we proceed to scale the slip fields in such a way as to increasingly separate the dislocations. Consider a slip system s and let $(c_1^s, \ldots, c_n^s)$ be a Bravais basis for the crystal such that $(c_1^s, \ldots, c_{n-1}^s)$ spans the

slip planes of the system, and let $(c_s^1, \dots, c_s^n)$ be the corresponding dual basis. Let ξ^s be the slip function for system s and let $h \in \mathbb{Z}$, $h \geqq 1$. The appropriate scaled slip function is

$$\hat{\xi}_h^s(k) = w_h^s(k)\hat{\xi}^s(hk), \tag{219}$$

where ξ is extended by periodicity outside B and

$$w_h^s(k) = \prod_{j=1}^{n-1} \frac{1 - \mathrm{e}^{-ihk\cdot c_j^s}}{1 - \mathrm{e}^{-ik\cdot c_j^s}} \equiv \frac{q^s(hk)}{q^s(k)} \tag{220}$$

is a slip-plane window function. The effect of this scaling transformation may be ascertained by applying it to the function

$$\xi^s(l') = \begin{cases} 1 & \text{if } l' = l, \\ 0 & \text{otherwise.} \end{cases} \tag{221}$$

The Fourier transform of this function is $\hat{\xi}^s(k) = \Omega \mathrm{e}^{-ik\cdot x(l)}$, and, hence, in this case $\hat{\xi}_h^s(k) = \Omega w_h^s(k)\mathrm{e}^{-ik\cdot x(hl)}$. Thus, by linearity, the scaling transformation maps the value $\xi^s(l)$ at $x(l)$ of a general slip function ξ^s onto the area $\{x(l + \nu),\ \nu_i = 1, \dots, h,\ i = 1, \dots, n-1\}$ of the corresponding slip plane, which in turn has the effect of expanding the dislocation lines within their planes. In addition, the scaling transformation separates the planes containing the dislocations. We additionally define the continuum window functions

$$w_0^s(k) = \prod_{j=1}^{n-1} \frac{1 - \mathrm{e}^{-ik\cdot c_j^s}}{ik \cdot c_j^s} \equiv \frac{q^s(k)}{q_0^s(k)}, \tag{222}$$

and introduce the diagonal matrices $W_h = \mathrm{diag}\{w_h^1, \dots, w_h^N\}$ and $W_0 = \mathrm{diag}\{w_0^1, \dots, w_0^N\}$ for notational convenience. The properties

$$|h^{1-n} w_h^s(h^{-1}\eta)| \leqq 1 \tag{223}$$

and

$$\lim_{h\to\infty} |h^{1-n} w_h^s(h^{-1}\eta)| = w_0(\eta) \tag{224}$$

are noted for subsequent reference.

It should be carefully noted that in the scaling just described, the scaled dislocation ensemble consists of long straight segments of directions defined by the vectors $(c_1^s, \dots, c_{n-1}^s)$. Evidently, the corresponding limiting energy depends on the choice of these vectors. However, the dislocation segments of many crystals classes exhibit preferred directions. For instance, dislocations in BCC crystals are known to consist predominantly of screw and edge segments. In these cases, the vectors $(c_1^s, \dots, c_{n-1}^s)$ may conveniently be taken to coincide with the preferred orientations of the dislocation segments.

Next we wish to elucidate the behavior of the stored energy of the crystal under the scaling transformation just defined, i.e., the behavior of the sequence of functions

$$\begin{aligned} E_h(\xi) &= E(\xi_h) \\ &= \frac{1}{(2\pi)^n} \int_B \frac{1}{2} \langle G(k) W_h(k) \hat{\xi}(hk),\, W_h^*(k) \hat{\xi}^*(hk) \rangle \, dk. \end{aligned} \tag{225}$$

Alternatively, effecting a change of variables to $\eta = hk$ we obtain

$$\begin{aligned} E_h(\xi) &= \frac{h^{-n}}{(2\pi)^n} \int_{hB} \frac{1}{2} \langle G(h^{-1}\eta) W_h(h^{-1}\eta) \hat{\xi}(\eta),\, W_h^*(h^{-1}\eta) \hat{\xi}^*(\eta) \rangle \, d\eta \\ &= \frac{1}{(2\pi)^n} \int_B \frac{1}{2} \langle G_h(k) \hat{\xi}(k),\, \hat{\xi}^*(k) \rangle \, dk, \end{aligned} \tag{226}$$

where

$$G_h(k) = h^{-n} \sum_{\nu \in \mathbb{Z}^n \cap [-h,h]^n} (W_h G W_h^*)\big(h^{-1}(k + 2\pi \nu_i a^i)\big). \tag{227}$$

The limit of $E_h(\xi)$ as $h \to \infty$ now characterizes the stored energy of a crystal containing well-separated, or dilute, dislocations.

The following lemmas set the stage for the determination of the dilute limit of the stored energy. We begin by ascertaining the form

$$G_0(k) = \lim_{\varepsilon \to 0} G(\varepsilon k) \tag{228}$$

of $G(k)$ in the long wavelength limit.

Lemma 1. *Suppose that:*

(i) *there is a constant $C > 0$ such that*

$$C|k|^2 |\zeta|^2 \leqq \langle D(k)\zeta, \zeta^* \rangle \tag{229}$$

for a. e. $k \in B$ and for every $\zeta \in \mathbb{C}^n$;

(ii) *for every $\zeta \in \mathbb{C}^n$, the functions $\varepsilon^{-2} \langle D(\varepsilon k)\zeta, \zeta^* \rangle$ converge for a. e. k to*

$$\langle D_0(k)\zeta, \zeta^* \rangle = c_{ijkl} k_j k_l \zeta_i \zeta_k^*. \tag{230}$$

Then,

$$G_0^{rs}(k) = \left[c_{ijkl} - (D_0^{-1})_{pm}(k) c_{pqij} c_{mnkl} k_q k_n \right] \frac{b_i^r}{d^r} m_j^r \frac{b_k^s}{d^s} m_l^s. \tag{231}$$

for a. e. k.

Proof. Fix k throughout. From (183) and (184) we have

$$\langle G(k)\zeta, \zeta^*\rangle = \min_{c\in\mathbb{C}^n} \langle E(k)[Q(k)c - \eta(k)], [Q(k)c - \eta(k)]^*\rangle \tag{232}$$

for all $\zeta \in \mathbb{C}^N$, where $Q(k)$ is the matrix representation (41) of d^0,

$$\eta(k) = -\sum_{r=1}^{N} \zeta^r [m^r \cdot i\partial_k Q(k)] \frac{b^r}{d^r} \tag{233}$$

and

$$E(k) = \frac{1}{\Omega^2}\hat{\Psi}(k). \tag{234}$$

By (109) we have the identity

$$\langle D(k)c, c^*\rangle = \langle E(k)Q(k)c, [Q(k)c]^*\rangle. \tag{235}$$

Scaling k in (232) we obtain

$$\begin{aligned}\langle G(\varepsilon k)\zeta, \zeta^*\rangle &= \min_{c\in\mathbb{C}^n} \langle E(\varepsilon k)[Q(\varepsilon k)c - \eta(\varepsilon k)], [Q(\varepsilon k)c - \eta(\varepsilon k)]^*\rangle \\ &= \min_{c\in\mathbb{C}^n} \langle E(\varepsilon k)[Q(\varepsilon k)\varepsilon^{-1}c - \eta(\varepsilon k)], [Q(\varepsilon k)\varepsilon^{-1}c - \eta(\varepsilon k)]^*\rangle. \end{aligned} \tag{236}$$

By assumption (229) the quadratic functions $\langle \varepsilon^{-2} D(\varepsilon k)c, c^*\rangle$ are convex and equicoercive. Therefore, we have

$$\begin{aligned}\langle G_0(k)\zeta, \zeta^*\rangle &= \lim_{\varepsilon\to 0} \langle G(\varepsilon k)\zeta, \zeta^*\rangle \\ &= \min_{c\in\mathbb{C}^n} \lim_{\varepsilon\to 0} \langle E(\varepsilon k)[Q(\varepsilon k)\varepsilon^{-1}c - \eta(\varepsilon k)], [Q(\varepsilon k)\varepsilon^{-1}c - \eta(\varepsilon k)]^*\rangle. \end{aligned} \tag{237}$$

But,

$$\lim_{\varepsilon\to 0} \varepsilon^{-1} Q(\varepsilon k) = k \cdot \partial_k Q(0), \tag{238a}$$

$$\lim_{\varepsilon\to 0} \eta(\varepsilon k) = -\sum_{r=1}^{N} \zeta^r [m^r \cdot i\partial_k Q(0)] \frac{b^r}{d^r}, \tag{238b}$$

$$\langle E(0)a \cdot \partial_k Q(0)c, [a \cdot \partial_k Q(0)c]^*\rangle = c_{ijkl} c_i a_j c_k^* a_l^*, \tag{238c}$$

where in arriving at the last identity we have made use of (168) and (235). Hence,

$$\langle G_0(k)\zeta, \zeta^*\rangle = \min_{c\in\mathbb{C}^n} c_{ijkl} \left(i c_i k_j - \sum_{r=1}^{N} \zeta^r s_i^r m_j^r \right) \left(i c_k k_l - \sum_{s=1}^{N} \zeta^s s_k^s m_l^s \right)^*. \tag{239}$$

A direct calculation of the minimizer finally gives (231). □

We note that $G_0(k)$ is determined by the properties of the limiting linear elastic continuum, namely, by the elasticity of the crystal through the elastic moduli c_{ijkl} and the elastic dynamical matrix (153). The following lemma reveals the essential structure of the continuum kernel $G_0(k)$.

Lemma 2. *Suppose that the elastic moduli c_{ijkl} are positive definite and finite. Then, there is a constant $C > 0$ such that*

$$\langle G_0(k)\zeta, \zeta^*\rangle \leqq CN \sum_{r=1}^{N} \left(1 - \frac{(k \cdot m^r)^2}{|k|^2}\right) |\zeta^r|^2. \tag{240}$$

Proof. By (239) and convexity we have

$$\begin{aligned}
\langle G_0(k)\zeta, \zeta^*\rangle &\leqq \min_{c\in\mathbb{C}^n} \frac{1}{N} \sum_{r=1}^{N} c_{ijkl} \left(ic_i k_j - N\zeta^r m_i^r s_j^r\right) \left(ic_k k_l - N\zeta^r m_k^r s_l^r\right)^* \\
&\leqq \min_{c\in\mathbb{C}^n} \frac{1}{N} \sum_{r=1}^{N} C|ic \otimes k - N\zeta^r m^r \otimes s^r|^2 \qquad (241) \\
&= CN \sum_{r=1}^{N} \left(1 - \frac{(k \cdot m^r)^2}{|k|^2}\right) |\zeta^r|^2. \quad \square
\end{aligned}$$

Finally, in order to investigate the Γ-convergence of the energy $E_h(\xi)$ we need to ascertain the precise manner in which it scales with h. Begin by noting that

$$h^{2-n} G_h(k) = \sum_{v\in\mathbb{Z}^n\cap[-h,h]^n} \left((h^{1-n} W_h) G (h^{1-n} W_h^*)\right)\left(h^{-1}(k + 2\pi v_i a^i)\right). \tag{242}$$

Thus, in view of (224) and definition (228) we expect

$$h^{2-n} G_h(k) \sim \sum_{v\in\mathbb{Z}^n\cap[-h,h]^n} (W_0 G_0 W_0^*)(k + 2\pi v_i a^i) \tag{243}$$

for large h. The behavior of the right-hand side of this asymptotic equation is established by the following lemma.

Lemma 3. *Let $n \geqq 2$, $\mathbb{Z} \ni h > 1$. Suppose that the elastic moduli C_{ijkl} are positive definite and finite. Then, there is a constant $C > 0$ such that*

$$\frac{1}{\log h} \sum_{v\in\mathbb{Z}^n\cap[-h,h]^n} \langle (W_0 G_0 W_0^*)(k + 2\pi v_i a^i)\zeta, \zeta^*\rangle \leqq C|\zeta|^2 \tag{244}$$

for all $\zeta \in \mathbb{C}^N$.

Proof. Fix k and $\zeta \in \mathbb{C}^N$. By lemma 2 there is a constant $C > 0$ such that

$$\langle G_0(k) W_0(k)\zeta, W_0^*(k)\zeta^*\rangle \leqq C \sum_{r=1}^{N} \left(1 - \frac{(k \cdot m^r)^2}{|k|^2}\right) |w_0^r(k)|^2 |\zeta^r|^2. \tag{245}$$

Let $k_p^r = k - (k \cdot m^r)m^r$ be the projection of k onto the slip planes of system r and let $\theta_i^r = k \cdot c_i^r$. Then,

$$\begin{aligned}\left(1 - \frac{(k \cdot m^r)^2}{|k|^2}\right)|w_0^r(k)|^2 &= \frac{|k_p^r|^2}{|k|^2}|w_0^r(k)|^2 \\ &\leqq C\frac{\sum_{i=1}^{n-1}(\theta_i^r)^2}{\sum_{i=1}^{n}(\theta_i^r)^2}|w_0^r(k)|^2 \\ &\leqq C\sum_{i=1}^{n-1}\left(\prod_{\substack{j=1\\ j\neq i}}^{n-1}\frac{\sin^2\frac{1}{2}\theta_j^r}{\left(\frac{1}{2}\theta_j^r\right)^2}\right)\frac{4\sin^2\frac{1}{2}\theta_i^r}{\sum_{k=1}^{n}(\theta_k^r)^2}. \quad (246)\end{aligned}$$

But

$$\begin{aligned}&\sum_{\nu_i=-h}^{h}\sum_{\nu_n=-h}^{h}\frac{4\sin^2\frac{1}{2}(\theta_i^r + 2\pi\nu_i)}{\sum_{k=1}^{n}(\theta_k^r + 2\pi\nu_k)^2} \\ &= 2\left|\sin\frac{\theta_i^r}{2}\right|\sum_{\nu_i=-h}^{h}\sum_{\nu_n=-h}^{h}\frac{2\left|\sin\frac{1}{2}(\theta_i^r + 2\pi\nu_i)\right|}{\sum_{k=1}^{n}(\theta_k^r + 2\pi\nu_k)^2} \\ &\leqq 2\left|\sin\frac{\theta_i^r}{2}\right|\sum_{\nu_i=-h}^{h}\sum_{\nu_n=-h}^{h}\frac{2\left|\sin\frac{1}{2}(\theta_i^r + 2\pi\nu_i)\right|}{(\theta_i^r + 2\pi\nu_i)^2 + (\theta_n^r + 2\pi\nu_n)^2} \\ &\leqq 2\left|\sin\frac{\theta_i^r}{2}\right|\sum_{\nu_i=-h}^{h}\sum_{\nu_n=-\infty}^{\infty}\frac{2\left|\sin\frac{1}{2}(\theta_i^r + 2\pi\nu_i)\right|}{(\theta_i^r + 2\pi\nu_i)^2 + (\theta_n^r + 2\pi\nu_n)^2} \\ &= 2\left|\sin\frac{\theta_i^r}{2}\right|\sum_{\nu_i=-h}^{h}\frac{1}{|\theta_i^r + 2\pi\nu_i|}\frac{\left|\sin\frac{1}{2}(\theta_i^r + 2\pi\nu_i)\right|\left|\sinh(\theta_i^r + 2\pi\nu_i)\right|}{\cosh(\theta_i^r + 2\pi\nu_i) - \cos\theta_n^r}. \quad (247)\end{aligned}$$

By virtue of the bound

$$\frac{\sin\frac{\eta}{2}\sinh\eta}{\cosh\eta - \cos\xi} \leqq C \approx 2.23743 \quad (248)$$

in the range $\eta \in [0, \infty)$, $\xi \in [-\pi, \pi]$, we further have

$$\begin{aligned}&\sum_{\nu_i=-h}^{h}\sum_{\nu_n=-h}^{h}\frac{4\sin^2\frac{1}{2}(\theta_i^r + 2\pi\nu_i)}{\sum_{k=1}^{n}(\theta_k^r + 2\pi\nu_k)^2} \\ &\leqq 2C\left|\sin\frac{\theta_i^r}{2}\right|\sum_{\nu_i=-h}^{h}\frac{1}{|\theta_i^r + 2\pi\nu_i|} \\ &\leqq 2C\left|\sin\frac{\theta_i^r}{2}\right|\left(\frac{1}{|\theta_i^r|} + \frac{1}{\pi}\log h\right) \\ &\leqq C\left(1 + \frac{1}{\pi}\log h\right). \quad (249)\end{aligned}$$

In addition we have

$$\sum_{\nu_j=-h}^{h} \frac{4\sin^2 \frac{1}{2}(\theta_j^r + 2\pi\nu_j)}{(\theta_j^r + 2\pi\nu_j)^2} \leqq 1. \tag{250}$$

Combining the preceding bounds we obtain

$$\sum_{\nu\in\mathbb{Z}^n\cap[-h,h]^n} \langle (W_0 G_0 W_0^*)(k + 2\pi\nu_i a^i)\zeta, \zeta^*\rangle \leqq C\left(1 + \frac{1}{\pi}\log h\right)|\zeta|^2, \tag{251}$$

which proves the assertion. □

The preceding lemma suggests the behavior $E_h(\xi) \sim h^{n-2}\log h$ for large h. Therefore, we introduce the scaled sequence of functions

$$F_h(\xi) = \frac{h^{2-n}}{\log h} E_h(\xi) = \frac{1}{(2\pi)^n}\int_B \frac{1}{2}\langle K_h(k)\hat{\xi}(k), \hat{\xi}^*(k)\rangle\, dk, \tag{252}$$

where

$$K_h(k) = \frac{h^{2-n}}{\log h} G_h(k). \tag{253}$$

The behavior of the sequence $F_h(\xi)$ as $h \to \infty$ is characterized by the following proposition.

Proposition 5. *Let $n \geqq 2$, $\mathbb{Z} \ni h > 1$. Suppose that:*

(i) *for every $\zeta \in \mathbb{C}^N$ the function $\langle K_h(\cdot)\zeta, \zeta^*\rangle$ is measurable on B;*
(ii) *there is a constant C such that*

$$0 \leqq \langle K_h(k)\zeta, \zeta^*\rangle \leqq C|\zeta|^2 \tag{254}$$

for a. e. $k \in B$ and for every $\zeta \in \mathbb{C}^N$;
(iii) *for every $\zeta \in \mathbb{C}^N$, the function $\langle K_h(k)\zeta, \zeta^*\rangle$ converges for a. e. k to $\langle K_0(k)\zeta, \zeta^*\rangle$ as $h \to \infty$.*

Let

$$F_0(\xi) = \frac{1}{(2\pi)^n}\int_B \frac{1}{2}\langle K_0(k)\hat{\xi}(k), \hat{\xi}^*(k)\rangle\, dk. \tag{255}$$

Then,

$$\Gamma - \lim_{h\to\infty} F_h = F_0 \tag{256}$$

in $X = \{\xi \in C_1^N$ s. t. $\hat{\xi} \in [L^2(B)]^N\}$.

Proof. Let $\xi \in X$. Then, from assumptions (i)–(iii) and dominated convergence, it follows that $F_h(\xi) \to F_0(\xi)$. Hence, F_h converges to F_0 pointwise. Consider now the space $Y = \{\xi : E_1 \to \mathbb{R}^N \text{ s. t. } \hat{\xi} \in [L^2(B)]^N\}$ obtained by lifting the integer-valuedness constraint and allowing the slip fields to take real values. By assumption (ii) it follows that the functions F_h are convex and equibounded, hence equi-lower semicontinuous, over Y. Since X is a closed subspace of Y it follows that the sequence F_h is likewise equi-lower semicontinuous over X. The proposition then follows from a standard result regarding the equivalence of pointwise convergence of equi-lower semicontinuous sequences and Γ-convergence (see [10], Proposition 5.9). □

The conditions of the theorem may be verified simply for specific force constant models. The $h^{n-2} \log h$ scaling of the stored energy $E_h(\xi)$ is consistent with the known solutions from linear elasticity for point dislocations in two dimensions and for dislocation loops in three dimensions (cf., e.g., [19]). The factor h^{n-2} accounts for the increase in dislocation length, or dislocation stretching, with increasing h. The factor $\log h$ corresponds to the familiar logarithmic divergence of the dislocation energy with the size of the domain occupied by the dislocations. It bears emphasis that the limiting energy (255) involves an integral over the Brillouin zone B and is defined for discrete slip fields. In this particular sense, the limit just derived retains the discreteness of the lattice on the scale of the dislocation cores and, as a consequence, remains free of the logarithmic core-divergence of linear elastic dislocation mechanics.

5.5.2. Continuously-distributed dislocations. Lemma 2 establishes the structure of the continuum kernel $G_0(k)$ and, by extension, sets the natural functional framework for the analysis of continuously distributed dislocations. Thus, the bound (240) suggests that the natural norm for a continuum slip field $\eta : \mathbb{R}^n \to \mathbb{R}^N$ is

$$||\eta||_X = \left[\sum_{s=1}^{N} \frac{1}{(2\pi)^n} \int \left(1 - \frac{(k \cdot m^s)^2}{|k|^2}\right) |\hat{\eta}^s(k)|^2 dk\right]^{1/2}. \tag{257}$$

Correspondingly, we may define the space X of continuum slip fields as the space of distributions resulting from the completion of C_0^∞ under the norm (257). Since

$$0 \leqq 1 - \frac{(k \cdot m^s)^2}{|k|^2} \leqq 1, \tag{258}$$

it follows that

$$||\eta||_X \leqq ||\eta||_{L^2} \tag{259}$$

and $L^2(\mathbb{R}^n, \mathbb{R}^N)$ is a subspace of X. Moreover, it follows from (259) that sequences converging strongly in L^2 also convergence strongly in X.

In addition to L^2-fields, the space X contains discontinuous slip fields such as

$$\eta^s = f(x_p^s)\delta(x_n^s), \tag{260}$$

where $(x_1^s, \dots, x_n^s)$ is a local system of cartesian coordinates for system s, with $(x_1^s, \dots, x_{n-1}^s)$ spanning the in-plane directions and x_n^s measuring distance in the direction normal to the slip planes; δ is the Dirac measure; and, for simplicity, we assume simple slip and set $\eta^r = 0$, $r \neq s$. Indeed, in this case,

$$\begin{aligned} ||\eta||_X^2 &= \frac{1}{(2\pi)^n} \int \frac{|k_p^s|^2}{|k^s|^2} |\hat{f}(k_p^s)|^2 dk^s \\ &= \frac{1}{(2\pi)^{n-1}} \int |k_p^s| \, |\hat{f}(k_p^s)|^2 dk_p^s = ||f||_{1/2}^2. \end{aligned} \tag{261}$$

Thus, the slip field (260) is in X provided that $f \in H^{1/2}(\mathbb{R}^{n-1})$.

For $\varepsilon > 0$, consider now the sequence of stored energy functions $E_\varepsilon : X \to \bar{\mathbb{R}}$:

$$E_\varepsilon(\xi) = \begin{cases} \frac{1}{(2\pi)^n} \int \frac{1}{2} \langle G(\varepsilon k) \hat{\xi}(k), \hat{\xi}^*(k) \rangle \, dk & \text{if } \operatorname{supp}(\hat{\xi}^s) \subset \varepsilon^{-1} B, \\ & \text{and } \xi^s(\varepsilon x(l)) \in \varepsilon \mathbb{Z}, \\ & l \in \mathbb{Z}^n, \ s = 1, \dots, N, \\ +\infty & \text{otherwise,} \end{cases} \tag{262}$$

obtained by scaling down both the crystal lattice and the Burgers vectors by a factor of ε simultaneously. In addition, consider the following candidate limiting energy $E_0 : X \to \bar{\mathbb{R}}$:

$$E_0(\eta) = \frac{1}{(2\pi)^n} \int \frac{1}{2} \langle G_0(k) \hat{\eta}(k), \hat{\eta}^*(k) \rangle \, dk. \tag{263}$$

The behavior of the sequence $E_\varepsilon(\xi)$ as $\varepsilon \to 0$ is characterized by the following proposition.

Proposition 6. *Suppose that:*

(i) *for every $\zeta \in \mathbb{C}^N$ the function $\langle G(\cdot)\zeta, \zeta^* \rangle$ is measurable on B;*
(ii) *there is a constant C such that*

$$0 \leqq \langle G(k)\zeta, \zeta^* \rangle \leqq C \sum_{r=1}^{N} \left(1 - \frac{(k \cdot m^r)^2}{|k|^2} \right) |\zeta^r|^2 \tag{264}$$

for a. e. $k \in B$ and for every $\zeta \in \mathbb{C}^N$;
(iii) *for every $\zeta \in \mathbb{C}^N$, the functions $\langle G(\varepsilon k)\zeta, \zeta^* \rangle$ converge for a. e. k to $\langle G_0(k)\zeta, \zeta^* \rangle$ as $\varepsilon \to 0$.*

Then,

$$\Gamma - \lim_{\varepsilon \to 0} E_\varepsilon = E_0 \tag{265}$$

in the weak topology of X.

Proof. Let $\eta \in X$. Let $u_i \in C_0^\infty$ be such that $u_i \to \eta$ in X. Approximate u_i by simple functions taking values in $\varepsilon\mathbb{Z}$ and converging strongly to u_i in X. Finally, sample the simple functions pointwise on a lattice of size ε (cf. Section A.4.2). Let ξ_ε be a diagonal sequence extracted from the preceding sequences. Then ξ_ε satisfies the integer-valuedness constraint in (262) and converges strongly to η in X. By assumption (ii) we have

$$\langle G(\varepsilon k)\hat{\xi}_\varepsilon(k), \hat{\xi}_\varepsilon^*(k)\rangle \leqq C\sum_{r=1}^{N}\left(1-\frac{(k\cdot m^r)^2}{|k|^2}\right)|\hat{\xi}_\varepsilon^r(k)|^2. \tag{266}$$

By assumption (iii) and the dominated convergence theorem it follows that

$$\lim_{\varepsilon\to 0}\int\langle G(\varepsilon k)\hat{\xi}_\varepsilon(k), \hat{\xi}_\varepsilon^*(k)\rangle dk = \int\langle G_0(k)\hat{\eta}(k), \hat{\eta}^*(k)\rangle dk \tag{267}$$

and, hence,

$$\lim_{\varepsilon\to 0} E_\varepsilon(\hat{\xi}_\varepsilon) = E_0(\eta). \tag{268}$$

Let now $\eta_\varepsilon \rightharpoonup \eta$ in X. We need to show that

$$E_0(\eta) \leqq \liminf_{\varepsilon\to 0} E_\varepsilon(\eta_\varepsilon). \tag{269}$$

Suppose that $\liminf_{\varepsilon\to 0} E_\varepsilon(\eta_\varepsilon) < +\infty$, otherwise there is nothing to prove. Pass to a subsequence, to be renamed ξ_ε, which gives the lim inf as a limit. In view of (267) it suffices to prove that

$$\lim_{\varepsilon\to 0}\int\Big(\langle G(\varepsilon k)\hat{\xi}_\varepsilon(k), \hat{\xi}_\varepsilon^*(k)\rangle - \langle G(\varepsilon k)\hat{\eta}(k), \hat{\eta}^*(k)\rangle\Big)dk \geqq 0. \tag{270}$$

Let $A(k) = \mathrm{diag}\{1-(k\cdot m^1)^2/|k|^2, \ldots, 1-(k\cdot m^N)^2/|k|^2\}$. Consider the identity

$$\begin{aligned}
&\langle G(\varepsilon k)\hat{\xi}_\varepsilon(k), \hat{\xi}_\varepsilon^*(k)\rangle - \langle G(\varepsilon k)\hat{\eta}(k), \hat{\eta}^*(k)\rangle \\
&\quad= \langle G(\varepsilon k)\big(\hat{\xi}_\varepsilon(k) - \hat{\eta}(k)\big), \hat{\xi}_\varepsilon^*(k) - \hat{\eta}^*(k)\rangle \\
&\qquad +2\langle A^{-1/2}(k)G(\varepsilon k)\hat{\eta}(k), A^{1/2}(k)\big(\hat{\xi}_\varepsilon^*(k) - \hat{\eta}^*(k)\big)\rangle
\end{aligned} \tag{271}$$

In the last term, $A^{1/2}(k)\big(\hat{\xi}_\varepsilon(k) - \hat{\eta}(k)\big) \rightharpoonup 0$ in L^2, whereas, by dominated convergence, $A^{-1/2}(k)G(\varepsilon k)\hat{\eta}(k) \to A^{-1/2}(k)G_0(k)\hat{\eta}(k)$ also in L^2. Hence,

$$\int\langle G(\varepsilon k)\hat{\eta}(k), \big(\hat{\xi}_\varepsilon^*(k) - \hat{\eta}^*(k)\big)\rangle\, dk \to 0 \tag{272}$$

and

$$\begin{aligned}
&\lim_{\varepsilon\to 0}\int\Big(\langle G(\varepsilon k)\hat{\xi}_\varepsilon(k), \hat{\xi}_\varepsilon^*(k)\rangle - \langle G(\varepsilon k)\hat{\eta}(k), \hat{\eta}^*(k)\rangle\Big)\, dk \\
&\quad= \lim_{\varepsilon\to 0}\int\langle G(\varepsilon k)\big(\hat{\xi}_\varepsilon(k) - \hat{\eta}(k)\big), \hat{\xi}_\varepsilon^*(k) - \hat{\eta}^*(k)\rangle\, dk \\
&\quad\geqq 0
\end{aligned} \tag{273}$$

as required. □

The energy (263) follows directly by minimizing out the displacement field in continuum plasticity with the aid of the Fourier transform. However, the preceding discussion does add to that formal result by providing an understanding of the precise manner in which the continuously distributed dislocation limit is approached, and an understanding of the natural functional setting in which to couch that limit. Thus, for instance, it is interesting to note that the energy (263) is well-defined for discontinuous slip of the form (260), provided that the slip distribution $f \in H^{1/2}(\mathbb{R}^{n-1})$ on the slip plane. By contrast, the limiting theory does not support Volterra dislocations, since a piecewise constant function $f \in H^{1/2}(\mathbb{R}^{n-1})$ is necessarily constant [14].

Appendix A. The discrete Fourier transform

Appendix A.1. Definition and fundamental properties

Begin by introducing the usual l^p spaces of lattice functions. Let f be a complex-valued lattice function, i.e., a function $f : \mathbb{Z}^n \to \mathbb{C}$. Its l^p-norm is

$$||f||_p = \left\{ \sum_{l \in \mathbb{Z}^n} |f(l)|^p \right\}^{1/p}. \tag{A.274}$$

Let l^p be the corresponding Banach spaces. In particular, l^1 can be turned into a Banach algebra with involution by taking the convolution

$$(f * g)(l) = \sum_{l' \in \mathbb{Z}^n} f(l - l')g(l') \tag{A.275}$$

as the multiplication operation and complex conjugation as the involution (cf., e.g., [42]). The discrete Fourier transform of $f \in l^1$ is

$$\hat{f}(\theta) = \sum_{l \in \mathbb{Z}^n} f(l)\mathrm{e}^{-i\theta \cdot l}. \tag{A.276}$$

In addition we have

$$f(l) = \frac{1}{(2\pi)^n} \int_{[-\pi,\pi]^n} \hat{f}(\theta)\mathrm{e}^{i\theta \cdot l} d\theta, \tag{A.277}$$

which is the inversion formula for the discrete Fourier transform. It follows from this expression that $f(-l)$ is the Fourier-series coefficient of $\hat{f}(\theta)$. The discrete Fourier transform characterizes all complex homomorphisms of the Banach algebra l^1. In particular we have the identity

$$\widehat{f * g} = \hat{f}\hat{g}, \tag{A.278}$$

which is often referred to as the *convolution theorem*. Suppose in addition that $f, g \in l^2$. Then, from the identity

$$\sum_{l\in\mathbb{Z}^n}\left(\frac{1}{(2\pi)^n}\int_{[-\pi,\pi]^n}\hat{f}(\theta)\mathrm{e}^{i\theta\cdot l}d\theta\right)g^*(l)$$
$$=\frac{1}{(2\pi)^n}\int_{[-\pi,\pi]^n}\hat{f}(\theta)\left(\sum_{l\in\mathbb{Z}^n}g^*(l)\mathrm{e}^{-i\theta\cdot l}\right)d\theta \tag{A.279}$$

we obtain

$$\sum_{l\in\mathbb{Z}^n}f(l)g^*(l)=\frac{1}{(2\pi)^n}\int_{[-\pi,\pi]^n}\hat{f}(\theta)\hat{g}^*(\theta)d\theta, \tag{A.280}$$

which is the Parserval identity for the discrete Fourier transform. If, in particular, $g = f$, Parseval's identity reduces to

$$\sum_{l\in\mathbb{Z}^n}|f(l)|^2=\frac{1}{(2\pi)^n}\int_{[-\pi,\pi]^n}|\hat{f}(\theta)|^2d\theta, \tag{A.281}$$

which shows that the DFT is an l^2-isometry. Since $l^\infty \subset \widehat{l^1}$ is dense in l^2, it follows that the DFT has a unique continuous extension to an isometric isomorphism of l^2 onto $L^2([-\pi,\pi]^n)$.

Appendix A.2. Wave-number representation

The ordinary Fourier transform of continuum fields is most often expressed in terms of wave-numbers. In applications concerned with the passing to the continuum, it is therefore natural to adopt a wave-number vector representation of the discrete Fourier transform. In particular, this representation ensures that the discrete and ordinary Fourier transforms of physical fields of the same kind have matching units. We begin by effecting a change of variables in all discrete Fourier transforms $\hat{f}(\theta)$ from angles θ to wave-number vector $k \equiv \theta_i a^i$. In addition, we multiply $\hat{f}(\theta)$ by the atomic volume. The resulting function $\hat{f}(k)$ is supported on the Brillouin zone B in dual space, and is given directly by

$$\hat{f}(k)=\Omega\sum_{l\in\mathbb{Z}^n}f(l)\mathrm{e}^{-ik\cdot x(l)}, \tag{A.282}$$

where $x(l) = l^i a_i$ are the coordinates of the vertices of the lattice. We note that the identity $k\cdot x(l) = \theta\cdot l$ holds, so that (A.282) is indeed equivalent to (A.276) except for the scaling factor of Ω. The inverse mapping is given by

$$f(l)=\frac{1}{(2\pi)^n}\int_B\hat{f}(k)\mathrm{e}^{ik\cdot x(l)}dk. \tag{A.283}$$

In this representation the convolution (A.275) becomes

$$(f*g)(l)=\Omega\sum_{l'\in\mathbb{Z}^n}f(l-l')g(l') \tag{A.284}$$

and the convolution theorem remains of the form (A.278). In addition, the Parseval identity (A.280) now is

$$\Omega \sum_{l\in\mathbb{Z}^n} f(l)g^*(l) = \frac{1}{(2\pi)^n}\int_B \hat{f}(k)\hat{g}^*(k)dk, \tag{A.285}$$

which establishes an isometric isomorphism of l^2 onto $L^2(B)$.

Appendix A.3. Periodic functions

The extension of the Fourier transform formalism to periodic functions is of particular interest in applications. Consider a set $Y \subset \mathbb{Z}^n$, the *unit cell*, such that the translates $\{Y + L^i A_i,\ L \in \mathbb{Z}^n\}$, for some translation vectors $A_i \in \mathbb{Z}^n, i = 1, \ldots, n$, define a partition of $\mathbb{Z}^n$. Let A^i be the corresponding dual basis, and $B^i = 2\pi A^i$ the reciprocal basis. A lattice function $f : \mathbb{Z}^n \to \mathbb{R}$ is Y-periodic if $f(l) = f(l+L^i A_i)$, for all $L \in \mathbb{Z}^n$. Proceeding formally, the discrete Fourier transform of a Y-periodic lattice function can be written in the form

$$\begin{aligned}\hat{f}(t) &= \sum_{L\in\mathbb{Z}^n}\sum_{l\in Y} f(l)\mathrm{e}^{-it\cdot(l+L^jA_j)}\\ &= \frac{1}{|Y|}\left\{\sum_{l\in Y} f(l)\mathrm{e}^{it\cdot l}\right\}\left\{|Y|\sum_{L\in\mathbb{Z}^n}\mathrm{e}^{it\cdot(L^jA_j)}\right\},\end{aligned} \tag{A.286}$$

where $|Y|$ is the number of points in Y. But

$$|Y|\sum_{L\in\mathbb{Z}^n}\mathrm{e}^{it\cdot(L^jA_j)} = (2\pi)^n\sum_{H\in\mathbb{Z}^n}\delta(t - H_iB^i) \tag{A.287}$$

and, hence,

$$\hat{f}(t) = \frac{(2\pi)^n}{|Y|}\sum_{\theta\in Z}\hat{f}(\theta)\delta(t-\theta), \tag{A.288}$$

where

$$\hat{f}(\theta) = \sum_{l\in Y} f(l)\mathrm{e}^{-i\theta\cdot l} \tag{A.289}$$

and Z is the intersection of the lattice spanned by B^i and $[-\pi,\pi]^n$. In addition, the inverse Fourier transform specializes to

$$f(l) = \frac{1}{|Y|}\sum_{\theta\in Z}\hat{f}(\theta)\mathrm{e}^{i\theta\cdot l}. \tag{A.290}$$

For periodic functions, Parseval's identity takes the form

$$\sum_{l\in Y} f(l)g^*(l) = \frac{1}{|Y|}\sum_{\theta\in Z}\hat{f}(\theta)\hat{g}^*(\theta). \tag{A.291}$$

Likewise, let f and g be complex-valued lattice functions, where the latter is periodic. Inserting representation (A.288) into the convolution theorem gives

$$\begin{aligned}\widehat{(f * g)}(t) &= \hat{f}(t)\left(\frac{(2\pi)^n}{|Y|}\sum_{\theta\in Z}\hat{g}(\theta)\delta(t-\theta)\right)\\ &= \frac{(2\pi)^n}{|Y|}\sum_{\theta\in Z}\hat{f}(\theta)\hat{g}(\theta)\delta(t-\theta),\end{aligned} \tag{A.292}$$

whence it follows that

$$\widehat{(f * g)}(\theta) = \hat{f}(\theta)\hat{g}(\theta). \tag{A.293}$$

Finally, the average of a periodic function follows as

$$\langle f\rangle = \frac{1}{|Y|}\sum_{l\in Y} f(l) = \frac{1}{|Y|}\hat{f}_0. \tag{A.294}$$

Appendix A.4. Sampling and interpolation

In passing to the continuum the question arises of how to sample a function over $\mathbb{R}^n$ on a lattice and, conversely, how to extend a lattice function to $\mathbb{R}^n$. The former operation may be regarded as *sampling* a continuum function, whereas the latter operation may be regarded as *interpolating* a lattice function. Evidently, functions can be sampled and interpolated in a variety of ways. In this section we collect the particular schemes that arise in applications.

Appendix A.4.1. Filtering. A simple device for sampling a function $f \in H^s$ is to restrict its ordinary Fourier transform $\hat{f}(k)$ to the Brillouin zone B of the lattice, i.e., to set

$$\widehat{s_B f}(k) = \hat{f}(k), \quad k \in B. \tag{A.295}$$

The corresponding lattice function then follows from an application of the inverse discrete Fourier transform (A.283), with the result

$$s_B f(l) = \frac{1}{(2\pi)^n}\int_B \hat{f}(k)\mathrm{e}^{ik\cdot x(l)}dk \tag{A.296}$$

for $l \in \mathbb{Z}^n$. Conversely, for every lattice function $f(l)$ we can define an interpolant over $\mathbb{R}^n$ of the form

$$i_B f(x) = \frac{1}{(2\pi)^n}\int_B \hat{f}(k)\mathrm{e}^{ik\cdot x}dk. \tag{A.297}$$

A projection $P_B : H^s \to H^s$ can now be defined as $P_B = i_B \circ s_B$, i.e., by applying the sampling and interpolation operations in succession. Thus, for every $f \in H^s$ we have

$$\widehat{P_B f}(k) = \begin{cases} f(k) & \text{if } k \in B,\\ 0 & \text{otherwise.}\end{cases} \tag{A.298}$$

Clearly, the projection is orthogonal. Suppose now that the lattice is scaled down in size by a factor $\varepsilon \to 0$. The Brillouin zones of the scaled lattices are $B_\varepsilon = B/\varepsilon$. Let $f \in H^s$ and $f_\varepsilon = P_{B_\varepsilon} f$. Then it follows trivially that $\hat{f}_\varepsilon \to \hat{f}$ pointwise. In addition,

$$||\hat{f}_\varepsilon - \hat{f}||_s^2 = \frac{1}{(2\pi)^n} \int_{\mathbb{R}^n \setminus B_\varepsilon} |\hat{f}(k)|^2 \, d\mu_s(k), \tag{A.299}$$

where $d\mu_s(k) = (1 + |k|^2)^s dk$, which, by dominated convergence, shows that $f_\varepsilon \to f$ in H^s.

Appendix A.4.2. Pointwise sampling. An alternative scheme for sampling a function on a lattice is to sample the function pointwise, i.e.,

$$s_B f(l) = f(x(l)) \tag{A.300}$$

for $l \in \mathbb{Z}^n$, provided that the pointwise value of f at $x(l)$ is defined. This method of sampling has the property of preserving the range of the function, i. e., if f takes values in a subset $A \subset \mathbb{R}$, then so does $s_B f$. In terms of Fourier transforms we have

$$\begin{aligned}
\widehat{s_B f}(k) &= \Omega \sum_{l \in \mathbb{Z}^n} f(x(l)) \mathrm{e}^{-ik \cdot x(l)} \\
&= \Omega \sum_{l \in \mathbb{Z}^n} \left\{ \frac{1}{(2\pi)^n} \int \hat{f}(k') \mathrm{e}^{ik' \cdot x(l)} dk' \right\} \mathrm{e}^{-ik \cdot x(l)} \\
&= \frac{1}{(2\pi)^n} \int \left\{ \Omega \sum_{l \in \mathbb{Z}^n} \mathrm{e}^{i(k-k') \cdot x(l)} \right\} \hat{f}(k') dk' \\
&= \frac{1}{(2\pi)^n} \int \left\{ (2\pi)^n \sum_{m \in \mathbb{Z}^n} \delta(k - k' - 2\pi m_i a^i) \right\} \hat{f}(k) dk. \qquad \text{(A.301)}
\end{aligned}$$

Hence, the discrete Fourier transform of the sampled lattice function is given by the Poisson summation formula

$$\widehat{s_B f}(k) = \sum_{m \in \mathbb{Z}^n} \hat{f}(k + 2\pi m_i a^i), \qquad k \in B. \tag{A.302}$$

Conversely, for every lattice function $f(l)$ we define an interpolant over $\mathbb{R}^n$ of the form (A.297). As in the preceding section, a projection $P_B : L^2 \to L^2$ can now be defined as $P_B = i_B \circ s_B$, i.e., by applying the sampling and interpolation operations in succession. Thus, if $f \in L^2$ and $f_B = P_B f$ we have

$$\widehat{P_B f}(k) = \begin{cases} \sum_{m \in \mathbb{Z}^n} \hat{f}(k + 2\pi m_i a^i) & \text{if } k \in B, \\ 0 & \text{otherwise.} \end{cases} \tag{A.303}$$

It is verified that

$$P_B f(x(l)) = \frac{1}{(2\pi)^n} \int_B \left(\sum_{m\in\mathbb{Z}^n} \hat{f}(k + 2\pi m_i a^i) \right) \mathrm{e}^{ik\cdot x(l)}\, dk$$
$$= \frac{1}{(2\pi)^n} \int \hat{f}(k) \mathrm{e}^{ik\cdot x(l)}\, dk = f(x(l)), \tag{A.304}$$

which shows that the projection preserves the value of the function on the lattice and, hence, is orthogonal. Suppose now that the lattice is scaled down in size by a factor $\varepsilon \to 0$. The Brillouin zones of the scaled lattices are $B_\varepsilon = B_\varepsilon$. Let $f \in L^2$ and let $f_\varepsilon = P_{B_\varepsilon} f$. Then, we have

$$\hat{f}_\varepsilon(k) = \begin{cases} \sum_{m\in\mathbb{Z}^n} \hat{f}(k + \varepsilon^{-1} 2\pi m_i a^i) & \text{if } k \in B_\varepsilon, \\ 0 & \text{otherwise.} \end{cases} \tag{A.305}$$

We verify that

$$\begin{aligned} &||\hat{f}_\varepsilon - \hat{f}||_0^2 \\ &= \frac{1}{(2\pi)^n} \int_{B_\varepsilon} |\hat{f}_\varepsilon(k) - \hat{f}(k)|^2\, dk + \frac{1}{(2\pi)^n} \int_{\mathbb{R}^n\setminus B_\varepsilon} |\hat{f}(k)|^2\, dk \\ &= \frac{1}{(2\pi)^n} \int_{B_\varepsilon} \Big| \sum_{m\in\mathbb{Z}^n\setminus\{0\}} \hat{f}(k + \varepsilon^{-1} 2\pi m_i a^i) \Big|^2\, dk + \frac{1}{(2\pi)^n} \int_{\mathbb{R}^n\setminus B_\varepsilon} |\hat{f}(k)|^2\, dk \\ &\leqq \frac{1}{(2\pi)^n} \int_{B_\varepsilon} \sum_{m\in\mathbb{Z}^n\setminus\{0\}} |\hat{f}(k + \varepsilon^{-1} 2\pi m_i a^i)|^2\, dk + \frac{1}{(2\pi)^n} \int_{\mathbb{R}^n\setminus B_\varepsilon} |\hat{f}(k)|^2\, dk \\ &= 2\frac{1}{(2\pi)^n} \int_{\mathbb{R}^n\setminus B_\varepsilon} |\hat{f}(k)|^2\, dk. \end{aligned} \tag{A.306}$$

Hence, by dominated convergence, $||\hat{f}_\varepsilon - \hat{f}||_0 \to 0$ as $\varepsilon \to 0$.

Acknowledgements. The authors gratefully acknowledge the support of the Department of Energy through Caltech's ASCI ASAP Center for the Simulation of the Dynamic Response of Materials. MO wishes to gratefully acknowledge support received from NSF through an ITR grant on Multiscale Modeling and Simulation and Caltech's Center for Integrative Multiscale Modeling and Simulation. We are greatly indebted to SERGIO CONTI, ADRIANA GARRONI and STEFAN MÜLLER for technical guidance and for many helpful discussions and suggestions. This work was partially carried during MO's stay at the Max Planck Institute for Mathematics in the Sciences of Leipzig, Germany, under the auspices of the Humboldt Foundation. MO gratefully acknowledges the financial support provided by the Foundation and the hospitality extended by the Institute.

References

1. ABRAHAM, F.F., SCHNEIDER, D., LAND, B., LIFKA D., SKOVIRA, J., GERNER, J., ROSENKRANTZ, M.: Instability dynamics in the 3-dimensional fracture - an atomistic simulation. *Journal of the Mechanics and Physics of Solids* **45**, 1461–1471 (1997)
2. ABRAHAM, R., MARSDEN, J.E., RATIU, T.: *Manifolds, Tensor Analysis and Applications*. Addison-Wesley, London, 1983
3. BACON, D.J., BARNETT, D.M., SCATTERGOOD, R.O.: Anisotropic Continuum Theory of Lattice Defects. *Progress in Material Sciences* **23**, 51–262 (1979)

4. BORN, M., HUANG, K.: *Dynamical theory of crystal lattices*. Oxford University Press, London, 1954
5. BOTT, R., TU, L.W.: *Differential Forms in Algebraic Topology*. Springer-Verlag, 1982
6. BRADLEY, C.J., CRACKNELL, A.P.: *The Mathematical Theory of Symmetry in Solids*. Clarendon Press, Oxford, 1972
7. BRAIDES, A., GELLI, M.S.: The passage from discrete to continuous variational problems: a nonlinear homogenization process. In: P.Ponte Castaneda, editor, *Nonlinear Homogenization and its Applications to Composites, Polycrystals and Smart Materials*. Kluwer, 2004
8. CIORANESCU, D., DONATO, P.: *An Introduction to Homogeneization*. Oxford University Press, 1999
9. CUITIÑO, A.M., ORTIZ, M.: Computational modeling of single-crystals. *Modelling and Simulation in Materials Science and Engineering* **1**, 225–263 (1993)
10. DAL MASO, G.: *An Introduction to* Γ*-Convergence*. Birkhauser, Boston, 1993
11. DAW, M.S.: The embedded atom method: A review. In *Many-Atom Interactions in Solids*, of *Springer Proceedings in Physics*, Springer-Verlag, Berlin, **48**, pp. 49–63 1990
12. ERICKSEN, J.L.: On the symmetry of deformable crystrals. *Archive for Rational Mechanics and Analysis* **72**, 1–13 (1979)
13. FINNIS, M.W., SINCLAIR, J.E.: A simple empirical n-body potential for transition- metals. *Philosophical Magazine A-Physics of Condensed Matter Structure Defects and Mechanical Properties* **50**, 45–55 (1984)
14. GARRONI, A., MÜLLER, S.: Γ-limit of a phase-field model of dislocations. Preprint 92, Max-Planck-Institut für Mathematik in den Naturwissenschaften, Leipzig, Germany, 2003
15. GARRONI, A., MÜLLER, S.: A variational model for dislocations in the line tension limit. Preprint 76, Max-Planck-Institut für Mathematik in den Naturwissenschaften, Leipzig, Germany, 2004
16. HAMERMESH, M.: *Group Theory and its Applications to Physical Problems*. Dover Publications, New York, 1962
17. HANSEN, N., KUHLMANN-WILSDORFF, D.: Low Energy Dislocation Structures due to Unidirectional Deformation at Low Temperatures. *Materials Science and Engineering* **81**, 141–161 (1986)
18. HIRANI, A.: *Discrete Exterior Calculus*. PhD thesis, California Institute of Technology, 2003
19. HIRTH, J.P., LOTHE, J.: *Theory of Dislocations*. McGraw-Hill, New York, 1968
20. HOLZ, A.: Topological properties of linked disclinations in anisotropic liquids. *Journal of Physics A* **24**, L1259–L1267 (1991)
21. HOLZ, A.: Topological properties of linked disclinations and dislocations in solid continua. *Journal of Physics A* **25**, L1–L10 1992
22. HOLZ, A.: Topological properties of static and dynamic defect configurations in ordered liquids. *Physica A* **182**, 240–278 (1992)
23. KLEMAN, M., MICHEL, L., TOULOUSE, G.: Classification of topologically stable defects in ordered media. *Journal de Physique* **38**, L195–L197 (1977)
24. KOSLOWSKI, M., CUITIÑO, A.M., ORTIZ, M.: A phase-field theory of dislocation dynamics, strain hardening and hysteresis in ductile single crystals. *Journal of the Mechanics and Physics of Solids* **50**, 2597–2635 (2002)
25. KOSLOWSKI, M., ORTIZ, M.: A multi-phase field model of planar dislocation networks. *Modeling and Simulation in Materials Science and Engineering* **12**, 1087–1097 (2004)
26. KRÖNER, E.: Berechnung der elastischen Konstanten des Vielkristalls aus den Konstanten des Einkristalls. *Zeitung der Physik* **151**, 504–518 (1958)
27. KUHLMANN-WILSDORF, D.: Theory of plastic deformation: properties of low energy dislocation structures. *Materials Science and Engineering* **A113**, 1 (1989)
28. LEOK, M.: *Foundations of Computational Geometric Mechanics*. PhD thesis, California Institute of Technology, 2004
29. LUBARDA, V.A., BLUME, J.A., NEEDLEMAN, A.: An Analysis of Equilibrium Dislocation Distributions. *Acta Metallurgica et Materialia* **41**, 625–642 (1993)

30. MERMIN, N.D.: The topological theory of defects in ordered media. *Reviews of Modern Physics* **51**, 591–648 (1979)
31. MORGAN, F.: *Geometric Measure Theory*. Academic Press, London, 2000
32. MORIARTY, J.A.: Angular forces and melting in bcc transition-metals – a case-study of molybdenum. *Physical Review B* **49**, 12431–12445 (1994)
33. MUGHRABI, H.: Description of the Dislocation Structure after Unidirectional Deformation at Low Temperatures. In A.S. Argon, editor, *Constitutive Equations in Plasticity*, Cambridge, Mass, 1975. MIT Press pp. 199–250
34. MUNKRES, J.R.: *Elements of Algebraic Topology*. Perseus Publishing, 1984
35. MURA, T.: Continuous distribution of moving dislocations. *Philosophical Magazine* **8**, 843 (1963)
36. MURA, T.: *Micromechanics of defects in solids*. Kluwer Academic Publishers, Boston, 1987
37. NEUMANN, P.: Low Energy Dislocation Configurations: A Possible Key to the Understanding of Fatigue. *Materials Science and Engineering* **81**, 465–475 (1986)
38. NYE, J.F.: Some geometrical relations in dislocated crystals. *Acta Metallurgica* **1**, 153–162 (1953)
39. ORTIZ, M., PHILLIPS, R.: Nanomechanics of defects in solids. *Advances in Applied Mechanics* **36**, 1–79 (1999)
40. PEIERLS, R.E.: The Size of a Dislocation. *Proceedings of the Royal Society of London* **A52**, 34 (1940)
41. PETTIFOR, D.G., OLEINIK, I.I., NGUYEN-MANH, D., VITEK, V.: Bond-order potentials: bridging the electronic to atomistic modelling hierarchies. *Computational Materials Science* **23**, 33–37 (2002)
42. RUDIN, W.: *Functional Analysis*. McGraw-Hill, 1991
43. SARKAR, S.K., SENGUPTA, S.: On born-huang invariance conditions. *Phys. Status Solidi (b)* **83**, 263–271 (1977)
44. SCHWARZENBERGER, R.L.E.: Classification of crystal lattices. *Proceedings of the Cambridge Philosophical Society* **72**, 325–349 (1972)
45. SENGUPTA, S.: *Lattice Theory of Elastic Constants*. Trans Tech Publications, Aedermannsdorf, Switzerland, 1988
46. STILLINGER, F.H., WEBER, T.A.: Computer simulation of local order in condensed phases of silicon. *Phys. Rev. B* **31**, 5262–5271 (1985)
47. TOULOUSE, G., KLEMAN, M.: Principles of a classification of defects in ordered media. *Journal de Physique* **37**, L149–L151 (1976)
48. TREBIN, H.R.: The topology of non-uniform media in condensed matter physics. *Advances in Physics* **31**, 195–254 (1982)
49. WANG, C.C.: On representations for isotropic functions .i. isotropic functions of symmetric tensors and vectors. *Archive for Rational Mechanics and Analysis* **33**, 249 (1969)
50. YUAN, X.Y., TAKAHASHI, K., OUYANG, Y.F., ONZAWA, A.: Development of a modified embedded atom method for bcc transition metals. *Journal of Physics-Condensed Matter* **15**, 8917–8926 (2003)

Division of Engineering and Applied Science
California Institute of Technology
Pasadena, CA 91125, USA
e-mail: ortiz@aero.caltech.edu

and

Escuela Técnica Superior de Ingenieros Industriales
Universidad de Seville
e-mail: mpariza@us.es

(*Accepted January 10, 2005*)
Published online September 16, 2005 – © Springer-Verlag (2005)